# Development of Nonlinear Real-Time Intelligent Controllers for Anti-lock Braking Systems (ABS)

**Samuel John (0418571X)**

A thesis submitted to the Faculty of Engineering and the Built Environment, University of the Witwatersrand, Johannesburg, in fulfilment of the requirements for the degree of Doctor of Philosophy.

Johannesburg, October 2012

# Declaration

I declare that this thesis is my own, unaided work, except where otherwise acknowledged. It is being submitted for the degree of Doctor of Philosophy in the University of the Witwatersrand, Johannesburg. It has not been submitted before for any degree or examination at any other university.

Signed this ___ day of ___________ 20___

_______________________________

Samuel John (0418571X).

# Acknowledgements

I will like to acknowledge those who in one way or the other supported me in the course of this work. first and foremost, I will like to thank my supervisor Prof. Jimoh O. Pedro whose scholarship guidance made this work to become a reality. Next, I will like to thank the management of the Polytechnic of Namibia for the support I received through the Institutional Research and Publication Committee (IRPC) in the form of research time and for the funds used to procure the ABS test rig. I also wish to thank the Polytechnic computer support team in general and Mr. Fredericks in particular for his support in providing computer hardware and software for the simulations and experimentation phases. I received several encouragement and academic support from my colleagues; the staff of the Department of Mechanical Engineering of the Polytechnic of Namibia, their constructive critique and inputs were valuable to the success of this work. Last and by no means the least, I wish to thank my family for their sacrifices and moral support in the course of this work. May God reward each one of you in a special way.

# Abstract

The objective of the Anti-lock Braking System (ABS) is to control the wheel slip to maximize the friction coefficient between the wheel and the road, irrespective of the road surface and condition. The introduction of new braking system in road vehicles such as the electro-mechanical brakes used in brake-by-wire (BBW) system, which has a more continuous braking operation with a high level of accuracy, necessitates the continual review and improvement of the anti-lock braking system. From the control view point, therefore, more refinement of the ABS operation could be achieved with these improved hardware components. This thesis proposes a hybrid controller; combining feedback linearization and *proportional, integral and derivative* (PID) controllers, and a neural network-based feedback linearisation wheel slip controller. Furthermore, the thesis investigated the viability of a hybrid system of the proposed neural network and a (PID) wheel slip controller system. The hybrid systems, combines the accuracy of slip tracking ability of the PID controller and the robustness of the feedback linearization controller to achieve shorter stopping distance and good slip tracking. The performance of the proposed ABS systems are validated in software simulation and on a laboratory ABS test bench. The results for both controllers revealed their robustness to different road conditions and good slip tracking. This work further confirms the feasibility of a future neural network-based ABS controllers in road vehicles.

# Published Work

Aspects of this thesis have been published in the following conference proceedings:

1. S. John and J.O. Pedro, ‘Non-Linear Slip Control for Anti-Lock Braking System’, Proceedings of the IASTED International Conference on Modelling and Simulation (AfricaMS 2012), Gaborene, Botswana, September 2012, pp 169 - 176

2. S. John and J.O. Pedro, ‘Performance of Vehicle Slip Controller Combined with Passive Suspension’, Proceedings of the IEEE Region 8 Africon 2011, Victoria Falls, Zambia, September 2011

3. S. John, J.O. Pedro and L.T. Koczy, ‘Adaptive Improvement of a Passive Antilock Brake Control’, Proceedings of the IEEE Region 8 Africon 2011, Victoria Falls, Zambia, September 2011

4. S. John, J.O. Pedro and C.R. Pozna, ‘Enhanced Slip Control Performance Using Nonlinear Passive Suspension System’, Proceedings of the IEEE/ASME International Conference on Advanced Intelligent Mechatronics, pp.277-282, Budapest, Hungary, July 2011

5. J O Pedro, O T C Nyandoro, S John, ‘Neural Network Based Feedback Linearisation Slip Control of an Anti-lock Braking’, Proceedings of the 7th Asian Control Conference, pp. 1251 - 1257, Hong Kong, August 2009

6. S John and J.O. Pedro , ‘Modelling of Vehicle Dynamics for Anti-Lock Braking System (ABS)Controller Design ’, Proceedings of the Fifth International Conference of Dynamics of Rigid and deformable Bodies, pp. 239-246, Usti nad Labem, Czech Republic, October 2007

7. S John and J.O. Pedro , ‘Review of Tyre/Road Friction Coefficient Estimation for ABS Controller’, Proceedings of the Fifth South African Conference on Computation and Applied Mechanics, pp. 432-440, Cape-Town, South Africa, January 2006

Journal papers from this work:

1. S. John and J.O. Pedro, 'Neural Network-Based Adaptive Feedback Linearization Control of Antilock Braking System', *International Journal of Artificial Intelligence* (IJAI), CESER Publications - **in press**.

2. S. John and J.O. Pedro 'Hybrid Feedback Linearization Slip Control for Antilock Braking System', *Journal of Applied Sciences, Acta Polytechnica Hungarica* Obuda University Budapest, Hungary. - **in press**

# Contents

# List of Figures

# List of Tables

# List of Symbols

### Alphabet Symbols

| | |
|---|---|
| $B$ | Viscous friction of the wheel bearings |
| $C$ | Aerodynamic drag of vehicle |
| $F_x$ | Braking or tractive force between tyre and surface |
| $F_z$ | Normal force exerted on the wheel |
| $g$ | Acceleration due to gravity |
| $I_z$ | Moment of inertia in yaw direction |
| $J$ | Rotational inertia of the wheel |
| $k_b$ | Hydraulic braking gain |
| $m$ | Mass of quarter car |
| $M$ | Mass of full car |
| $P_b$ | Hydraulic braking pressure |
| $r$ | Wheel radius |
| $T_b$ | Braking torque |
| $v_x$ | Longitudinal velocity of vehicle |

### Greek Symbols

| | |
|---|---|
| $\alpha$ | Steering angle |
| $\lambda_x$ | Longitudinal tyre slip |

| | |
|---|---|
| $\mu_x$ | Tyre/road friction coefficient |
| $\tau$ | Time constant |
| $\omega$ | Angular velocity of wheel |

**Abbreviations / Acronyms**

| | |
|---|---|
| ABS | Anti-Lock Braking Systems |
| BBW | Brake-By-Wire |
| EMB | Electro-Mechanical Brake |
| ESP | Electronic Stability Programme |
| FBL | Feedback Linearization |
| FBLPID | Feedback Linearization with Proportional Integral and Derivative |
| MF | Magic Formulae |
| MLP | Multi-layered Perceptron |
| NNFBL | Neural Network Feedback Linearization |
| NNFBLPID | Neural Network Feedback Linearization with Proportional Integral and Derivative |
| PID | Proportional Integral and Derivative |
| SMC | Sliding Mode Control |
| VSC | Vehicle Stability Control |

# 1 Introduction

## 1.1 Background

There are basically two broad safety categories in road vehicles: passive and active safety devices. The passive safety devices include seat belts and air-bags while the active safety devices include such systems like the anti-lock brake system (ABS), vehicle stability control (VSC) and active suspension system. With recent advances in auto-electronics, active safety systems are increasingly being improved. This work focuses on the active safety system namely the ABS safety device.

The operation of the ABS is briefly described as follows: during emergency braking, usually the driver suddenly applies the brakes in panic and this leads to the locking of the wheels while the vehicle's body momentum is still high, this causes the car to skid. During skidding, the driver loses the control of the steering wheel and the outcome could be disastrous. The anti-lock braking system, is a device that senses when the wheels of the vehicle are about to lock during braking and it releases the brakes so that locking does not occur. This operation results in the improving of the longitudinal stability and hence driver's control of the steering, thereby improving the driver's ability to avoid obstacles. The ABS also tries to maximise the frictional forces between the tyres and the road, consequently minimising the braking distance.

This chapter discusses the research rationale and motivation for the current work and gives the problem statement. A literature review of related works is given, covering mathematical modeling and control methods. The gaps identified lead to the development of the research objectives, scope and methodology.

## 1.2 Research Rationale and Motivation

The braking system in road vehicles has evolved from simple wooden blocks to the latest electromechanical brakes (EMB) applied in brake-by-wire (BBW) systems. Considering the contribution of the ABS to vehicle safety makes it necessary for continual review and improvement as newer and faster vehicles are developed. Furthermore, with the introduction of the electromechanical brake system, a more continuous braking operation can be achieved with a high level of accuracy. From the control viewpoint, therefore, more refinement of the ABS operation could be achieved with these improved hardware components. Anwar (2004) demonstrates the positive impact EMB systems could have on ABS performance.

A study was conducted in Australia (Burton et al., 2004) to ascertain the effectiveness of ABS in preventing vehicle occupant injury risk and injury severity. The study was based on crash data from 12 local vehicle suppliers, comparing ABS fitted vehicles to those without ABS. The findings reveal that ABS fitted vehicles reduce the rate of rear-end, head-on and pedestrian crashes. Similar studies have been conducted in the United States and the findings show similar results with those of the Australian study (Hertz, 1998, 2000; Kahane, 1994). Both studies conclude that vehicles fitted with ABS have beneficial effect in preventing most types of crashes.

Austin and Morrey (2000) claim that there have been a lot of research effort toward the development of more intelligent ABS controllers. The main reason is that conventional ABS has short-comings in new and advanced technologies. Secondly, there have been technological advances in model based design methods; for example the emergence of mechatronics design methods has made it possible to have more compact and integrated ABS controller systems, with the solenoid valve coils all located in a single printed circuit board. These new approaches lead to reduced system cost and improved performance.

## 1.3 Problem Statement

There are several control challenges which researchers must address in tackling the next generation ABS. These include, but not limited to, the following: first, noise attenuation; this problem is common with the table rule control method commonly used by the automotive industry, which introduces chattering due to the on/off nature of the solenoid valves. Second, the controller should be robust with regards to vehicle dynamics, road conditions and disturbance that might affect the control performance. Thirdly, the accuracy in slip tracking should be improved. The overall goal of the ABS is to provide ride comfort and control in an emergency braking situation by being able to shorten the braking distance and enable the driver to have control of steering.

To put the problem statement quantitatively, Solyom (2002) proposes that the ABS must track a reference trajectory for the tyre slip, while braking to achieve the following:

- No wheel-lock is allowed to occur for speeds above 4 m/s.
- Wheel-lock for a period of less than 0.2 seconds is allowed for speeds in the range 4 to 0.8 m/s.
- For speeds below 0.8 m/s - 4 m/s the wheels are allowed to lock.
- The controller should be robust with respect to other un-modelled dynamics such as the actuator dynamics and the time delay for micro-controller communication.

The overall operation to be realised by the ABS controller, is to have precise vehicle velocity estimation, good estimation of the road conditions and not too long time delay in the control system. In addition, the controller should be easy to tune.

## 1.4 Literature Review

### 1.4.1 Introduction

Review of literature is carried out to determine current knowledge in the field of research. In this section, the current commercial ABS and its control method is explained. General classifications and applicable mathematical models used in the literature is described. One of the challenges for developing a controller for the ABS is the fact that it is non-linear and hence linear control methods may not give good performance. The sources of the non-linearity in ABS are discussed. The braking actuator dynamics has an impact on the design of ABS controllers, since braking systems have been improved upon over the years, it is important to discuss this in the literature review. A brief survey of linear, non-linear and intelligent-based control methods is presented. From the literature review, gaps leading to the current research objectives are identified.

### 1.4.2 Anti-lock braking systems

The concept of the anti-lock braking system was first applied to rail-road vehicles in 1943, while its application to aircraft was in the late 1940s' to early 1950s' (Solyom, 2002). For example, the ABS was applied to the B-47 bombers to avoid tyre blow-out on dry concrete runways, and to avoid "spin-outs" on icy runways (Petersen, 2003).

Most commercially available ABS controllers are table and relay feedback based. They are designed to work with hydraulic braking systems. These early systems operated on analog computers with vacuum-actuated modulators (Petersen, 2003).

From the middle to the late 80's the Bosch ABS was introduced by Mercedes, BMW and Audi, and this was available on luxury and sport cars. About the same period, Ford motors introduced the first Teves ABS system (Petersen, 2003). With electronics in vehicles, the ABS has become a standard component on most modern vehicles (Gillespie, 1992). The current rule based controllers typically have several hundred rules to capture all braking manoeuvring (Wellstead and Pettit, 1997). The controllers are tuned in a trial-and-error method, using simulations and several field testing. The next generation vehicles will utilise brake-by-wire (electromechanical) system, which provides opportunity for up-grading current ABS. In a brake-by-wire system, the actuators supply continuous and more accurate braking pressure to the four wheels independently. This system gives the advantage of controlling tyre slip at arbitrary set points which can be used to improve the control of the vehicle.

### 1.4.3 Classification of anti-lock braking systems

There are four variants of ABS, which are based on the brake circuit configuration, vehicle drive-train configuration and functional requirements (Dietsche and Klingebiel, 2007). These variants are further differentiated according to the number of control channels and wheel speed sensors. The four variants are briefly described as follows:

- Two variants of the 4-channel 4-sensors exist, these variants allow independent control of the braking pressure on the four individual wheels by the four hydraulic channels. In one variant the split front/rear brake circuit configuration (type II) is used and in the second variant, the diagonal brake circuit configuration (type X) is used.
- In the 3-channel 3-sensors variant, a single sensor is used for both rear wheels. This sensor is fitted in the differential to measure the wheel speed differences and a single hydraulic channel is used for controlling the rear braking pressure. This variant requires a type II brake circuit configuration and can only be fitted to rear wheel drive vehicles. These include small commercial vehicles and light trucks.
- The 2-channel 3-sensors front-rare variants are been phased out due to their limited functionality. These consist of a speed sensor on the rear axle differential and a single control channel with no return pumps. These prevent the rear wheel from locking but not the front wheels, which is a disadvantage.

These variants of ABS are installed in light passenger cars as well as light to heavy trucks; however, the four-channels four-sensors variant is acclaimed to be more effective (Dietsche and Klingebiel, 2007). In the United States of America, for example, the National Highway Traffic Safety Administration (NHTSA) requires that air-braked and hydraulically braked trucks, buses and trailers be fitted with ABS (Kahane, 1994). Though much research work is based on passenger vehicles, (Petersen, 2003; Solyom, 2004; Yoo, 2006) some works focus on heavy trucks ABS applications (Jiang and Gao, 2001; Kienhofer et al., 2008).

### 1.4.4 Anti-lock braking systems mathematical models

There are three main forms of vehicle models employed by researchers in developing the ABS mathematical models: quarter-car, half-car and full-car models. These models range from two-degrees-of-freedom to eight-degrees-of-freedom models. The quarter-car model is employed by most researchers (Cao et al., 2008; Poursamad, 2009; Tanelli et al., 2006); this could be attributed to its simplicity and ease of modelling. The quarter-car model, excludes such dynamics as pitching, roll and yaw effects. If these dynamics are important and necessary for the accurate evaluation of the controller being considered, then the half-car or full-car models will be inevitable. If an active or passive suspension system is integrated with the ABS, it will be necessary to consider using a half-car or full-car model. In such situations, some authors have simplified these models by decomposing the half-car into two quarter-cars and decompose the full-car into two half-cars, based on certain symmetrical assumptions (Jun, 1998; Wang, 2001).

However, for the design of anti-lock braking systems, the essential characteristics are the longitudinal velocity of the vehicle and the rotational speed of the wheels. In this case, a two-degree-of-freedom (quarter-car) model or a three-degree-of-freedom (half-car) model will suffice.

### 1.4.5 Sources of nonlinearity in anti-lock braking systems

The braking and traction of road vehicles are greatly influenced by the frictional forces developed between the tyre and the road surface. This tyre-road friction in wheeled vehicles is a complex non-linear problem which has attracted a lot of research work in the eighties to nineties (Bakker et al., 1989; Lidner, 1993; Oosten and Bakker, 1993; Pacejka and Bakker, 1993). When the rotation of the wheel around its axle is free, partly or fully locked, three phenomena are likely to take place; these are free rolling, skidding and full locking. The available maximum acceleration / deceleration of the vehicle body is determined by the maximum friction coefficient describing the contact of the road and the wheels. For this reason the behaviour of various tyres under various environmental conditions are extensively studied (Bakker et al., 1989; Canudas-de Wit and Tsiotras, 1999; Lacombe, 2000; Lidner, 1993; Olson, 2001).

The physics involved in the modelling of the rolling phenomenon is complex. Bakker et al. (1989) in the late eighties and Zanten et al. (1990) in the early nineties concentrated on clarifying the role of the so called *"wheel slip"* parameter that is defined as the ratio of the difference of the velocity of the contact point of the tyre and that of the car body with respect to the road and this latter quantity. The *wheel slip* was found to be a critical parameter on which the available maximal friction coefficient depends. A parameter essentially identical to this wheel slip later was found to be crucial by measurements (Yagi et al., 2005). However, a practically useful model need not be so complex. The development of a practical friction model may enhance the performance of the ABS controller.

More recent investigations toward practical friction models for application in ABS have been presented by various researchers (Berzeri et al., 2004; Bian et al., 2004; Chen and Wang, 2011; Woods, 2004). As a result, various empirical mathematical friction models have been advanced in the literature (Chen and Wang, 2011; Li et al., 2006; Svendenius, 2003) for the estimation of the friction coefficient and slip values. There are, broadly speaking, static models; that are based on heuristic data and there are dynamic models, which are derived from the physical behaviour of the tyre/road surface interaction.

Bakker et al. (1989) developed an empirical formulae known as the *magic formulae* that has been shown to fit experimental data accurately, making it the desired friction model by most researchers. The equation describing the magic formulae is of the form:

$$F_x(\lambda) = D\sin\{C\arctan(B\lambda - E(B\lambda - \arctan(B\lambda)))\} \tag{1.1}$$

The coefficients B, C, D and E are curve fit parameters and are named according to their role in the equation as follows; $B$ - stiffness factor, $C$ - shape factor, $D$ - peak factor, $E$ -curvature factor, and $F(\lambda)$ is the braking force. This model is equally used to estimate the lateral tyre force and the aligning torque characteristics. Figure 1.1 presents typical plots of the magic formulae for different road conditions.

The magic formulae however, requires a number of parameters that can only be determined experimentally using sophisticated test equipment (Lacombe, 2000). Organizations with moderate testing equipment therefore, find it difficult to implement their analysis using the magic formula.

Due to some of the problems mentioned above, some researchers have proposed a number of modifications to the magic formulae. These efforts are directed toward reducing the cost of estimating the parameters, thereby making the model more experimentally affordable. However, there are other less complicated tyre friction

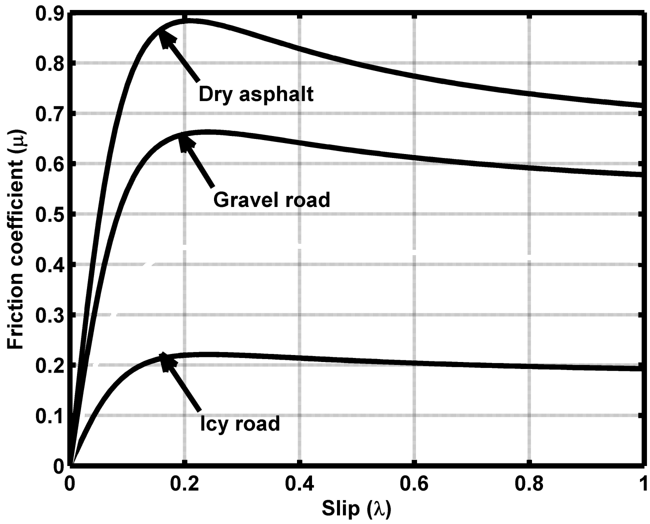


Figure 1.1: $\mu - \lambda$ Curves for different road conditions

Table 1.1: Coefficients of Burckhardt friction model

| Surface Condition | $C_1$ | $C_2$ | $C_3$ |
|---|---|---|---|
| Dry asphalt | 1.2801 | 23.99 | 0.52 |
| Wet asphalt | 0.857 | 33.822 | 0.3470 |
| Snow | 0.1946 | 94.129 | 0.0646 |
| Ice | 0.05 | 306.39 | 0 |

models in the literature (Bian et al., 2004; Canudas-de Wit and Tsiotras, 1999; Olson, 2001).

A variation of the magic formula as expressed by Burckhardt is widely used (Park and Lim, 2008; Petersen, 2003). The expression is given in Equation (1.2) and it assumes a constant vertical force ($F_z$) on the tyre.

$$\mu_x(\lambda, v) = \left[C_1(1 - e^{-C_2\lambda}) - C_3\lambda\right] e^{-C_4\lambda v} \qquad (1.2)$$

The parameters are based on the surface conditions as shown in Table 1.1

where

- $C_1$ is the maximum value of friction curve
- $C_2$ is the friction curve shape

- $C_3$ is the friction curve difference between the maximum value and the value at $\lambda = 1$
- $C_4$ is the wetness characteristics which is in the range $0.02 \leq C_4 \leq 0.04 s/m$

The Burchkhardt friction model provides a simplified model in terms of parameter estimation in comparison with the magic formulae.

The static friction models have the advantage of being simple and less expensive in implementation in comparison with the dynamic models given in the next section.

**Dynamic tyre-road friction models**

Dynamic friction models are modelled as lumped or distributed models, for example Canudas-de Wit and Tsiotras (1999) proposed a lumped model which took into consideration the Stribeck relative velocity and the tyre's stiffness and damping coefficients. The model also incorporated a non-linear estimator (observer) which estimates the changes in the road condition. One of the greatest advantages of this model is that it uses only the wheel rotational speed to estimate the $(\lambda - \mu)$ characteristic of the tyre/road interaction. Distributed dynamic models are presented as more superior in their ability to provide a more precise estimate of the $(\lambda - \mu)$ characteristic (Canudas-de Wit and Horowitz, 1999; Claeys et al., 2001).

The advantages of the dynamic friction models include the ability to be robust with respect to physical characteristics of wheels such as hysteresis and pre-sliding displacement of the tyre.

The various friction models are compared using simulation on a simple ABS model by the author (John and Pedro, 2006).

**Tyre-road friction model for current work**

With the review of the tyre-road friction models in the previous sections, this section presents the model used for the current work. First, the numerical problems associated with most friction models will be discussed. The friction models are based on the definition of slip ($\lambda$) as given by the equation:

$$\lambda = \frac{v - r\omega}{v} \tag{1.3}$$

in which $v(t) > 0$ is the velocity of the vehicle. This equation has some physical deficiency, because of the normalization with $v$ in the definition of $\lambda$ no any dependence on the *absolute value* of $|v|$ is taken into account, though the relative velocity of the skidding surfaces is determined by $v - r \cdot \omega$. The magic formulae given by Equation 1.1 which is based on this same definition, suffers from this physical deficiency (John, Pedro and Koczy, 2011; Villella, 2004). The Burckhardt's model expressed by (Equation 1.2) on the other hand contains the relative velocity of the car body to road, $v$. This formulae was evidently developed for $v > 0$ ($\lambda$ cannot even be defined for $v = 0$) and for $r \cdot \omega \in [0, v]$. Since $\omega$ and $v$ are physically independent variables, different possible $\omega/v$ ratios may occur in practice. For example the $v \to 0$ situation may happen while $\omega \neq 0$ that makes $\lambda$ indefinite. Besides this problem, it can be observed that the indefinite quantities may appear in the exponent of the approximating functions in the model. In order to eliminate these numerical difficulties, which could make the simulation unreliable, the present work has adopted a static tyre-road friction model proposed by Lin and Ting (2007) given as:

$$\mu(\lambda) = 2\mu_0 \frac{\lambda_0 \lambda}{\lambda_0^2 + \lambda^2} \tag{1.4}$$

in which $\lambda_0$ can be interpreted as the "optimal slip ratio" and $\mu_0$ denotes the available maximum of the friction coefficient. This model has the advantage that it gives good result when $\lambda \to \pm\infty$ and its sign modification can also be physically interpreted as turning from braking to accelerating phase and vice versa. However, it also has the special property that for $v - r \cdot \omega = 0$ (i.e. for rolling without skidding) it yields $\mu = 0$. Therefore, it can describe the case of locked wheels when $v = 0$.

In ABS controller design, the actuator dynamics and the wheel dynamics should be considered as a single plant (Aly et al., 2011). The actuators used in ABS will be described in the next section.

### 1.4.6 Actuators used in anti-lock braking systems

The actuator dynamics affect the performance of the ABS controller. Most production ABS largely uses conventional hydraulic brake systems.

However, with the more auto electronics in modern vehicles and the introduction of active chassis systems like the Traction Controls Systems (TCS) and Electronic Stability Program (ESP) the braking actuator has increased in complexity (Yoo, 2006). The "x-by-wire" introduced in the automotive industry, is a gradual move from mechanical components to more electronic ones. The "x" in the "x-by-wire" represents the variable safety components like steering, braking, suspension or throttle control. The aim is to provide electronic active safety assistance to the driver in emergency situations, thereby improving the over-all performance and vehicle safety (Petersen, 2003).

The brake-by-wire (BBW) is therefore a major leap in automotive braking actuators. The common design of the BBW consists of distributed electronic brake controllers, central electronic control unit, electro-mechanical disc brake actuators, brake-by-wire pedal unit and 42 *volt* electrical systems (Petersen, 2003; Solyom, 2004; Yoo, 2006). Brake-by-wire implies that there are no mechanical or hydraulic connections between the brake pedal and the brake actuators. The driver's brake command is communicated through a micro-controller to the actuator, which necessitate the use of electromechanical actuators (Petersen, 2003). The BBW system makes it possible for a shift in ABS controllers from the current acceleration / deceleration control, to a slip set-point control. Other potential advantages are (Petersen, 2003):

- Assistance functions (ABS, brake assistance (BA), ESP etc) which could be realized by software and sensors, without additional mechanical or hydraulic components.
- Easier adaptation of assistance systems due to electrical interface instead of hydraulic interfaces.
- Reduction in system weight, resulting in improved vehicle performance and cost.
- Reduced maintenance requirements.
- Intelligent error response.
- As the supervisory monitoring system will not interface with the pedal movement, the current pulsation on driver's foot in the current ABS will be eliminated.

A comparative study on the performance of the ABS using hydraulic and electromechanical brakes was conducted by Emereole (2004). His findings reveal that electromechanical brakes enhances the performance of the ABS with respect to fast and accurate effective braking torques.

### 1.4.7 Control of anti-lock braking systems

Due to the non-linearity of the anti-lock braking systems and other challenges posed by the dynamics involve, authors have proposed different control methods. The slip control is expected to operate optimally in the face of un-modeled dynamics and external disturbances. To achieve this, correct slip estimation, which is crucial in the performance of the controller is important (Aly et al., 2011). On off-roads, the slip ratio could vary rapidly due to tyre bouncing, posing additional problems that the control has to handle. Communication delay time for the micro-controller could impact on the performance of the controller.

In this section a review of major ABS control methods proposed in the literature will be reviewed.

#### Current anti-lock braking systems control methods

Most commercial ABS have a design objective of maximising the friction force between the tyres and the road surface to achieve shorter braking distance and steering wheel control (Petersen, 2003; Solyom, 2002). They are implemented using an algorithm that is based on complicated logic rules (table rules), which attempt to capture all possible operating scenarios. These rules are executed by a control computer that switches on and off solenoid valves to ensure the right pressures are delivered to the wheels while avoiding slippage (Wellstead and Pettit, 1997). The basic concept is illustrated in Figure 1.2.

It consists of an electronic control unit (ECU), speed sensors located at the four wheels and a modulator that regulates the solenoid valves. The speed sensors send speed signals to the ECU, which decides when to increase, or decrease the braking pressure at the wheels on the application of the brakes by the driver. The ECU computes the deceleration of the vehicle and compares it with the actual speed sensor to determine if the slippage is becoming excessive. If this is the case, the ECU sends signals to release the pressure on the braking pads; otherwise, it keeps the pressure. Another method is for the ECU to monitor the deceleration rate of the wheels and determine when the wheels are about to lock and then decreases the

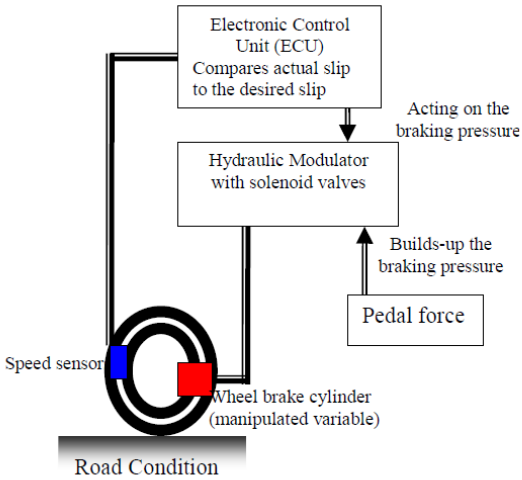


Figure 1.2: Closed loop ABS Schematic

pressure on the braking pads (Dietsche and Klingebiel, 2007) . In both cases, on the determination of a wheel lock-up point, the solenoid valves releases the pressure on the wheels momentarily thereby maximizing the friction/slip relations, by staying within the control region; the region with an optimum coefficient of friction.

### Application of PID control to ABS

Current ABS research is based on slip control. The aim of the controller is to continuously monitor the slip value ($\lambda$) and by manipulating the braking pressure $P_b$, it is possible to avoid a slip value of 100% (wheel lock) and maintain the slip at about the desired ($\lambda_d$) value, which is estimated for most road conditions to be about 20% (Chikhi et al., 2005; Xu et al., 2009). Since it is difficult to measure the slip ($\lambda$) directly, an estimator (observer) is usually employed for the estimation of ($\lambda$) using the vehicle speed ($v$) and the wheel speed ($\omega$). A block diagram illustrating this process is presented as Figure 1.3.

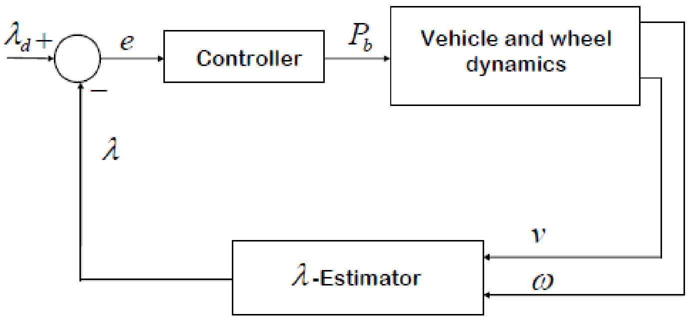


Figure 1.3: Block diagram of a typical ABS model

The proportional-integral-derivative (PID) controller has been used extensively in industrial applications and has been applied to the ABS controller (Jiang and Gao, 2001; Yoo, 2006). Solyom (2002) proposes a slip controller scheme, in which the design objective is for each wheel to follow a reference longitudinal wheel slip trajectory. A gain scheduled linear PI(D) controller was implemented for his design. Secondly, tuning the controller did not take as long as commercial ABS. However, the effects of pitching, side-slip, and the suspension dynamics were not considered in his work. Braking from an initial speed of $30m/s$ the vehicle achieved a stopping distance of between $36m$ to $41m$, which is about 15% to 20% improvement over commercially available ABS

Jiang and Gao (2001) propose a non-linear PID (NPID) for the ABS. The NPID incorporates two non-linear functions to the classical linear PID. The method of gain scheduling implemented for the NPID is the same as for the linear PID. Comparison between the two control methods revealed that the NPID has a better robustness compared with linear PID with respect to vehicle stopping distance, road conditions and tyre conditions. The NPID performance was rated to achieve a 25% improvement over the linear PID when tested on trucks. With respect to tuning, the NPID requires the tuning of five parameters and this appears to pose a challenge.

**Robust control methods**

The robust performance of a control system, is described by its ability to track a desired reference signal, belonging to a class of signals, with as little deviations as possible in the face of various classes of uncertainties (Bhattacharyya et al., 1995). The sliding mode control (SMC) is one of the proposed robust control method for ABS in the literature. The non-linearity of the ABS makes it difficult to capture all the dynamics in a mathematical model and hence, the motivation for the introduction of the sliding mode control (SMC). The SMC consists of a robust controller, an equivalent controller and a sliding surface estimator. The robust controller compensates for broad range of uncertainties while the equivalent controller tracks the desired slip. The robustness of the SMC is its main strength in ABS controller application. However, the major drawback with the SMC is the chattering caused by the non-linearity in the ABS model, which could affect the life-span of the ABS elements. According to a study by Austin and Morrey (2000), some researchers have tried to solve the chattering problem by introducing a saturation function in place of the sign function for switching control for different road conditions. The introduction of the saturation function eliminates the chattering, but introduces a steady state error (Austin and Morrey, 2000; Buckholtz, 2002).

Jing et al. (2009) proposed a moving sliding surface, based on global sliding mode control (GSMC) strategy for the slip control. In this method, unlike in the conventional SMC, the sliding surface moves to the desired sliding surface from the initial condition, thus achieving fast tracking of the desired slip. This strategy aimed at eliminating the reaching phase that causes chattering in the conventional SMC method. In addition, the radial basis neural network functions are used for the sliding mode controller. Simulation results on a quarter-car model comparing the proposed method and the conventional SMC method, indicates that the proposed method reduced the chattering.

A new SMC methodology called the grey sliding mode control method, provides robustness to partially unknown parameters and alleviates the chattering in the conventional SMC. Since its introduction in the eighties (Kayacan et al., 2009), it has been applied to various control problems (Li et al., 2008; Lu, 2004) including the ABS (Kayacan et al., 2009; Oniz et al., 2007). Kayacan et al. (2009) proposed a grey sliding mode controller for the regulation of the wheel slip on the basis of the vehicle longitudinal speed. The slip controller anticipates the slip value as a means of control input. Simulations and experimental validations were carried out using a quarter-car model on sudden changes of road conditions, to evaluate its robustness. The proposed controller achieved faster convergence and better noise attenuation than the conventional SMC. It was concluded that the GSMC, with its predictive capabilities can be a viable alternative approach when the conventional SMC cannot meet the desired performance specifications.

### 1.4.8 Control methods directly related to this work

Some of the major challenges in the implementation of ABS controllers are;

- the non-linearity associated with the mathematical model,
- the imprecise nature of the model due to un-modelled or inaccurate mathematical modelling of some of the dynamics.

The PID, SMC methods and the current on-off (*bang-bang*) commercial ABS controllers discussed in the previous sections, cannot handle these non-linearities effectively. Adaptive control method is a possible approach to explore. Some adaptive controls and hybrid methods in the literature are discussed in the following section.

### Application of feedback linearization control to ABS

The feedback linearisation control method as applied to non-linear systems is one natural method to turn to for solving the slip control problem. However, there exists minimum literature on the application of feedback linearisation control method to ABS. Park and Lim (2008) presented simulation results of a wheel slip control employing the feedback linearisation control method with an adaptive sliding mode control. The novelty of this work is the introduction of a time delay to the input. The time delay is necessary because in practice, there exists a time delay in the actuator dynamics. To compensate for the time delay, the sliding mode controller is incorporated to bound the uncertainties, using a method proposed by Shin et al. (2006). The simulation results presented did not show a significant difference between the model incorporating time delay to the model without the time delay.

A feedback linearisation controller scheme is more robust with respect to un-modelled dynamics compared to the PID and SMC methods. To get maximum benefit with respect to accurate slip tracking using PID and SMC, which is necessary for effective ABS performance, requires a comprehensive mathematical model. Further improved performance of the ABS can be achieved using intelligent control schemes; a review of these methods is presented in the following section.

### Application of intelligent control techniques

With the changes in technology, there is the need to design systems to maintain acceptable performance levels in the face of significant uncertainties. Recent approaches to this problem has been the development of control system schemes that emulate intelligent biological systems. Computational intelligent methods such as neural networks, fuzzy logic, evolutionary algorithms and machine learning have been incorporated into control systems design to ensure more robust systems. The ability of intelligent systems to adapt well even when the mathematical model is not accurate enough is a good reason for employing intelligent schemes. Due to the difficulty involved in developing a mathematical model that will capture all possible vehicle braking dynamics some researchers are turning to intelligent control methods for the development of ABS controllers (Hsu et al., 2008; Lin and Hsu, 2003; Poursamad, 2009).

An adaptive neural network-based hybrid controller for anti-lock braking systems is proposed by Poursamad (2009). The hybrid controller is based on the non-linear feedback linearization method, combined with two radial basis feedforward neural networks that are used to learn the non-linearities of the anti-lock braking system The neural network weight adaptation law used, is the steepest descent gradient approach and backpropagation algorithm. An on-line weight adaptation is used and the Lyapunov stability criterion was applied to study the stability of the proposed controller. Simulations are conducted to show the effectiveness of the proposed controller under various road conditions and parameter uncertainties. The author concluded that the proposed controller is more effective and superior than the standard feedback linearization control method. It is further concluded that the robustness of the NN-based hybrid controller to external disturbance, measurement noise and changes in initial conditions is more favourable than the standard feedback linearization control.

The fuzzy logic application to slip control has received a lot of attention. The fuzzy logic controller for example, has several advantages; it can easily adapt to complex changes in the vehicle operation condition and the non-linearity of the vehicle tyre and suspension systems which gives it a good robust performance (Yu et al., 2002).

Yu et al. (2002) developed a fuzzy logic controller with the objective of tracking an optimal slip ratio in real time, to obtain a shorter stopping distance while enhancing side slip stability. The fuzzy logic controller consisted of 25 fuzzy rules and the triangular membership functions were employed. From typical simulation results presented, the proposed controller was found robust in that it was able to adapt to changes in road conditions. It further shortens the stopping distance by 15% compared to a controller with a fixed slip ratio scheme.

In another work, Mirzaei et al. (2006) developed an optimal fuzzy controller for the ABS. The fuzzy membership functions and rules were of the Takagi-Sugeno-Kang

(TSK) type. These were optimized using genetic algorithm and an error-based optimization techniques. The objective was to maintain a desired wheel slip value, to obtain maximum traction forces on the wheels and maximum vehicle deceleration. The error-based optimization was then used to get a faster convergence of the slip. The performance of the controller was tested on a vehicle model incorporating the hydraulic dynamic and also considering the dynamic load transfer from the rear to the front axle. Simulations were conducted on alternating dry-asphalt and icy-asphalt road surface. Initial vehicle speed of $30m/s$ ($108km/h$) was used. The stopping distance was $20m$ less than the stopping distance with lock-up wheels.

In a laboratory ABS test rig, Precup et al. (2010) implemented four Takagi-Sugeno fuzzy controllers (T-S FCs), employing parallel distributed compensation (PDC) method. This method was proposed by Wang et al. (1995) for obtaining the state feedback gain matrices. Two controllers were designed to guarantee global stability while the other two controllers were designed using the linear-quadratic regulator (LQR). The main advantage of their approach is the relative simple design and low cost of implementation of the Takagi-Sugeno fuzzy controllers. The drawbacks of the method is that, only two of the four Takagi-Sugeno fuzzy controllers provide near optimum results, around an operating point. The disadvantage of this result therefore is that it would not be able to handle the so called "split-$\mu$" braking condition.

Aly (2010) presents an intelligent fuzzy controller for the ABS , with the goal of being able to handle the split-$\mu$ braking situation. In this work, the fuzzy controllers act as observers to determine the optimal wheel slip for any sudden change in surface condition, and to cause the actual wheel slip to track the reference optimal wheel slip. However this work uses the bang-bang ABS controller which has several drawbacks (see section 1.4.7)

Experiments on a prototype fuzzy ABS, performed in the early nineties (Von Altrock, 1994), show considerable improvement in performance against current ABS methods. The fuzzy controller used had six-fuzzy logic rules. This prototype ABS controller improved the performance of the commercial ABS considerably on a split-$\mu$ braking condition, that is on an alternating road conditions from snowy to wet asphalt (Von Altrock, 1994).

To complete the discussion regarding the efforts for the development of future ABS controller, it is imperative to look at some efforts towards hybrid systems.

### Review of hybrid ABS control schemes

Hybrid systems are usually defined as a combination of *continuous time* and *discrete* systems. However, in the literature, it is also referred to as a combination of two or more control methods. This latter definition is applicable in the rest of this thesis unless defined otherwise.

To compensate for the shortcomings of various ABS controller designs, hybrid controllers seem to be one of the proposed ways out. There are some proposals in the literature (Assadian, 2001; Jun, 1998; Zhang et al., 2010). By comparing the performances of four different control methods; threshold control, PID control, variable structure control and fuzzy logic control, Jun (1998) concludes that it is difficult for any single control method to provide optimal control, accuracy and robustness under all possible braking conditions.

The quest for hybrid systems has been an area of focus by few researchers, for example, Assadian (2001) investigated a mixed $H_\infty$ and fuzzy logic controller. In the study, simulations provided showed that using fuzzy logic mapping to vary the commanded slip value based on the vehicle deceleration input provides optimal results with $H_\infty$ as the main controller or regulator of the torque. In another work by Johansen et al. (2001) experimental results are presented for a gain scheduled explicit constrained LQ ABS controller and the results were compared with the conventional ABS. The authors presented only experimental results for braking on snow surface, with an optimum friction value of (0.07).

Austin and Morrey (2000) reported the development of a hybrid PID ABS controller with a sliding mode-based optimizer. The optimizer determines the optimal slip that corresponds to the maximum deceleration of the vehicle and tracks it. The tracking is done by regulating the braking torque on the wheels of the vehicle.

There is a window of opportunity for hybrid systems in the light of advances in auto-electronics, which provides more flexibility.

## 1.5 Identified Gaps in the Literature

The above review reveals the following

- The PID control method has the advantages of accuracy and ease of tuning. However, the PID control method has the problem of robustness with respect to un-modelled dynamics. The attempt by Jiang and Gao (2001) to improve on this short-coming by introducing the 'Non-linear PID' (NPID) is a step in the right direction to expanding its application to non-linear systems like the ABS. However, not much has been done in this direction to warrant proposing it as a solution to the problem of robustness. More investigation is required on NPID. The acceptance and wide use of the PID controller in industry is an advantage that cannot be overlooked.

- The sliding mode controller (SMC) is more robust compared to the PID controller, it also has the ability to track the desired slip accurately. However, two major problems have been identified with SMC; these are the introduction of chattering effect and steady-state error. Therefore the advantage of its robustness seems to have been compromised. The introduction of the grey sliding mode control (GSMC) algorithm seems to provide some solution to the inherent chattering problem of the sliding mode control.

- Among the non-intelligent controllers discussed above therefore, the feedback linearisation seems to provide a good compromise between accuracy and robustness. More investigation in the implementation of this controller scheme should therefore be pursued further.

- The intelligent control schemes discussed, revealed that their application to ABS is still very much in the simulation arena. it can be concluded that the fuzzy logic and neural network control schemes may have a lot of advantages due to their adaptation capabilities to handle un-modelled vehicle dynamics and external disturbances and hence seems to hold some solutions to most of the problems encountered with the traditional or non-intelligent ABS controller schemes. The challenges are the difficulty and cost of implementation.

- The hybrid system appears to be attractive for further investigation. Some combination already investigated like the $H_\infty$-fuzzy scheme, requires more convincing simulation results and experimental validation.

## 1.6 Research Objectives

The research objectives therefore are;

1. to design a hybrid *Feedback Linearization* (FBL) / *Proportional-Integral-Derivative* (PID) ABS controller, and a *Neural Network-Based Feedback Linearization* (NNFBL) ABS controller,
2. to implement and evaluate the performance of individual ABS controllers (FBL and PID), the hybrid (FBLPID) ABS controller and the neural network-based (NNFBL) controller schemes against their robustness and accuracy through simulations on the following specification criteria:
   (a) good tracking of the desired slip, in terms of rise time and steady-state conditions, and
   (b) nominal stability.
3. to validate the simulation results of the neural network controller, using a laboratory experimental quarter-car ABS test rig, incorporating a real-time embedded digital micro-controller.

## 1.7 Research Scope and Limitations

The scope of this research will involve the development of a mathematical model, implementation through simulation and verification of the simulation results of the proposed neural network controller, using a laboratory experimental quarter-car ABS test rig, incorporating a real-time embedded digital micro-controller.

This work is limited to laboratory test and hence, there will not be any field testing.

## 1.8 Research Strategy and Methodology

The research approach for the current work is model-based. A mathematical model must be complex enough for the specific application but should not be overly complex. The mathematical model for the deceleration of the vehicle, will be developed capturing the longitudinal braking condition with the actuator dynamics.

In model-based design, computer aided simulation is the means by which models are tested under different conditions for review and optimization. In the automotive industry this is an established procedure and practice. This work therefore employs Matlab® / Simulink® for the evaluation of the proposed ABS model. After a mathematical model has been developed, simulations under different conditions can then be conducted. Advances in numerical methods and the availability of several programming packages has made simulation possible. Figure 1.4 shows the flow-chart of the research methodology in this work.

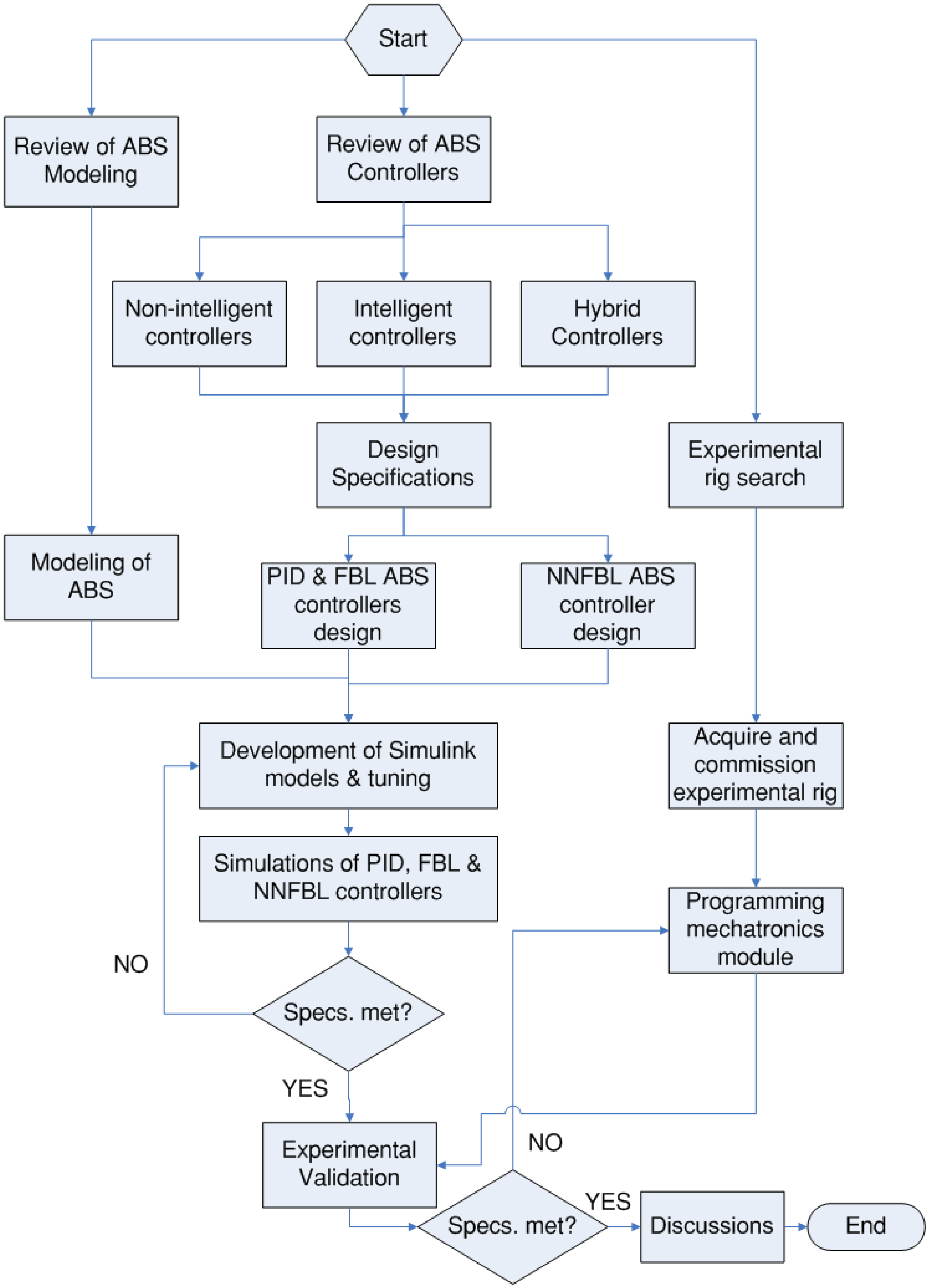


Figure 1.4: Flowchart of research scope, strategy and methodology

## 1.9 Research Contributions

The contributions of this thesis is summarised as follows:

### 1.9.1 Hybrid wheel slip controller design

A hybrid wheel slip controller is proposed, combining the advantages of a linear PID and feedback linearization non-linear control schemes.

### 1.9.2 Neural network-based feedback linearization wheel slip controller design

A new intelligent wheel slip controller is developed using neural network feedback linearisation control mode. In addition, an investigation has been conducted into new intelligent hybrid wheel slip controller using neural network feedback linearisation and PID control modes. A laboratory experimental quarter-car ABS test rig validates the proposed ABS controller simulation results. These results provide some evidence for field testing the proposed ABS controller.

### 1.9.3 Comparative analysis of ABS control modes:

This thesis investigates four ABS controller schemes: a linear controller (PID), a non-linear controller (FBL), a hybrid controller (FBLPID) and a neural network-based FBL (NNFBL) controller. These analyses have contributed to the design of ABS. Most of these contributions are in widely circulated conference proceedings. [(John and Pedro, 2011; John, Pedro and Koczy, 2011; John, Pedro and Pozna, 2011; Pedro et al., 2009)].

## 1.10 Thesis Layout

The rest of this thesis is organised as follows:

- Chapter 2 presents the physical and theoretical background for the modelling of the vehicle dynamics. This chapter presents a comprehensive modelling of the quarter-car model during straight line braking.

- In chapter 3 the controller specifications and performance criteria are defined. The design and stability analysis of the PID wheel slip controller are presented in section 3.2. The tuning process used in the current work for the selection of the PID gains is explained. The FBL controller design and stability analysis are presented in section 3.3, while the proposed wheel slip solution, which is a hybrid combination of the FBL and the PID (FBLPID) controller is presented in section 3.3.8. Section 3.4 presents the second proposed controller, which is the neural network feedback linearization (NNFBL) controller

- Chapter 4 presents the comparative study of the simulation results for the four controllers for dry asphalt, gravel and icy road conditions.

- Chapter 5 gives the experimental study of the proposed neural network ABS system and discusses the experimental results.

- Conclusions and recommendations for further studies are presented in chapter 6.

# 2 Physical and Mathematical Model of the Anti-lock Braking System

## 2.1 Introduction

The quarter-car model is extensively used in the design of slip control for ABS as discussed in Section 1.4.4 and is applied in this work. This chapter presents the physical model of the quarter-car, the modeling assumptions and analytical mathematical model of the longitudinal dynamics of the vehicle, wheel and braking dynamics.

## 2.2 Modeling Assumptions

The physical model of a quarter car is illustrated in Figure 2.1. It consists of a single wheel carrying a quarter mass $m$ of the vehicle and at any given time $t$, the vehicle is moving with a longitudinal velocity $v(t)$. Before brakes are applied, the wheel moves with an angular velocity of $\omega(t)$, driven by the mass $m$ in the direction of the longitudinal motion. Due to the friction between the tyre and the road surface, a tractive force $F_x$ is generated. As the tyre reacts to this force, it will generate a torque that will produce a rolling motion $\omega$ of the wheel. When the driver applies the braking torque, it will cause the wheel to decelerate until it comes to a stop.

The following assumptions are made in developing the quarter-car model:

- only the longitudinal dynamics of the vehicle are considered,
- the vertical and lateral motions are ignored,
- it is assumed that the vehicle is braking on a flat road,

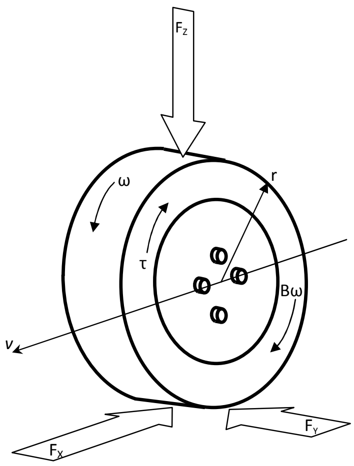


Figure 2.1: A quarter-car model

- since a quarter-car is employed, interaction between the four wheels is ignored,
- the pitching, yaw and suspension dynamics are not considered.

Though the model appears simple, it captures the essential dynamic elements of the ABS (Kayacan et al., 2009; Park and Lim, 2008).

## 2.3 Dynamic Equations of the System

The focus of the current work is the controller design and the approach adopted is by developing the longitudinal dynamics of a quarter-car. The quarter-car model has been extensively used by researchers (Oniz et al., 2007; Petersen, 2003; Precup et al., 2010; Solyom, 2002) for the development of different ABS controller schemes. This is because the quarter car model simplifies the mathematical model and provides a convenient model for the evaluation of several possible active safety systems including the ABS.

The free-body diagram of a quarter-car model is shown in Figure 2.2. It consists of a single wheel carrying a quarter mass $m$ of the vehicle. The vehicle is moving at an initial velocity $v_0$ and at an instant time $t = t_0$, the brakes are applied, and at an instant time $t = t_f$, the vehicle's longitudinal velocity comes to zero; this implies that $v(t_f) = 0$.

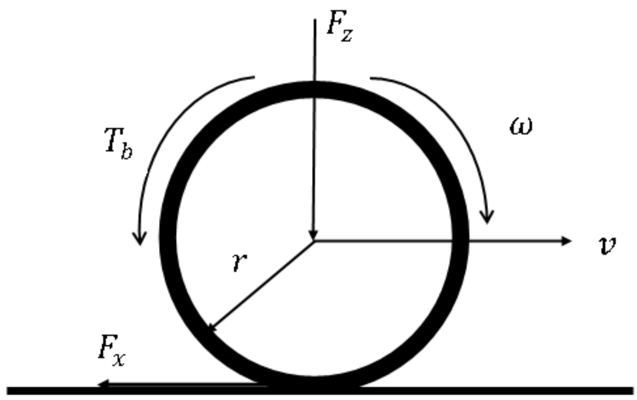


Figure 2.2: 2Dof Quarter car model

From Newton's second law of motion, the equations describing the vehicle, tyre and road interaction dynamics during braking are given by Equations 2.1 and 2.2.

$$\dot{v}_x = -\frac{1}{m}(\mu_x(\lambda_x)F_z + C{v_x}^2) \tag{2.1}$$

where $v_x$ is the longitudinal velocity of the vehicle, $C$ is the vehicle's aerodynamic friction coefficient, $\mu_x$ is the longitudinal friction coefficient between the tyre and the road surface $\lambda_x$ is the longitudinal tyre slip and $F_z$ is the normal force exerted on the wheel. Since it is assumed that the vehicle is braking on a straight line, the only forces affecting the deceleration of the vehicle will be $F_z$ and $F_x$.

The equation describing the wheel rotational dynamics is given by:

$$\dot{\omega} = \frac{1}{J}(r\mu(\lambda)F_z - B\omega - T_b(sign(\omega)) \tag{2.2}$$

where $\omega$ is the angular velocity of the wheel, $J$ is the rotational inertia of the wheel, $r$ is the radius of the tyre, $B$ is the viscous friction coefficient of the wheel bearings and $T_b$ is the effective braking torque, which is dependent on the direction of the angular velocity.

The hydraulic brake actuator dynamics is modelled as a first-order system given by:

$$\dot{T}_b = \frac{1}{\tau}(-T_b + k_b P_b) \tag{2.3}$$

where $k_b$ is the braking gain; which is a function of the brake radius, brake pad friction coefficient, brake temperature and the number of pads, $P_b$ is the braking pressure from the action of the brake pedal which is converted to torque by the gain $k_b$. The hydraulic time constant $\tau$ accounts for the brake cylinder's filling and dumping of the brake fluid (Alleyne, 1997).

The friction coefficient between the road and the tyre has influence on the braking or traction of the vehicle. The wheel slip results in the deformation and sliding of tread elements in the tyre/road patch. A simple representation of the longitudinal slip ($\lambda_x$) is given by:

$$\lambda_x = \frac{v_x - r\omega}{v_x} \tag{2.4}$$

and the lateral slip is given by:

$$\lambda_y = \frac{\omega r sin\alpha}{v} = (1 - \lambda_x) sin\alpha \tag{2.5}$$

The friction coefficient ($\mu_x$) can be expressed as: $\mu_x = F_x/F_z(\lambda, \mu_0, \alpha, v_x)$. This equation indicates that the friction coefficient is a function of the slip ($\lambda$), optimal friction coefficient ($\mu_0$) of the surface, the steering angle ($\alpha$) and the vehicle velocity ($v_x$). From now-on, $\mu_x = \mu$, $v_x = v$ and $\lambda_x = \lambda$ unless stated otherwise.

The wheel slip dynamics is obtained by taking the derivative of the longitudinal wheel slip (Equation 2.4) with respect to time, assuming that the radius of the tyre remains constant.

$$\frac{d\lambda}{dt} = \frac{\partial\lambda}{\partial v}\frac{dv}{dt} + \frac{\partial\lambda}{\partial\omega}\frac{d\omega}{dt} + \frac{\partial\lambda}{\partial r}\frac{dr}{dt} \tag{2.6}$$

$$\dot{\lambda} = \frac{\omega r}{v^2}\dot{v} - \frac{r}{v}\dot{\omega} \tag{2.7}$$

Substituting (2.1) and (2.2) into (2.7) yields the following:

$$\dot{\lambda} = -\frac{1}{v}\left(\frac{\omega r}{mv} + \frac{r^2}{J}\right) F_x + \omega r \left(\frac{B}{Jv} - \frac{C}{m}\right) + \frac{T_b r}{Jv} \tag{2.8}$$

Rearranging (2.8) and knowing that $F_x = \mu F_z(\lambda)$ yields the slip dynamics as

$$\dot{\lambda} = \omega r \left( \frac{B}{Jv} - \frac{C}{m} - \frac{\mu F_z}{mv^2} \right) + \frac{r^2 \mu F_z}{Jv} + \frac{T_b r}{Jv} \tag{2.9}$$

This can be written in the form:

$$\dot{\lambda} = (1 - \lambda) \left[ \frac{Bmv - CJv^2 - J\mu F_z}{mJv^2} \right] + \frac{r^2 \mu F_z}{Jv} + \frac{T_b r}{Jv} \tag{2.10}$$

From the slip dynamics (2.10), it can be seen that as $v \to 0$ the slip dynamics $\dot{\lambda} \to \infty$, which occurs during a wheel lock-up, and must be avoided by switching off the ABS controller at low velocities. This can be further clarified by the following proposition and its proof (Johansen et al., 2003).

**Proposition 1.** Considering the slip dynamics (Equation 2.10) and the vehicle dynamics (Equation 2.1) during braking, i.e. $T_b(t) \geq 0 \ \forall t \geq 0$; if $v(0) > 0$ and $\lambda(0) \in [0, 1]$, then $\lambda(t) \in [0, 1]$ and $\dot{v}(t) \leq 0 \ \forall t \geq 0$ where $v(t) > 0$

*Proof*: Since $v(t) > 0$ the slip $\lambda(t)$ will be a continuous trajectory. Therefore $\lambda$ can only be either $\lambda = 0$, or $\lambda = 1$. Consider the case for $\lambda = 0$; since $\mu = 0$ then from Equation (2.10) it follows that $\dot{\lambda} = \frac{r}{Jv} T_b \geq 0$ because of the fact that $T_b \geq 0$. Therefore $\lambda(0) \geq 0$ implies that $\lambda(t) \geq 0 \ \forall t \geq 0$. Next, if the case for $\lambda = 1$ is considered, it will imply $\omega = 0$ and from Equation (2.2) it follows that $\dot{\omega} \geq 0$ due to the singularity that will occur in equation (2.2). From equation (2.7) it can be seen that $\dot{\lambda} = -\frac{r\dot{\omega}}{v} \leq 0$, which implies $\lambda(t) \leq 1 \ \forall t \geq 0$. In conclusion it can be noted that $\dot{v} \leq 0$ from 2.1 due to the fact that $F_x \geq 0$ for $\lambda \in [0, 1]$.

From Equation (2.5) the lateral friction ($\mu_y$) is dependent on the side slip angle ($\alpha$). As the side slip angle increases, the longitudinal force decreases, thereby avoiding high longitudinal slip values. This process provides high steerability and lateral stability of the vehicle during braking. The trade-off between the longitudinal slip and the lateral slip is achieved when the longitudinal slip is maintained at the vicinity of its peak value (Petersen, 2003). For the current work, it will be assumed that the steering angle ($\alpha$) and hence the lateral slip ($\lambda_y$) are zero.

Furthermore from Equation (2.10) it can be seen that the longitudinal slip depends on the frictional forces between the tyres and the road condition. These frictional forces are non-linear and cannot be easily measured with sensors and hence must be estimated using observers. A comprehensive review of friction models used for the estimation of these forces is presented in Section (1.4.5) and the adopted friction model for the current work is presented by Equation (1.4), which is repeated herewith.

$$\mu(\lambda) = 2\mu_0 \frac{\lambda_0 \lambda}{\lambda_0^2 + \lambda^2} \tag{2.11}$$

### 2.3.1 State space form of the ABS equations

From Equations (2.1), (2.2) and (2.3), the state-space form of the slip dynamics is given as:

$$\begin{aligned}
&\dot{\omega} = \tfrac{1}{J}(r\mu(\lambda)F_z - B\omega - T_b(sign(\omega)) \\
&\dot{v} = -\tfrac{1}{m}(\mu(\lambda)F_z + Cv^2) \\
&\dot{T_b} = \tfrac{1}{\tau}(-T_b + k_b P_b) \\
&\lambda = \tfrac{v - r\omega}{v}
\end{aligned} \tag{2.12}$$

where the states are chosen as: $x_1 = \omega$, $x_2 = v$ and $x_3 = T_b$, the control input is $u = P_b$ which is the braking pressure and the output $y = \lambda$ is the slip. The state-space equation can therefore be presented in vector form as:

$$\begin{aligned}
\dot{\mathbf{x}} &= \mathbf{f}(\mathbf{x}, u) \\
y &= \mathbf{h}(\mathbf{x})
\end{aligned} \tag{2.13}$$

The development of the feedback linearization controller in section 3.3 is based on equation (2.13)

## 2.4 Summary

In this chapter, a mathematical model capturing the vehicle longitudinal dynamics, wheel rotational dynamics and actuator dynamics is developed. In addition, a simple and practical friction model is adopted for the current work. The next chapter presents the slip controller specifications and performance criteria for the ABS.

# 3 Wheel Slip-Based Controller Design for Anti-Lock Braking Systems

## 3.1 Design Specifications and Performance Criteria

### 3.1.1 Introduction

Advances in the automotive field like the drive-by-wire, brake-by-wire and other developments provide opportunities for the development of more efficient anti-lock braking systems, compared to the traditional table rule. With these advances, it is possible to maintain more accurate braking forces acting independently on all wheels of the vehicle. Several works have been conducted by researchers on the application of different controller methodologies in ABS design (Chen and Wang, 2011; Jing et al., 2009; Mao et al., 2010; Poursamad, 2009; Yu et al., 2002). In the current trend, the objective of the controller is to maintain a braking torque that regulates the longitudinal slip ($\lambda$ ) to an optimum slip value ($\lambda_d$ ). To ensure accuracy of performance, the controller must be robust enough to compensate for un-modelled system dynamics like the brake pads and disc, the tyre characteristics, pitching effect, yaw rate effect and external road disturbances.

This section presents the design specifications for the wheel slip control, and the performance criteria for the ABS controller. This is followed by the design of a linear PID controller and the design of a feedback linearisation controller. Problems associated with the FBL are discussed and the proposed hybrid FBLPID solution is presented. The chapter concludes with the design and analysis of the proposed neural network counterpart of the FBL controller.

### 3.1.2 Design specifications

Current work focuses on slip control, and the goal of the controller is to follow a pre-determined slip trajectory, which is the reference input to the controller. The specifications for the slip tracking are based on Liu and Luo (2006) and the Bosch Automotive Handbook (Dietsche and Klingebiel, 2007). To meet the desired research objectives (expanded from Section 1.6) therefore, the specifications are chosen as:

- desired response quality
  - rise time measured between 10% to 90% of the final slip value should not be greater than $0.25 sec$,
  - slip's maximum overshoot should not be greater than 5%,
  - the slip should settle about $\pm 2\%$, and
- stopping distance $\leq 50m$ from initial speed of $80 km/h$ ($22.23 m/s$).

The performance criteria are given in the next section.

### 3.1.3 Performance criteria

Performance criteria for controllers can be broadly described in three categories; *response quality*, *stability* and *robustness*. The robustness is based on response quality and stability of controller in the face of uncertainties like disturbances, un-modelled dynamics, and sensor noise (Cetinkunt, 2007). The response quality is assessed with respect to the transient response of the system to the input signal and the steady-state condition. The transient response is analysed with respect to system's rise time (measured between $10\% - 90\%$) and percent-overshoot of the output signal compared to the desired response of the input signal. A third measure of the transient response, is the time taken for the system to settle between a desired percentage range $\pm 2\%$ of the desired final value, referred to as the settling time. The steady-state condition is the condition of the system after sufficient time has passed. It is the measure of the deviation of the final value of the output as a percent of the input signal.

In order to evaluate the performance of the proposed controllers, three performance indices are adopted. These are: the integral squared error [ISE] of the slip

$\int_{t_0}^{t_f} (\lambda - \lambda_d)^2 dt$, the integral squared control input $\int_{t_0}^{t_f} {T_b}^2 dt$, and the stopping distance $\int_{t_0}^{t_f} vdt$ $(m)$ (Mirzaeinejad and Mirzaei, 2010). The desired performance will therefore be; small variations from the desired slip, less effective braking torque, to achieve a shorter stopping distance.

## 3.2 PID-Based Wheel Slip Control of ABS

### 3.2.1 Introduction

The *proportional integral and derivative* (PID) controller has been applied to various industrial processes. According to O'Dwyer (2009), 95% controllers in the process industry are PID controllers and in the pulp and paper industry, 98% of the controllers are made up of PI controllers. From the literature review, PID controllers have been applied in slip control by (Jiang and Gao, 2001; Wang et al., 2010; Yoo, 2006).

The PID controller has several advantages as a benchmark controller for the current work. It is a well known and accepted controller that is used to compensate most practical industrial processes, and it is easy to implement and tune. However, a major drawback of the PID is that it is poor with respect to tracking compared to non-linear controllers. To get the benefits of the PID controller, the slip curve is linearised around the optimum value (see Figure 3.2) and the PID controller is then made to regulate the braking pressure to maintain the desired slip value of $\lambda_d = 0.18$.

### 3.2.2 PID controller design

There are different structures of the PID controller, the structure chosen for the current work is the classical form given by:

$$U(s) = \left[K_p \left(\frac{T_i s + 1}{T_i s} \frac{T_d s + 1}{\Psi T_d s + 1}\right)\right] E(s) \tag{3.1}$$

where $E(s)$ and $U(s)$ are the error signal and plant input signal respectively, $K_p$

is the proportional gain, $T_d$ is the derivative time constant, $T_i$ is the integral time constant and $\Psi$ is the lag factor in the derivative component of the PID. The basic PID ABS structure of the controller is shown in Figure 3.1.

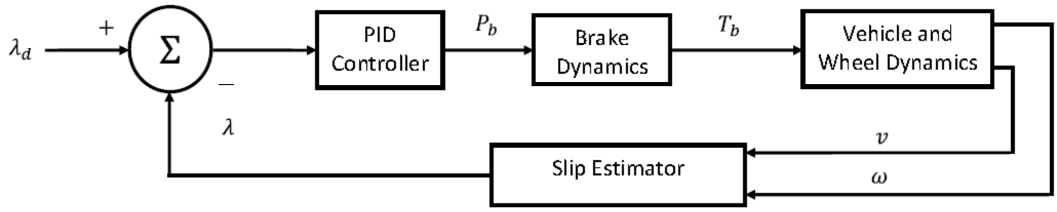


Figure 3.1: PID slip control structure

The stability of this controller is discussed next.

### 3.2.3 Stability analysis of the PID-based slip controller

This section analyses slip dynamics to understand the transient characteristic and the condition for stability. The current design strategy is to keep the wheel slip ($\lambda$) as close as possible to the optimum slip ratio ($\lambda_d$), which is the desired slip point, thereby getting the vehicle velocity to converge to zero as quickly as possible. The desired set slip ratio could be pre-determined by a higher level controller like the electronic stability programme (ESP) for example.

The non-linear friction curve is linearised around its optimum value, which is the ABS operating point (shown as the shaded portion of Figure (3.2)).

This yields an approximate friction coefficient as $\mu = m_i\lambda$; where $m_i$ is the gradient of the slope at the desired operating point (Yoo, 2006).

Substituting this into equation (2.10) and simplifying it will yield the linearised slip dynamics as follows:

$$\dot{\lambda} = \frac{r^2}{Jv}F_z(m_i\lambda) + \frac{r}{Jv}T_b \tag{3.2}$$

Equation (3.2) is a first-order system with the input variable to the model being the braking torque ($T_b$) and the output being the longitudinal slip ratio ($\lambda$). Taking the Laplace transform of (3.2) and simplifying it will give the system's transfer function

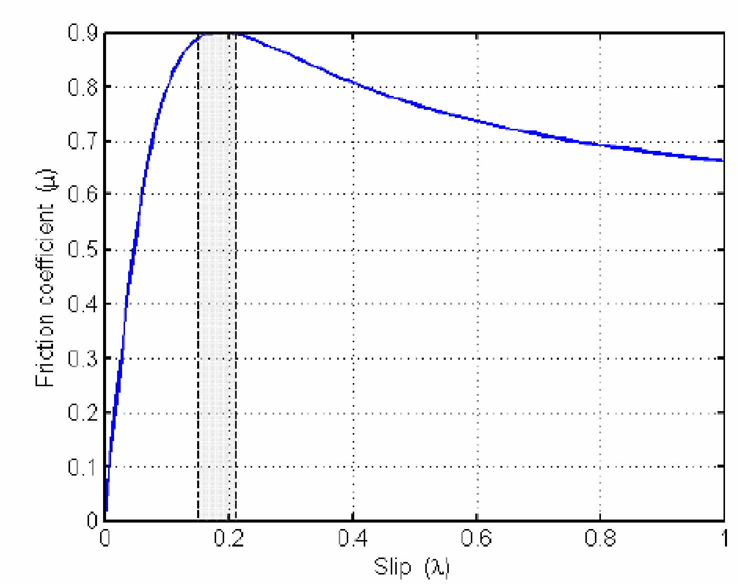


Figure 3.2: Controller operating region

as:

$$G_p(s) = \frac{\left(\frac{1}{rF_z m_i}\right)}{s\left(\frac{vJ}{r^2 F_z m_i}\right) + 1} \tag{3.3}$$

From (3.3) it can be seen that there exist a pole given by:

$$pole = -\left(\frac{r^2 F_z m_i}{Jv}\right) \tag{3.4}$$

Therefore it is clear that the stability of this system is dependent on the slope of the friction curve ($m_i$). Considering a piece-wise linear approximation around the operating point, the following analysis will then hold:

For $m_i < 0$ we will have a pole to the right side of the $s - plane$ which will give rise to an unstable situation. For $m_i > 0$ we will have a pole to the left side of the $s - plane$ which will give rise to a stable situation.

### 3.2.4 Controller simulation parameters

The process of selecting the parameters ($K_p, T_i, T_d$ and $\Psi$) of the PID controller given by equation (3.1) is called tuning. The Ziegler-Nichols method and its modified versions are frequently used in the literature (Garcia et al., 2006; O'Dwyer, 2009; Ogata, 2002). However, a numerical method is employed in the current work using

Table 3.1: PID gains

| Parameter | Gain |
|---|---|
| $K_p$ | 150 |
| $T_i$ | 0.011 |
| $T_d$ | 0.25 |
| $\Psi$ | 0.025 |

the optimization toolbox in Simulink®. In this method, the plant output, which in this case is the slip ($\lambda$) is constrained to the desired signal response according to the requirement of the design specification as stipulated in Section 3.1.2. The block diagram showing the set-up for the optimization process for the selection of the PID parameters is shown in Figure 3.3.

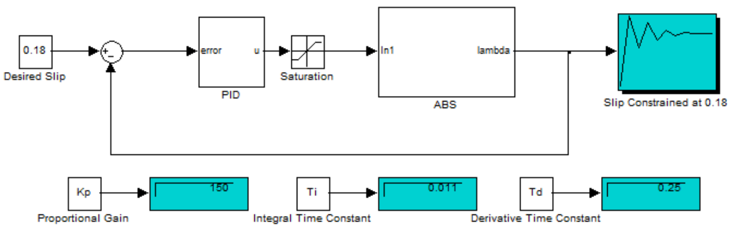


Figure 3.3: PID parameters tuning Set-up

The constraints imposed to the output slip for the tuning of the PID controller are illustrated in Figure 3.4. The gradient descent method is used, with a tolerance of 0.001 to search for the optimal gains. The iterations is limited to 100, however, the system stabilizes after 10 iterations. The gains are given in Table 3.1.

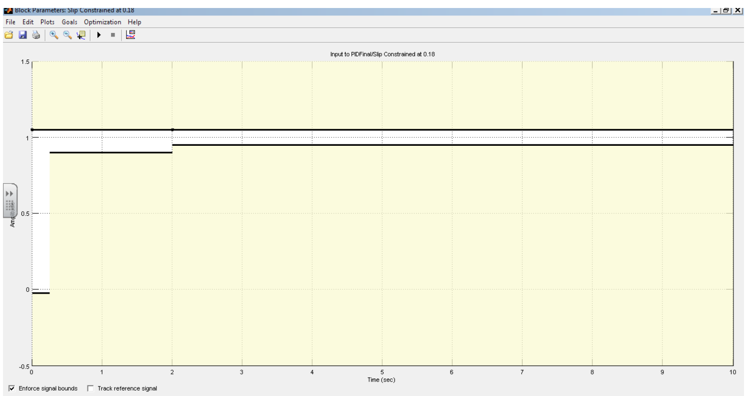

Figure 3.4: Enforced signal bounds

These controller parameters are used for simulation of the PID-based controller on different road conditions and the results are presented and discussed in Chapter 4

### 3.2.5 Summary

The structure of the PID controller used for the slip control is presented and it is shown that if the PID controller operations around the peak slip value, it remains stable. The next section presents the design of the feedback linearization ABS controller.

## 3.3 Feedback Linearization-Based Wheel Slip Control of ABS

### 3.3.1 Introduction

Feedback linearization is a control system solution for non-linear systems. It is a method that transforms non-linear models to an equivalent linear model, making it possible to apply linear control methods (Hedrick and Girard, 2005). Most approaches are based on input-output linearization or state-space linearization. In the former approach, the goal is to linearize the map between the transformed inputs and the actual outputs. The latter approach linearises the map between the transformed inputs and the transformed state variables (Henson and Seborg, 1997; Slotine and Li, 1991). Therefore, the concept of feedback linearization is to cancel the non-linearities in a non-linear system thereby making the closed loop dynamics of the system linear.

### 3.3.2 Proposed feedback linearization controller design

This section introduces the class of non-linear problems within which the slip control problem falls and presents the proposed FBL controller.

The wheel slip problem is a tracking problem; in which the output slip ($\lambda$) tracks the desired slip trajectory ($\lambda_d$) at the same time keeping the state variables bounded. Since ($\lambda_d$) and its derivatives are known, the non-linear affine system described in its general form by Equation (3.5) (Ball et al., 2005; Slotine and Li, 1991) is applied to the wheel slip control.

$$\frac{d}{dt}\begin{bmatrix} x_1 \\ x_2 \\ \vdots \\ x_{n-1} \\ x_n \end{bmatrix} = \begin{bmatrix} x_2 \\ x_3 \\ \vdots \\ x_n \\ f(\mathbf{x}) + g(\mathbf{x})u \end{bmatrix} \tag{3.5}$$

$$y = h(\mathbf{x}) \tag{3.6}$$

where $\mathbf{x} = [x_1, x_2, \ldots, x_n]^T$ and $f(\cdot), g(\cdot) : \mathbb{R}^n \to \mathbb{R}^n$ are smooth vector fields and $h(\cdot) : \mathbb{R}^n \to \mathbb{R}$, with $u(t)$ as input and $y(t)$ the output function. Applying this to the vehicle, wheel and slip dynamics yields the following:

$$\begin{aligned} \dot{x_1} &= 1/J(r\mu(\lambda)F_z - Bx_1 - u) \\ \dot{x_2} &= -1/m(\mu(\lambda)F_z + C{x_2}^2) \end{aligned} \tag{3.7}$$

$$\lambda = \frac{x_2 - rx_1}{x_2} \tag{3.8}$$

where the states are $\mathbf{x} = \begin{bmatrix} x_1 & x_2 \end{bmatrix}^T$ with $x_1$ and $x_2$ representing the wheel speed and the vehicle speed respectively, the input $u(t)$ is the braking torque ($T_b(t)$), and $\lambda(t)$ is the output function, which is the slip.

Before applying the feedback linearization method to the slip dynamics, the differential geometry notation used in subsequent sections is first introduced.

### 3.3.3 The differential geometry notation

It is essential to introduce the differential geometry notation known as the Lie derivative method, which is the notion of repeated differentiation (Nyandoro et al., 2011; Slotine and Li, 1991). This notation is subsequently used in the rest of the analysis.

If $h(\mathbf{x})$ is a scalar function and $\mathbf{f}(\mathbf{x})$ is a vector field, a new scalar function called the Lie derivative is defined as $L_{\mathbf{f}}h$. This means the derivative of $h$ with respect to $\mathbf{f}$. The following definition can then be introduced (Slotine and Li, 1991):

**Definition 1.** Let $h : \mathbf{R}^n \to \mathbf{R}$ be a smooth scalar function, and $\mathbf{f} : \mathbf{R}^n \to \mathbf{R}^n$ be a smooth vector field on $\mathbf{R}^n$, then the Lie derivative of $h$ with respect to $\mathbf{f}$ is a scalar function defined by $L_{\mathbf{f}}h = \nabla h\mathbf{f}$.

This means that $L_{\mathbf{f}}h$ is the directional derivative of $h$ along the direction of the vector $\mathbf{f}$; where $\nabla h = \frac{\partial h}{\partial \mathbf{x}}$ is the gradient of $h$. The following are therefore defined:

$$\begin{aligned} &L_{\mathbf{f}}^0 h = h \\ &L_{\mathbf{f}}^i h = L_{\mathbf{f}}(L_{\mathbf{f}}^{i-1}h) = \nabla(L_{\mathbf{f}}^{i-1}h)\mathbf{f} \\ &\textbf{for} \quad i = 1, 2 \ldots \end{aligned} \tag{3.9}$$

Similarly if $\mathbf{g}$ is another vector, then the scalar function $L_{\mathbf{g}}L_{\mathbf{f}}h(\mathbf{x})$ is

$$L_{\mathbf{g}}L_{\mathbf{f}}h = \nabla(L_{\mathbf{f}}h)\mathbf{g} \tag{3.10}$$

The benefit of this notation is shown with the following single-output system,

$$\begin{aligned} \dot{\mathbf{x}} &= \mathbf{f}(\mathbf{x}) \\ y &= h(\mathbf{x}) \end{aligned} \tag{3.11}$$

where the repeated derivatives can be derived for the output $y$ as:

$$\begin{aligned} \dot{y} &= \tfrac{\partial h}{\partial \mathbf{x}}\dot{\mathbf{x}} = L_{\mathbf{f}}h \\ \ddot{y} &= \tfrac{\partial [L_{\mathbf{f}}h]}{\partial \mathbf{x}}\dot{\mathbf{x}} = L_{\mathbf{f}}^2 h \end{aligned} \tag{3.12}$$

The Lie derivative method is applied in the FBL controller design and stability analysis, which follows.

### 3.3.4 Input-output feedback linearization ABS controller design

In the input-output linearization method, the output ($y$) is differentiated $r$ times to generate an explicit relationship between the output and the input. For any controllable system of order $n$, it will require at most $n$ differentiations of the output for the control input to appear. This implies that $r \leq n$, where $r$ is referred to as the *relative degree* of the system. If the control input never appears, the system is uncontrollable or undefined. If on the other hand $r < n$ there will exist *internal dynamics*, which cannot be seen from the external input-output relationship. Depending on whether the internal dynamics are stable or unstable, further transformation of the states and analysis is required. The internal dynamics are usually difficult to analyse and hence the *zero dynamics* are often times analysed instead (Hedrick and Girard, 2005; Slotine and Li, 1991).

For a well-defined system (i.e. $r \leq n$), a controller is designed to cancel the nonlinearity. For an undefined or uncontrollable system, it is not possible to linearise the system. The current work is based on a well-defined relative degree as shown next.

Considering the tracking problem of the desired slip trajectory of a wheel slip control, applying the Lie derivative method to the output function, (Equation (3.8) within the ABS operating region $\Omega_x$ in the state-space yields:

$$\dot{\lambda} = \nabla h(\mathbf{f} + \mathbf{gu}) = L_{\mathbf{f}}h(\mathbf{x}) + L_{\mathbf{g}}h(\mathbf{x})u \tag{3.13}$$

where $L_{\mathbf{f}}h(\mathbf{x}) = x_1 r\left(\frac{B}{Jx_2} - \frac{C}{m} - \frac{\mu F_z}{m{x_2}^2}\right) + \frac{r^2 \mu F_z}{Jx_2}$

and $L_{\mathbf{g}}h(\mathbf{x})u = \frac{r}{Jx_2}T_b$.

This means that the relative degree of the system is 1, because the output function is differentiated once to realise the input ($T_b$). The ABS operating region considered is for speeds $x_2(0) \leq x_2 \leq x_2(min)$, where $x_2(0)$ is vehicle initial speed before braking and $x_2(min)$ is defined to be $\leq 4km/h$ in the problem statement (Section 1.3) therefore $L_{\mathbf{g}}h(\mathbf{x}) \neq 0 \; \forall t > t_0$. And by continuity in this operating region, the input transformation is given by:

$$u = \frac{1}{L_{\mathbf{g}}h(\mathbf{x})}\left(\nu - L_{\mathbf{f}}h(\mathbf{x})\right) \tag{3.14}$$

where $\nu$ is a virtual input. Substituting (3.14) into (3.13) will yield a linear relation between the output $\lambda$ and the new input $\nu$ given as:

$$\dot{\lambda} = \nu \tag{3.15}$$

The next step is to check for any *internal dynamics* of the system.

### 3.3.5 Internal dynamics

Asymptotic stability of the zero dynamics is a necessary condition for nominal closed-loop stability Henson and Seborg (1997), however, there exist a special case in which $r = n$; this spacial case yields input-output linearization and input-state linearization simultaneously, in the operating region $\Omega_x$. This is stated in Lemma 1 (Slotine and Li, 1991):

**Lemma 1.** *An $n^{th}$ order non-linear system is input-state linearizable if, and only if, there exist a scalar function $\mathcal{Z}_1(\mathbf{x})$ such that the system's input-out linearization with $\mathcal{Z}_1(\mathbf{x})$ as output function has a relative degree $n$*

Since the wheel slip dynamics fulfil the condition of Lemma 1, the current system does not have internal dynamics, and it is not necessary to analyse the zero-dynamics. In addition, the internal dynamics is also coupled to the *external* closed-loop dynamics and hence if a Lyapunov function is found for the system, its analysis provides the solution (Slotine and Li, 1991). In the next section, the external dynamics are analysed for the stability of the system.

### 3.3.6 Stability analysis

The wheel slip control is an output tracking problem. The objective is to find a control action $u(t)$, that will ensure the plant follows the desired slip trajectory within acceptable boundaries, keeping all the states variables and controls bounded. On this basis some assumptions are made as follow (Yeşildirek and Lewis, 2001):

**Assumption 1.** *The vehicle velocity $v$ and wheel speed $\omega$ are measurable or observable.*

**Assumption 2.** *The desired trajectory vector defined within a compact subset of $\mathbb{R}^{\varrho}$, i.e. $\lambda_d(t) \in U_d$, is assumed to be continuous, available for measurement, and $\|\lambda_d(t)\| \leq \Omega_x$ with $\Omega_x$ as a known bound.*

Let the tracking error $(e)$ be given as:

$$e = \lambda(t) - \lambda_d(t) \tag{3.16}$$

and let the new input be chosen as:

$$\nu = \dot{\lambda}_d - \kappa e \tag{3.17}$$

where $\kappa$ is a positive constant. From (3.15) and (3.14) the closed loop tracking error dynamics will be:

$$\dot{e} + \kappa e = 0 \tag{3.18}$$

If the new input is defined as:

$$\nu = \kappa_v r + \Lambda_1 e^{n-1} + \cdots + \Lambda_{n-1} e + \cdots + \dot{x}_{nd} \tag{3.19}$$

where $r$ is the filtered error given by:

$$r = \frac{d^{n-1}e}{dt^{n-1}} + \Lambda_1 \frac{d^{n-2}e}{dt^{n-2}} + \cdots + \Lambda_{n-1} e \tag{3.20}$$

where the design parameters $\kappa_v$ and $\Lambda s$ are chosen heuristically (Behera and Kar, 2009). The derivative of $r$ will therefore be given by:

$$\dot{r} = -\kappa_v r \tag{3.21}$$

Considering the following Lyapunov function:

$$V = \frac{1}{2} r^2 \tag{3.22}$$

The derivative of (3.22) will yield:

$$\dot{V} = r = \frac{d^{n-1}e}{dt^{n-1}} + \Lambda_1 \frac{d^{n-2}e}{dt^{n-2}} + \cdots + \Lambda_{n-1} e \tag{3.23}$$

It can be seen that $e \to 0$ exponentially as $r \to 0$ over time, while the design parameters $\Lambda_1 \ldots \Lambda_{n-1}$ are chosen so that the system is stable. For example, if before braking $e(0) = \dot{e}(0) = 0$, then $e(t) \equiv 0 \ \forall t \geq 0$; this signifies perfect tracking of the slip.

### 3.3.7 Wheel slip controller

The structure of the input-output feedback linearization controller for the ABS is shown in Figure 3.5, where the indicated linear controller is essentially *pole placement.*

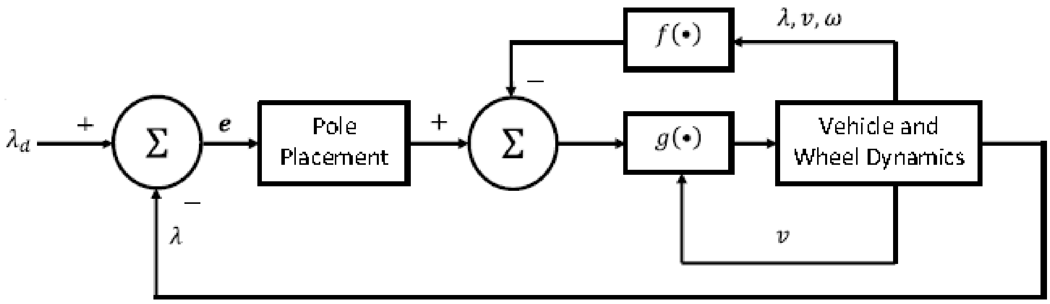


Figure 3.5: Feedback linearization slip controller structure

The input transformation (Equation 3.14) which is the actual control input $u$, indicates that the whole system is considered to be stable within the operating region. This is shown by the stability analysis (Section 3.3.6) and confirmed by the following theorem Slotine and Li (1991).

**Theorem 1.** *Assume that the system (3.5, 3.6) has relative degree $r$ and that its zero dynamics is locally asymptotically stable. Choose constants $\Lambda_i$ such that the polynomial 3.20 has all its roots strictly in the left-half plane. Then the control law (3.14) yields a locally asymptotically stable closed-loop system.*

The current work proposes a hybrid system that combines the PID and the FBL (FBLPID) controllers and this is presented in the next section.

### 3.3.8 Proposed hybrid FBL / PID controller design

There exist some hybrid systems with some promising outcomes (Section 1.4.8). Hybrid systems aimed at combining the advantages of two or more controllers to achieve better performance of the control robustness and accuracy. In this section a hybrid FBL and PID (FBLPID) controller system combination is introduced.

The FBLPID hybrid solution for the ABS takes advantage of the FBL approach, in which a non-linear system is transformed into a linear system (Hedrick and Girard,

Table 3.2: PID gains for hybrid system

| Parameter | Gain |
|---|---|
| $K_p$ | 1487 |
| $T_i$ | 0.1255 |
| $T_d$ | 0.25 |
| $\Psi$ | 0.025 |

2005; Henson and Seborg, 1997). This provides the opportunity and possibility to apply a linear PID controller in cascade with the FBL, instead of the traditional pole placement controller. A problem identified with the FBL method incorporating pole placement approach for the ABS, is that it inherently chatters (see Figures 4.10, 4.22 and 4.34). The linear controller realised from the input-output feedback linearization scheme contains *proportional* and *derivative* terms of the error signal. The proposed scheme therefore, added the *integral* term to reduce the chattering. The arrangement of the proposed hybrid system is shown in Figure 3.6.

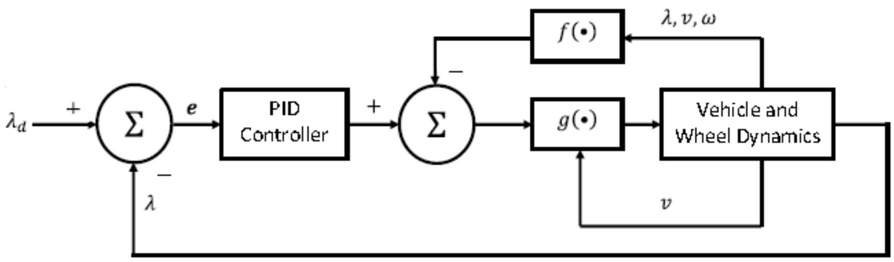


Figure 3.6: Hybrid FBLPID slip controller structure

The structure of the PID controller for the hybrid system is given by:

$$U(s) = \left[K_p \left(\frac{T_i s + 1}{T_i s} \frac{T_d s + 1}{\Psi T_d s + 1}\right)\right] E(s) \tag{3.24}$$

### 3.3.9 Controller simulation parameters

The Simulink® optimization toolbox using a gradient descent method is used to choose the gains for the PID controller. The gains are presented in Table 3.2. The outcome of this combination is tested in Chapter 4.

The hybrid system could be viewed as a PID controller with some disturbance, hence its stability is ensured (Zhang et al., 2010). Moreover, the stability of the FBL transformation is proven in Section 3.3.6.

### 3.3.10 Summary

Section 3.3.2 established the motivation for the application of the input-output feedback linearization solution to the ABS, which is mainly its good tracking ability. The ABS problem has been shown to fall within a special case of the input-output linearization, in which the relative degree is same with the order of the system. This case guarantees that there are no internal dynamics, and the input-output linearisation leads to input-state linearization simultaneously. This situation provides solutions for both state regulation and output tracking. The external dynamics were checked for stability in the Lyapunov sense.

Traditionally, the *pole placement* method is applied to the linearised model generated from the FBL method. The pole placement which is compared to a proportional controller, can handle only the current error component. The current work therefore proposes to also correct the previous error with the use of an integrator and to anticipate and minimise future errors by the use of the derivative component. This leads to the employment of the PID controller in place of the pole placement controller. This work therefore proposes that the realization and utilization of the fact that linear equations obtained by the technique of Feedback Linearization are not necessarily treated by the pole placement method that is quite common in linear control practice but causes inconvenient chattering in this case. The replacement of the pole placement with the much finer PID controller is able to solve the phenomenon of chattering, while the controller follows a predefined slip value with good and reliable tyre-road friction conditions which guaranteed good braking properties.

The accuracy of the FBL and FBLPID controllers depend on the accuracy of the model. The parameters of the system may be perturbed or unknown, the nonlinearities of the developed controller (3.14) may not be measured precisely leading to errors in performance. To ensure the robustness of the controller, a *neural network-based feedback linearization* controller is proposed as a second solution. This is discussed in the next section.

## 3.4 Neural Network Based Feedback Linearization Slip Control of ABS

### 3.4.1 Introduction

In Sections 3.2 and 3.3 two types of controller solutions are developed; PID, which is a linear controller and feedback linearization, a non-linear controller. Section 3.3.8 discusses the realization of a propose hybrid system of these two controllers. This section presents the proposed neural network-based feedback linearization (NNFBL) slip control, also referred to in literature as the *Non-linear Autoregressive-Moving Average* abbreviated as NARMA-L2 (Adaryani and Afrakhte, 2011; Awwad et al., 2008; Norgaard et al., 2003).

The motivation for the neural network approach to the slip control design, is based on the fact that there is high uncertainty associated with the estimation of the slip ($\lambda$). This is further compounded with the possible sudden changes in road conditions. In the feedback linearization control scheme, it is assumed that all state variables are measurable and/or observable. However, some parameters of the system may be perturbed. In addition, it is difficult to capture all vehicle dynamics in a mathematical model. NNFBL has been employed by researchers, to handle similar non-linear control problems (Pukrittayakamee et al., 2002; Srakaew et al., 2011; Wahyudi et al., 2008).

### 3.4.2 Class of non-linear systems

The class of non-linear systems within which the slip control problem is defined, is the single-input single-output (SISO) affine systems. Recalling the canonical form of this system given by Equation (3.25):

$$\begin{aligned} \dot{\mathbf{x}} &= f(\mathbf{x}) + g(\mathbf{x})u(t) \\ y(t) &= h(\mathbf{x}) \end{aligned} \tag{3.25}$$

with $\mathbf{x} = [x_1 x_2 \ldots x_n]^T \in \mathbb{R}^n$ the state vector, and $f(\cdot), g(\cdot) : \mathbb{R}^n \to \mathbb{R}^n$ are smooth functions, $h(\cdot) : \mathbb{R}^n \to \mathbb{R}$ smooth function, the output is $y(t)$ and the input is $u(t)$ and let $y(t), u(t) \in \mathbb{R}$.

The wheel slip tracking problem is to find a control action $u(t)$, that will ensure that the plant follows the desired slip trajectory within acceptable boundaries, keeping all the state variables and controls bounded (Yeşildirek and Lewis, 2001).

The PID, FBL and the FBLPID controllers developed for the ABS as described in Sections 3.2 and 3.3 are model-based. In these methods, it is assumed that all parameters of the model are known or observable. However, some of these parameters could be perturbed, and the model may not be able to handle both internal and external disturbances. Secondly, the functions $f(\cdot)$, $g(\cdot)$ and $h(\cdot)$ may be either partially known or completely unknown (Behera and Kar, 2009; Yeşildirek and Lewis, 2001). In the case of any unknown function, neural networks could be employed to estimate the unknown function or functions. The controller parameters are therefore up-dated to achieve convergence of the error to zero, by the selection of an appropriate learning algorithm. In the current work it is assumed that both functions $f(\cdot)$ and $g(\cdot)$ are unknown. This assumption is necessary for the sake of comparison between the standard feedback linearization solution to its neural network counterpart.

Following this assumption therefore, an indirect adaptive control method, using neural networks feedback linearization (NNFBL) model is chosen to estimate the ABS model. The NNFBL is based on input-output feedback linearization, and it has fast and accurate mapping capability (Akbarimajd and Kia, 2010). Two steps are involved in the indirect adaptive controller design, using neural networks: system identification, and controller design which are presented in Section 3.4.3. The simulation results are presented, discussed and compared with the performances of the PID, FBL and FBLPID slip controllers in Chapter 4. This section, ends with a summary.

### 3.4.3 System identification and controller design

The *system identification* process involves collecting a set of training data through experiments. This is achieved through varying inputs to the system and observing the behaviour on the outputs. A set of corresponding inputs and outputs data is then used to train the neural network to estimate the system's dynamics.

To illustrate the advantage of using NNFBL: if the nominal condition for the non-linear functions $f(\cdot)$ and $g(\cdot)$ are known, then it will be necessary to separate the known from the unknown portions of the dynamics. If for example the nominal dynamics are represented by Equation (3.26)

$$\dot{\lambda} = \mathbf{f}(\mathbf{x}) + \mathbf{g}(\mathbf{x})\mathbf{u} \tag{3.26}$$

where $\mathbf{f}(\mathbf{x})$ and $\mathbf{g}(\mathbf{x})$ are the nominal parameters.

Taking into account the deviations from the nominal condition and the noise in the measured parameters, the slip dynamics becomes:

$$\dot{\lambda} = [\mathbf{f}(\mathbf{x}) + \Delta\mathbf{f}(\mathbf{x})] + [\mathbf{g}(\mathbf{x}) + \Delta\mathbf{g}(\mathbf{x})]\,[\mathbf{u} + n(t)] \tag{3.27}$$

where the uncertainties are represented by $\Delta\mathbf{f}(\mathbf{x})$ and $\Delta\mathbf{g}(\mathbf{x})$ while $n(t)$ is the noise in the measured parameters. Therefore, the robustness of the chosen linear controller for the standard feedback linearization in Section (3.3.4) cannot be guaranteed, due to uncertainties. Therefore, to ensure the robustness of the controller, a neural network model is employed and trained to estimate the non-linear system and due to its adaptation capability, it will behave well under varying conditions. Neural networks have been shown to approximate arbitrary non-linear functions quite well (Hsu et al., 2008; Lin and Hsu, 2003; Poursamad, 2009; Yeşildirek and Lewis, 2001) .

The system identification procedure is illustrated in Figure 3.7, where $\lambda_f$ is the reference slip input to both the ABS system and the neural network model, $\lambda_p$ and $\lambda_m$ are the ABS system's and NN model's slip outputs respectively. The error signal is used for the training of the NN model to estimate the ABS system.

The steps involved in the system identification are as follows:

- Experimentation
- Model structure selection.
- Model estimation.
- Model validation

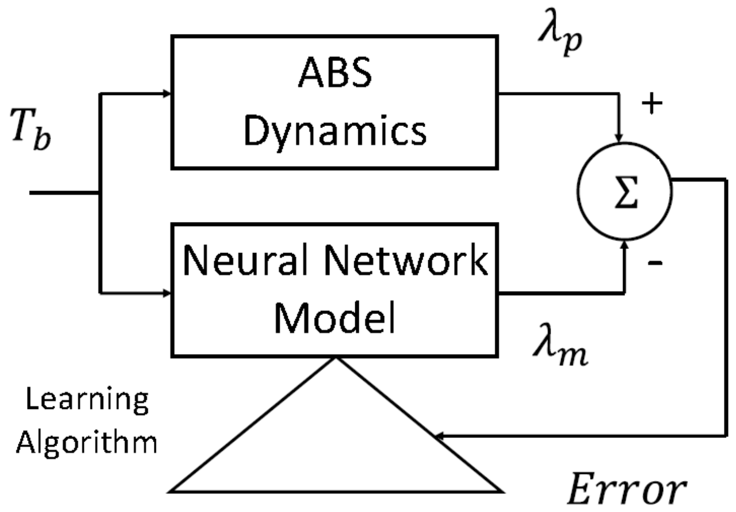


Figure 3.7: System identification of ABS dynamics for NNFBL control

**Experimentation**

In the experimental stage, a set of input/output data is collected through experiments with the ABS model. It is important that the collected data covers the entire operating range of the ABS. To ensure that every dynamic of the plant is captured, the sampling time had to be smaller than the fastest dynamic.

The Simulink® experimental model used for data collection is shown in Figure 3.8.

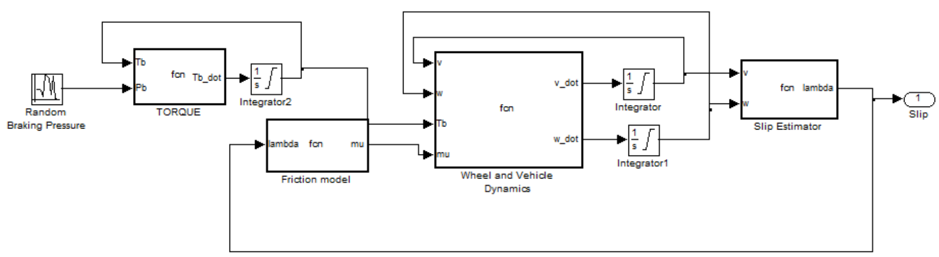


Figure 3.8: ABS Simulink® model for NNFBL system identification

The data set ${Z_i}^n$ collected can be presented by Equation 3.28.

$$ {Z_i}^n = f\{[u_i(k), y_i(k)]\,; k = 1, 2 \ldots, N\} \tag{3.28} $$

where $u_i(k)$ is the input to the system, which is the braking pressure ($P_b$) and $y_i(k)$ the corresponding slip ($\lambda$) output. $k$ is the number of the sample instant and the total number of samples taken is $n$ (Pedro et al., 2009). A total of 25000 samples were collected at a sampling rate of $T_s = 0.0001 sec$. The breaking pressure is a random input with a maximum value of $1500 N/m^2$ and a minimum value of 0. The output slip value is limited to a maximum value of 0.18 and a minimum value of 0.

### Model structure selection

The slip dynamics as developed in Section 2.3 is given by the equation:

$$\dot{\lambda} = x_1 r \left( \frac{B}{J x_2} - \frac{C}{m} - \frac{\mu F_z}{m {x_2}^2} \right) + \frac{r^2 \mu F_z}{J x_2} + \frac{r}{J x_2} T_b \tag{3.29}$$

This can be represented in the vector form as:

$$\dot{\lambda} = \mathbf{f}(\mathbf{x}) + \mathbf{g}(\mathbf{x})\mathbf{u} \tag{3.30}$$

where $\mathbf{f}(\mathbf{x}) = x_1 r \left( \frac{B}{J x_2} - \frac{C}{m} - \frac{\mu F_z}{m {x_2}^2} \right) + \frac{r^2 \mu F_z}{J x_2}$, $\mathbf{g}(\mathbf{x}) = \frac{r}{J x_2}$ and the output $\mathbf{u} = T_b$

The structure of the NN model to be selected, should be able to estimate the functions $f(\cdot)$ and $g(\cdot)$. Therefore the *Non-linear Autoregressive-Moving Average* model is selected for this work, which is presented in its discrete form as (Akbarimajd and Kia, 2010; Pedro et al., 2009):

$$\begin{aligned} y(k+d) \quad = \quad & F[y(k), y(k-1), \ldots, y(k-na+1), \\ & u(k), u(k-1), \ldots, u(k-nb+1)] \end{aligned} \tag{3.31}$$

where $F(\cdot)$ is a non-linear function, $na$ is the number of past outputs, $nb$ is the number of past inputs, and $d$ is the system delay. The network is trained during identification to approximate the non-linear function $F(\cdot)$. By Taylor expansion of $F(\cdot)$, Equation(3.31) becomes (Akbarimajd and Kia, 2010):

$$
\begin{aligned}
y(k+d) \quad = \quad & f[y(k), y(k-1), \ldots, y(k-na+1), \\
& u(k-1), \ldots, u(k-nb+1)] \\
& +g[y(k), y(k-1), \ldots, y(k-na+1), \\
& u(k-1), \ldots, u(k-nb+1)] \cdot u(k)
\end{aligned}
\tag{3.32}
$$

Equation 3.32 has elements similar to the ABS system dynamics presented in Equation (3.30). NNFBL operates on the same principles like the standard FBL, in which the goal is to cancel the non-linearity in the system to generate a linear system. This is achieved by training two *Multi-layered perceptron* (MLP) neural networks to approximate the non-linear functions $f(\cdot)$ and $g(\cdot)$ as:

$$
\begin{aligned}
\hat{y}(k+d) \quad = \quad & \hat{f}[y(k), y(k-1), \ldots, y(k-na+1), \\
& u(k-1), \ldots, u(k-nb+1)] \\
& +\hat{g}[y(k), y(k-1), \ldots, y(k-na+1), \\
& u(k-1), \ldots, u(k-nb+1)] \cdot u(k)
\end{aligned}
\tag{3.33}
$$

where $\hat{f}(\cdot)$ and $\hat{g}(\cdot)$ are used as approximates for the $f(\cdot)$ and $g(\cdot)$ non-linear functions. The controller design is then to have the system output to follow a reference trajectory, which is based on Equation (3.32).

$$
u(k) = \frac{y_r(k+d) - \hat{f}[y(k), \ldots, y(k-n+1), u(k-1), \ldots, u(k-n+1)]}{\hat{g}[y(k), \ldots, y(k-n+1), u(k-1), \ldots, u(k-n+1)]} \tag{3.34}
$$

However, the control law given by Equation (3.34) is not feasible, because to compute $u(k)$ , $y(k)$ is required. Therefore if the plant delay is chosen to be $d \geq 2$ with model order of $n = na = nb = 2$, the following practical NNFBL control law will be realised (Akbarimajd and Kia, 2010; Norgaard, 2000):

$$
u(k) = \frac{y_r(k+d) - \hat{f}[y(k), \ldots, y(k-n+1), u(k), \ldots, u(k-n+1)]}{\hat{g}[y(k), \ldots, y(k-n+1), u(k), \ldots, u(k-n+1)]} \tag{3.35}
$$

A brief description of the MLP neural network is presented in Section 3.4.4.

### 3.4.4 Model estimation

#### Multi-layered perceptron neural networks

The process of training the neural network to estimate the system dynamics using the experimental data is referred to as model estimation. A brief background of neural networks is presented.

Neural networks (NN) are classified as distributive or adaptive or in general non-linear learning machines. The network is made-up of processing elements known as neurons. A single neuron can be represented as shown in Figure 3.9, it consists of the input $x$, which is multiplied by the scalar weight $w$ to give the product $wx$, which is a scalar. Then the weighted input $wx$ is added to the bias $b$ to form the net input $n$. The bias is like a weight, except that it has a constant input of 1. Finally, the net input is passed through the transfer function $f$, which produces the output $y$. The number of neurons and their interconnectivity defines the structure or the architecture of the network. These neural networks, which are inspired by the behaviour of biological neurons, have the ability to approximate arbitrary non-linear functions (Garces et al., 2003). For this reason, they are regarded as possessing *artificial intelligence*. The neural networks can be further classified as static and dynamics networks. The static networks are described by an algebraic equation while the dynamic networks are represented by differential equations in continuous time domain, and by difference equation in the discrete time domain (Garces et al., 2003).

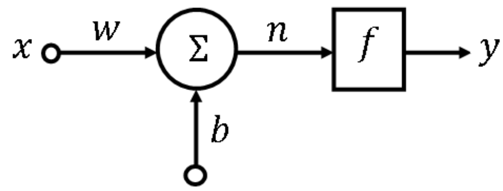


Figure 3.9: Structure of a single neuron with a bias

The MLP network is the most used neural network, and is known to be good at learning (training) non-linear dynamic systems (Norgaard et al., 2003). According to Hagan et al. (2002) and Hornik et al. (1989), a two-layer network with sigmoid transfer function in the hidden layer and linear transfer function in the output layer can be regarded as a universal function approximator . They are also known for their robustness, and the availability of fast training algorithms. In addition, the MLP responses fast in re-call mode, as it does not have to carryout any further iterations (Bruckner and Rudolph, 2000; Norgaard et al., 2003).

A schematic representation of a typical MLP with three layers neural network, made-up of an input layer an output layer and one hidden layer is shown in Figure 3.10.

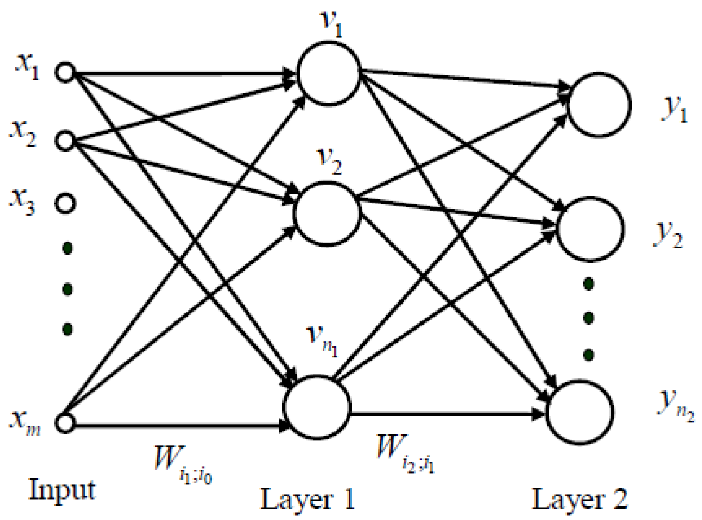


Figure 3.10: Two-layered neural network structure

Through the process of *training*, the adjustable weights are determined from a set of *training data* collected during the *experimentation* stage. Using the MLP shown in Figure 3.10, the predicted output is given by:

$$\hat{y}(t,\theta) = V_i \left[ \sum_{j=1}^{q} W_{ij} h_j(\mathbf{w}) + W_{i0} \right] \tag{3.36}$$

If the training set is given by:

$$\mathcal{Z}^N = \{[u(t), y(t)] | t = 1, \ldots, N\} \tag{3.37}$$

the goal is to determine a mapping from the training data set to possible weights, i.e. $Z^N \rightarrow \hat{\theta}$ so that the network predicts $\hat{y}(t)$ as close as possible to the system's output $y(t)$. The prediction error is based on the mean square error criterion (MSE). The *sigmoid* activation function $v_i$ is used in the hidden layer, and is given by Equation 3.38.

$$v_{i_2} = \frac{1}{1 + e^{-h_{i_1}}} \tag{3.38}$$

where $h_{i_1}$ is given by:

$$h_{i_1} = \sum_{i_1=0}^{m} W_{i_1 i_0} x_{i_0} \tag{3.39}$$

The back-propagation (BP) algorithm is employed to adjust the neural networks weights aimed at minimizing the cost function given by Equation (3.40). This learning method has a fast convergence rate (Behera and Kar, 2009; Norgaard et al., 2003) and it is recommended for most control applications and real-time implementations (Behera and Kar, 2009).

$$E_{i_2} = \frac{1}{n} \sum_{i=1}^{n} \left( y_{d i_2}(t) - y_{i_2}(t) \right)^2 \tag{3.40}$$

where $y_{d i_2}(t)$ is the desired response and $y_{i_2}$ is the model output of the $i_2^{th}$ unit of the output layer and $n$ is the number of training samples.

**Validation**

The 25000 data generated during the experimental phase is divided into three portions. 50% of the data is used for the training of the neural network model, 25% is used for testing the trained NN model and the remaining 25% is used for the validation.

The structure of the NNFBL used to estimate the functions $\hat{f}(\cdot)$ and $\hat{g}(\cdot)$ is shown in Figure 3.11.

The parameters used for the neural network identification process and their numerical values are presented in Table 3.3 and the results obtained are presented in Table 3.4. Figures 3.12, 3.13 and 3.14 show the plots of the training, testing and validation data respectively.

The closed-loop block diagram of the NNFBL controller is shown in Figure 3.15

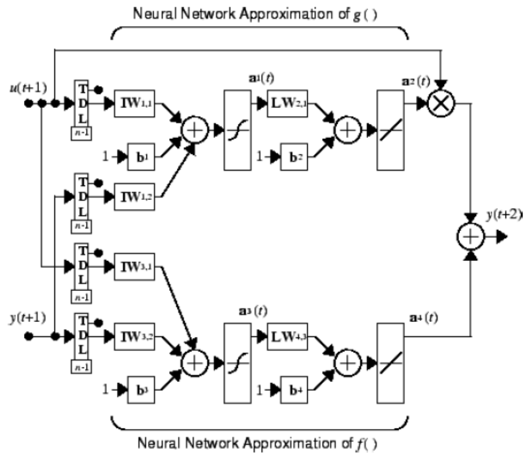


Figure 3.11: NNFBL model for approximation of $\hat{f}(\cdot)$ and $\hat{g}(\cdot)$

Table 3.3: System identification parameters and numerical values

| Parameters | Values |
|---|---|
| Number of layers | 2 |
| Number of hidden layer neurons | 3 |
| Number of past outputs | 2 |
| Number of past inputs | 2 |
| Total number of samples | 25000 |
| Number of iterations | 500 |
| Training algorithm | Levenberg-Marquardt |
| Sampling time | 0.0001 sec |
| Maximum plant input | 1500 $N/m^2$ |
| Minimum plant input | 0 |
| Maximum plant output | 0.18 |
| Minimum plant output | 0 |

Table 3.4: Result of system identification

| Parameters | Results |
|---|---|
| Performance (MSE) | $1.87 \times 10^{-10}$ |
| Number of epoch | 6 |

### 3.4.5 Summary

In this chapter, the category of non-linear systems within which the ABS problem is defined; the non-linear affine systems is introduced. The adopted neural network model structure is presented and the model identification and controller design are presented. The following chapter, presents and discusses the simulation results for

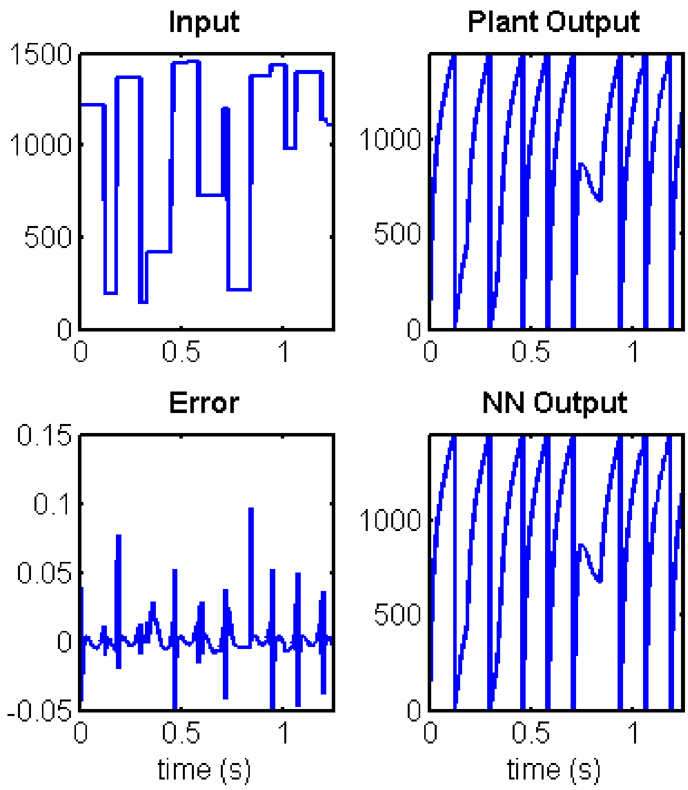


Figure 3.12: Training data for NNFBL

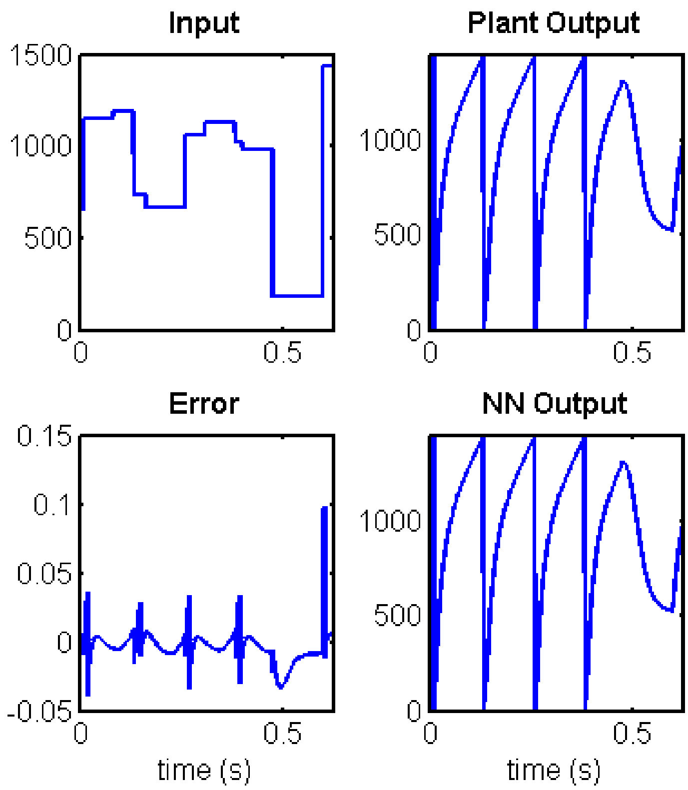


Figure 3.13: Testing data for NNFBL

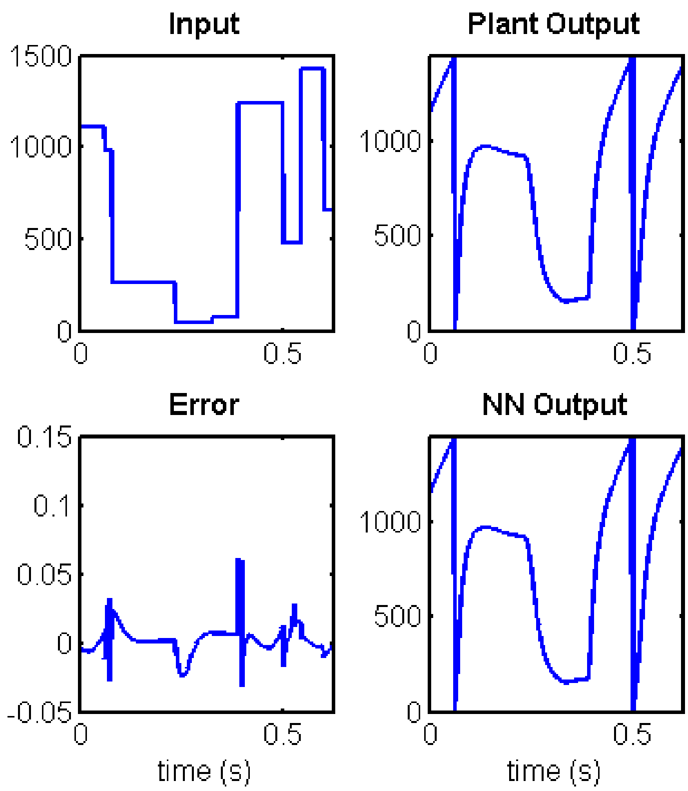


Figure 3.14: Validation data for NNFBL

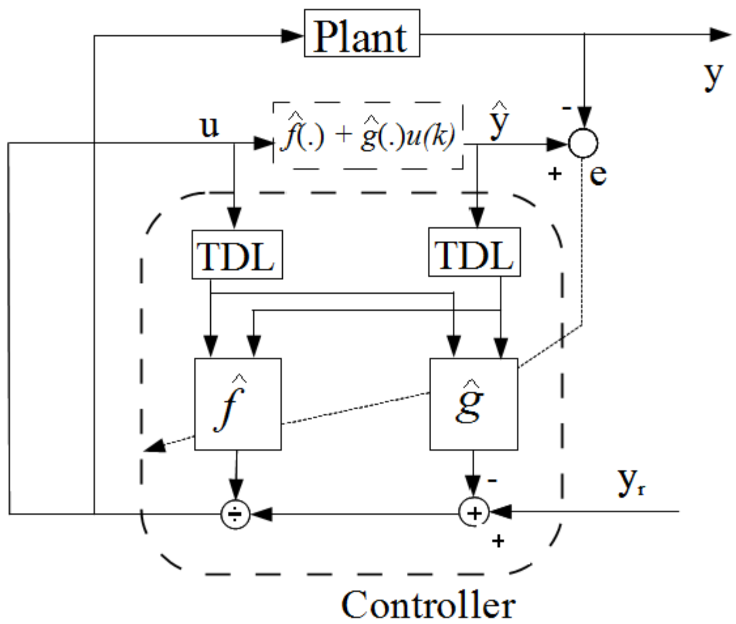


Figure 3.15: Block diagram of NNFBL controller

the PID, FBL, FBLPID and NNFBL ABS controller schemes. It also presents a comparative study of these controllers.

# 4 Comparative Study of the Control Schemes Applied to the ABS

## 4.1 Introduction

To evaluate completely the performance of the proposed controllers, experiments with an actual vehicle is required. However, performance evaluation in a simulation environment is a necessary step in model-based design. There are several software and computing tools that enable vehicle simulations, for example CARSIM, TruckSim, ADAMS MathModelica and Matlab® / Simulink® (Fritzson et al., 2002; Jiang and Gao, 2001; Schofield, 2008; Yoo, 2006), which produce the behaviour of actual vehicles, without actually building the hardware. This chapter introduces the simulation environment and numerical values used for simulating the ABS controllers, and discusses their performances.

## 4.2 Simulation Environment and Numerical Data

Due to its flexibility and ease of use, the Matlab® / Simulink® is selected to demonstrate the performances of the control strategies presented in Chapters 3.2, 3.3 and 3.4

During simulation, a quarter-car model with the parameters and numerical values shown in Table 4.1 is used. The slip between the tyre and the road is generated by the friction model (Equation 1.4).

In real-life, the driver may avoid an obstacle in an emergency by steering the vehicle. Other active safety systems like the *active steering control, obstacle avoidance control* and their combination (Benine-Neto et al., 2010; Bevan et al., 2010; Chang,

Table 4.1: System parameters and numerical values

| Symbol | Description | Value | Unit |
|---|---|---|---|
| $m$ | Quarter car mass | 395 | $kg$ |
| $J$ | Wheel inertia | 1.6 | $Nms^2/rad$ |
| $r$ | Radius of wheel | 0.3 | $m$ |
| $C$ | Vehicle viscous friction | 0.856 | $kg/m$ |
| $B$ | Wheel viscous friction | 0.08 | $Nkgm^2/s$ |
| $\tau$ | Hydraulic time constant | 0.3 | sec |
| $k_b$ | Hydraulic gain | 0.8 | constant |
| $g$ | Gravitational acceleration | 9.81 | $m/s^2$ |
| $\lambda_d$ | Desired slip ratio | 0.18 | Ratio |

2007; Hattori et al., 2006) with the ABS will provide a possible solution for this situation. These interaction of active safety systems may confuse results, and is not the focus of the current work. Evaluating the ABS on a straight-line braking therefore is sufficient and used here.

When simulating, braking commenced at an initial longitudinal velocity of $80km/h$ ($22.23m/s$) (Dietsche and Klingebiel, 2007), and the braking torque is limited to $1200Nm$. To impose a desired slip trajectory, the following reference model is adopted (Poursamad, 2009).

$$\dot{\lambda}_d(t) + 10\lambda_d(t) = 10\lambda_c(t) \tag{4.1}$$

where the slip command is chosen to be $\lambda_c = 0.18$.

Simulations are conducted for a high, medium and low friction surfaces with friction coefficients of $\mu = 0.85$, $\mu = 0.6$ and $\mu = 0.2$ corresponding to dry asphalt, gravel and icy road conditions respectively (MacIsaac Jr and Garrot, 2002). The simulations are terminated at speeds of $1m/s$ ($3.6km/h$), because as the speed of the wheel approaches zero, the slip becomes unstable. The ABS should disengage at low speed to allow the vehicle to stop.

Based on the criteria stipulated in Section (3.1.2) the performance of the controllers are evaluated against their stopping distance, slip regulation and the braking torque.

Comments are made on the over-all robustness of the controllers.

## 4.3 Simulation Results for High Friction Road Condition

A friction coefficient of 0.85 is used to simulate braking on a dry-asphalt road condition. Though higher values are used in other works (Nyandoro et al., 2011) the selected value of 0.85 is considered conservative for the evaluation of the controllers. Optimum performance of the controllers are demonstrated on this road condition. Figures 4.1 to 4.12 are the plots of the vehicle and wheel deceleration, slip tracking and braking torque for the PID, FBL, FBLPID and NNFBL controllers.

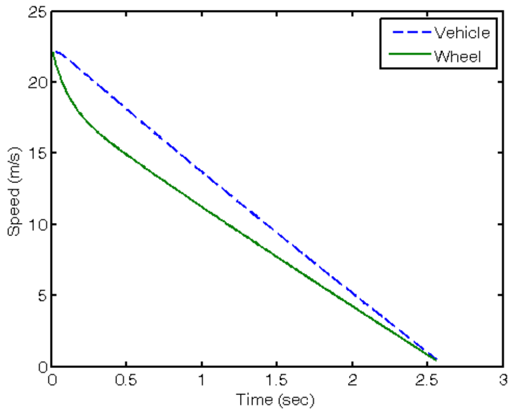


Figure 4.1: Vehicle and wheel deceleration on high friction surface ($\mu = 0.85$) using PID controller

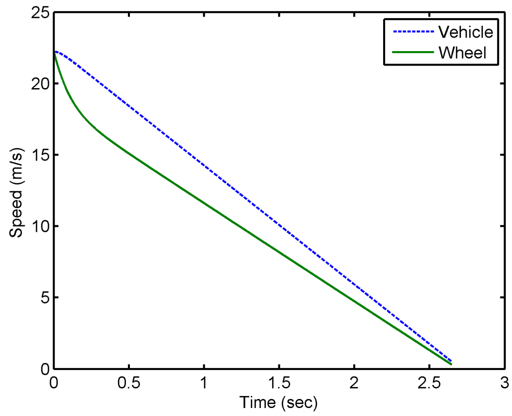


Figure 4.2: Vehicle and wheel deceleration on high friction surface ($\mu = 0.85$) using FBL controller

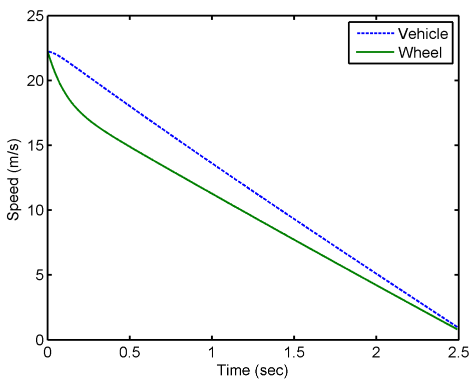


Figure 4.3: Vehicle and wheel deceleration on high friction surface ($\mu = 0.85$) using FBLPID controller

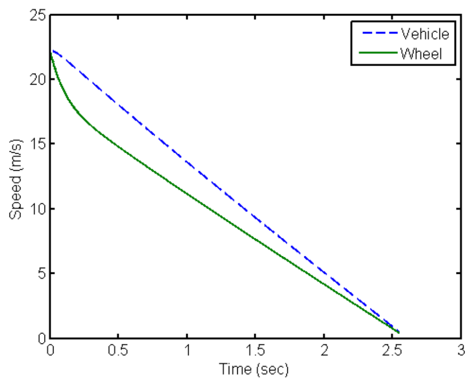


Figure 4.4: Vehicle and wheel deceleration on high friction surface ($\mu = 0.85$) using NNFBL controller

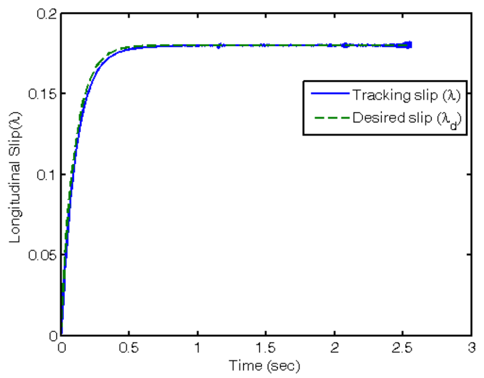


Figure 4.5: Slip tracking on high friction surface ($\mu = 0.85$) using PID controller

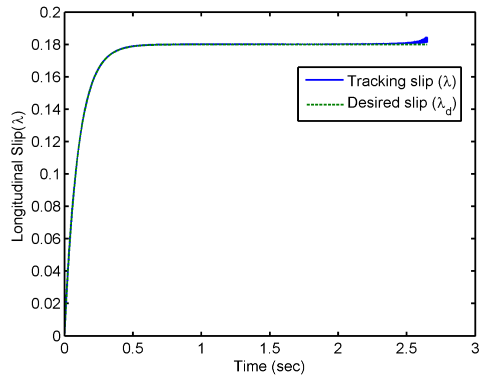


Figure 4.6: Slip tracking on high friction surface ($\mu = 0.85$) using FBL controller

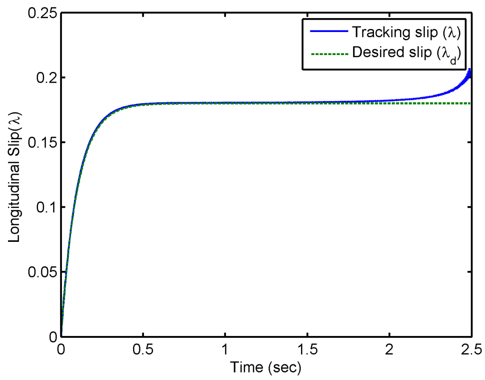


Figure 4.7: Slip tracking on high friction surface ($\mu = 0.85$) using FBLPID controller

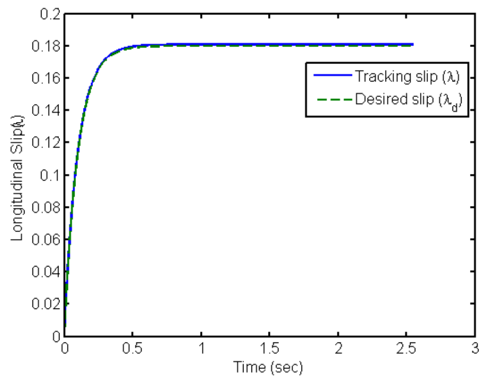


Figure 4.8: Slip tracking on high friction surface ($\mu = 0.85$) using NNFBL controller

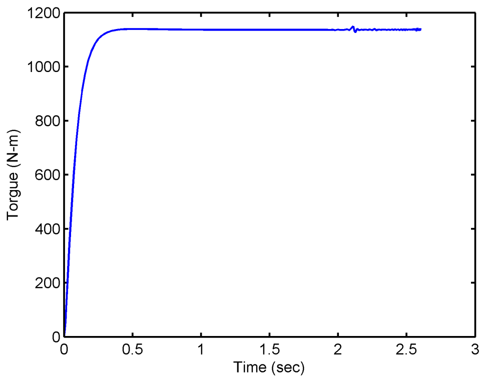


Figure 4.9: Braking torque on high friction surface ($\mu = 0.85$) using PID controller

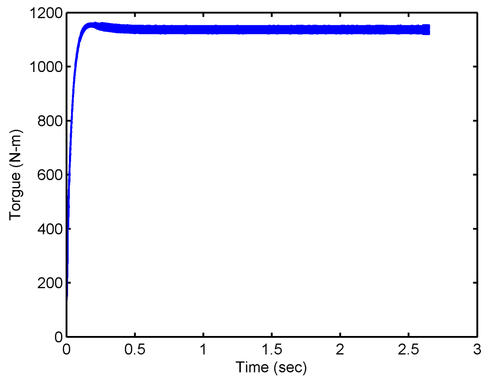


Figure 4.10: Braking torque on high friction surface ($\mu = 0.85$) using FBL controller

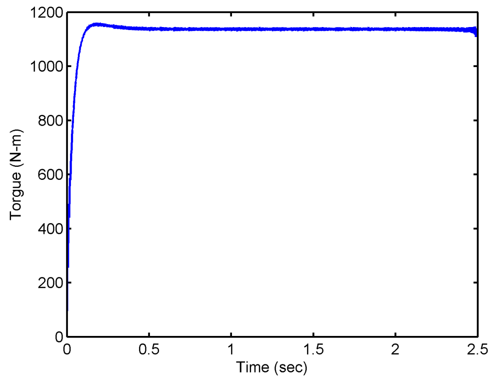


Figure 4.11: Braking torque on high friction surface ($\mu = 0.85$) using FBLPID controller

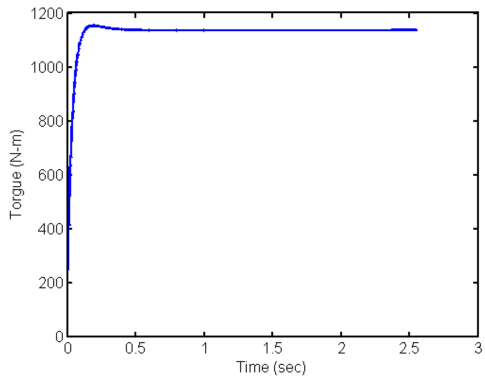


Figure 4.12: Braking torque on high friction surface ($\mu = 0.85$) using NNFBL controller

The summary of the performances of the four controllers based on performance indices specified in Section 3.1.2 are presented in Table 4.2 for the high friction road condition. The full discussion on these results is given in Section 4.6. The vehicle and wheel deceleration figures (Figures 4.1 to 4.4) show the vehicle deceleration as blue dash-lines while the wheel angular deceleration is shown in green continuous line. Figures 4.5 to 4.8 are the plots for the slip tracking with the desired slip shown in green dash-lines and the tracking slip is shown as continuous blue lines. It can be observed that in some cases the difference between the slip tracking and the desired slip is not obvious; this is a case of perfect tracking. Figures 4.9 to 4.12 are the plots of the braking torques.

Table 4.2: Simulation results for $\mu = 0.85$ road condition

| Performance parameters | Specs | PID | FBL | FBLPID | NNFBL |
|---|---|---|---|---|---|
| Slip tracking - $\int_{t_0}^{t_f} (\lambda - \lambda_d)^2 dt$ $10^{-6}$ | min | 108.200 | 65.990 | 0.2113 | 1.704 |
| Braking torque - $\int_{t_0}^{t_f} {T_b}^2 dt$ $(Nm)^2$ $10^5$ | min | 2.005 | 2.411 | 2.083 | 4.161 |
| Stopping distance - $\int_{t_0}^{t_f} vdt$ $(m)$ | $\leq 50m$ | 29.26 | 30.58 | 28.83 | 28.88 |

## 4.4 Simulation Results for Medium Friction Road Condition

Medium friction road condition are road surface with a friction coefficient of between 0.5 to 0.7. Wet asphalt and gravel road fall within this category of road. A friction

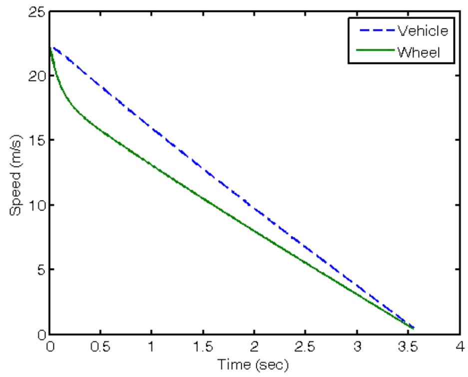


Figure 4.13: Vehicle and wheel deceleration on medium friction surface ($\mu = 0.6$) using PID controller

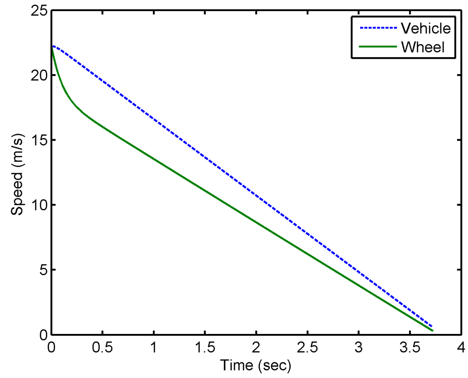


Figure 4.14: Vehicle and wheel deceleration on medium friction surface ($\mu = 0.6$) using FBL controller

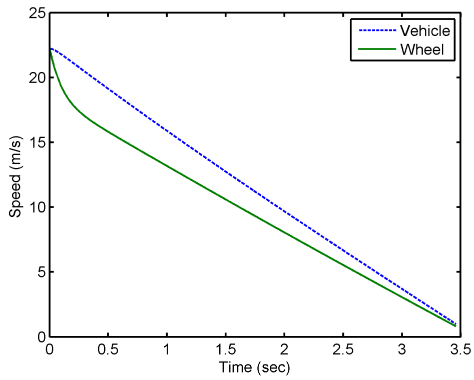


Figure 4.15: Vehicle and wheel deceleration on medium friction ($\mu = 0.6$) using FBLPID controller

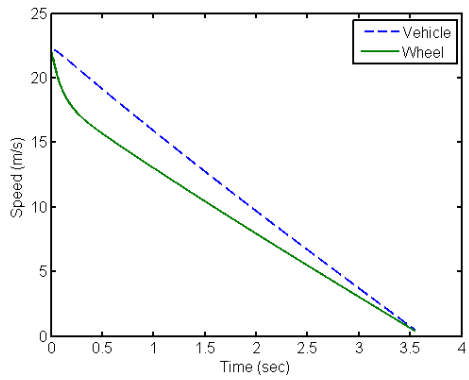


Figure 4.16: Vehicle and wheel deceleration on medium friction surface ($\mu = 0.6$) using NNFBL controller

coefficient of 0.6 is used to simulate braking on a gravel road. Controller performance on a gravel road is not considered to be the best of performances, however this provides a good basis for testing the robustness of the controllers. Figures 4.13 to 4.24 are the plots of vehicle and wheel deceleration, slip tracking and braking torque for the controllers.

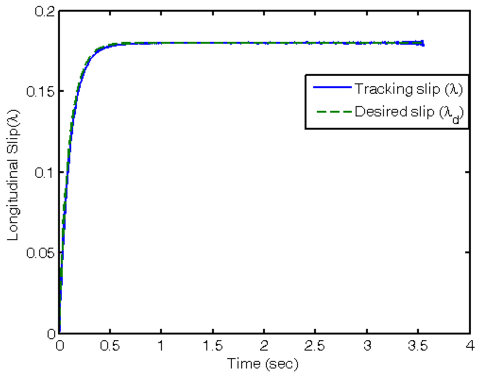


Figure 4.17: Slip tracking on medium friction surface ($\mu = 0.6$) using PID controller

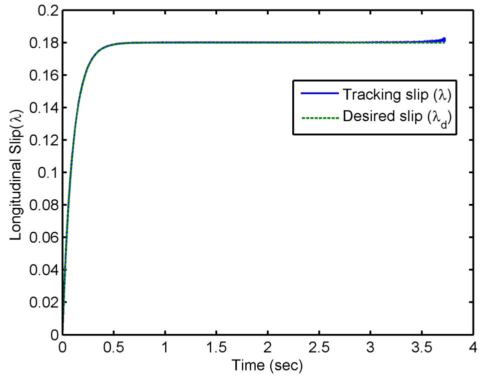


Figure 4.18: Slip tracking on medium friction surface ($\mu = 0.6$) using FBL controller

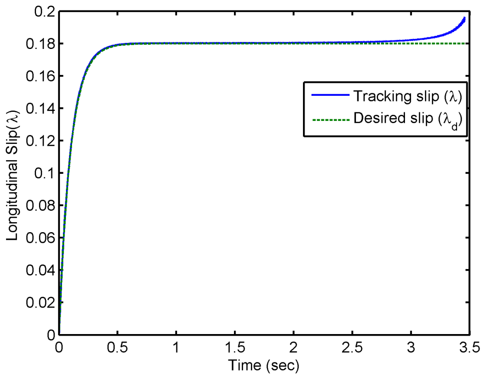


Figure 4.19: Slip tracking on medium friction ($\mu = 0.6$) using FBLPID controller

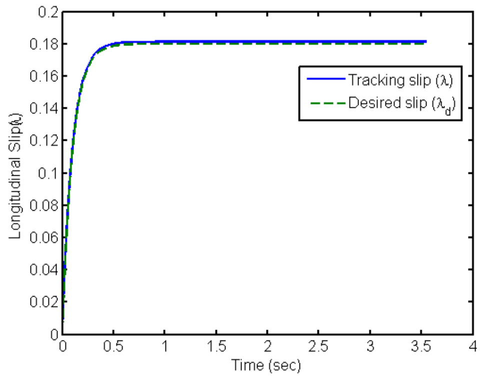


Figure 4.20: Slip tracking on medium friction surface ($\mu = 0.6$) using NNFBL controller

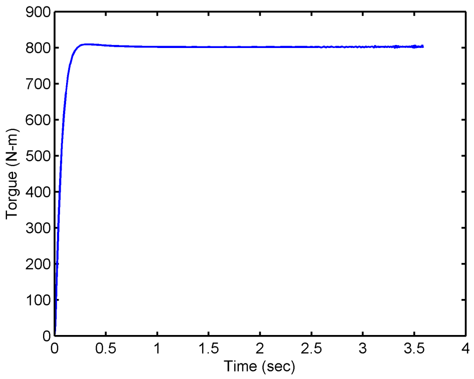


Figure 4.21: Braking torque on medium friction surface ($\mu = 0.6$) using PID controller

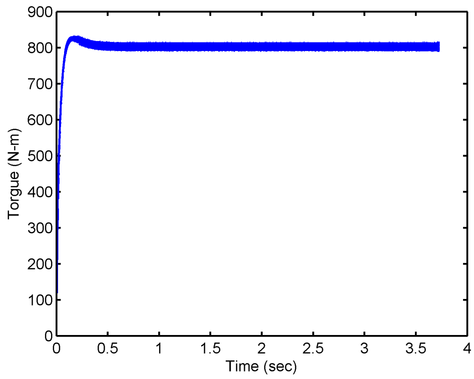


Figure 4.22: Braking torque on medium friction surface ($\mu = 0.6$) using FBL controller

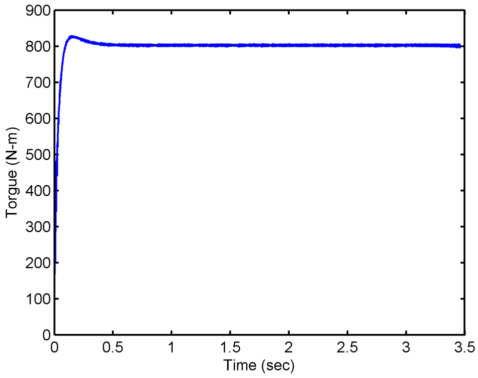


Figure 4.23: Braking torque on medium friction ($\mu = 0.6$) using FBLPID controller

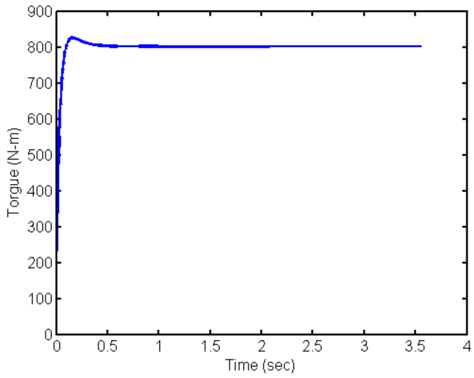


Figure 4.24: Braking torque on medium friction surface ($\mu = 0.6$) using NNFBL controller

Table 4.3: Simulation results for $\mu = 0.6$ road condition

| Performance parameters | Specs | PID | FBL | FBLPID | NNFBL |
|---|---|---|---|---|---|
| Slip tracking - $\int_{t_0}^{t_f} (\lambda - \lambda_d)^2 dt$ $(10^{-6})$ | min | 51.32 | 51.40 | 12.94 | 6.10 |
| Braking torque - $\int_{t_0}^{t_f} {T_b}^2 dt$ $((Nm)^2)$ $(10^5)$ | min | 1.003 | 1.749 | 1.472 | 2.907 |
| Stopping distance - $\int_{t_0}^{t_f} vdt$ $(m)$ | $\leq 50m$ | 40.00 | 42.92 | 39.61 | 39.67 |

Performance indices results for the four controllers as specified in Section 3.1.2 for the medium friction road condition are presented in Table 4.3. The full discussion on these plots is given in Section 4.6. The descriptions of the figures for the vehicle and wheel deceleration (Figures 4.13 to 4.16), slip tracking (Figures 4.17 to 4.20 and braking torque (Figures 4.21 to 4.24 follow a similar pattern to those for the high friction road condition.

## 4.5 Simulation Results for Low Friction Road Condition

Snow and icy roads are classified as low friction road condition in this work, and a friction coefficient of 0.2 is adopted based on other similar works (Petersen, 2003; Tanelli et al., 2006). As with gravel road condition, the icy road simulation results confirm the robustness of the controllers. Figures 4.25 to 4.36 are the plots of vehicle and wheel deceleration, slip tracking and braking torque for the controllers.

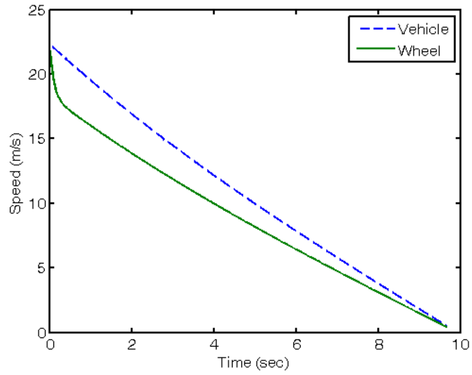


Figure 4.25: Vehicle and wheel deceleration on low friction surface ($\mu = 0.2$) using PID controller

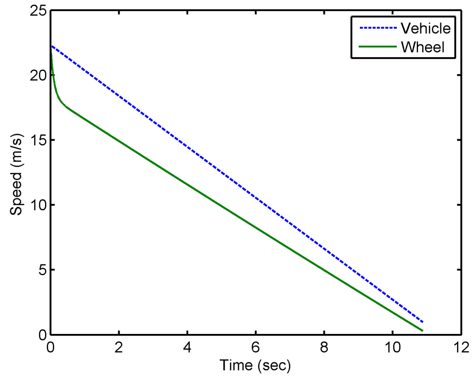


Figure 4.26: Vehicle and wheel deceleration on low friction surface ($\mu = 0.2$) using FBL controller

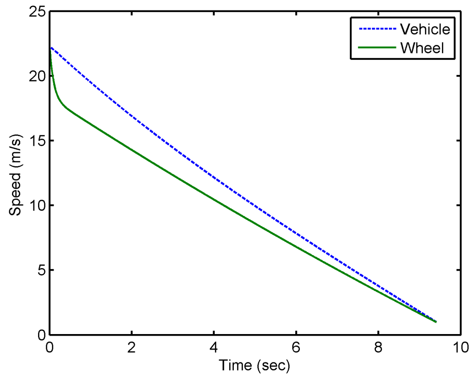


Figure 4.27: Vehicle and wheel deceleration on low friction surface ($\mu = 0.2$) using FBLPID controller

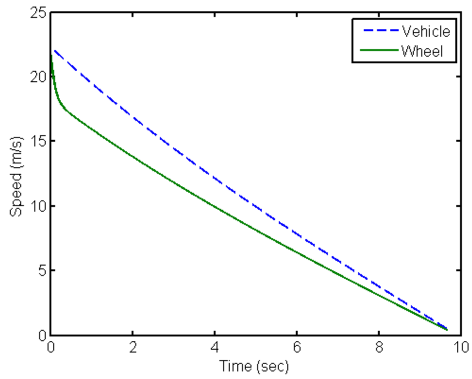


Figure 4.28: Vehicle and wheel deceleration on low friction surface ($\mu = 0.2$) using NNFBL controller

In-line with the previous two road conditions, the summary of the performance indices of the four controllers are presented in Table 4.4. The full discussion follows

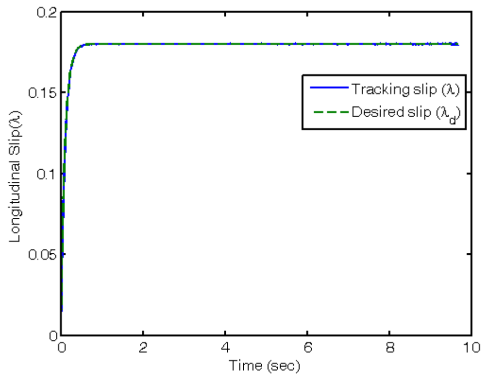


Figure 4.29: Slip tracking on low friction surface ($\mu = 0.2$) using PID controller

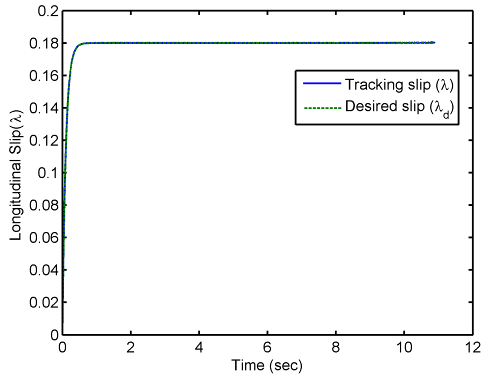


Figure 4.30: Slip tracking on low friction surface ($\mu = 0.2$) using FBL controller

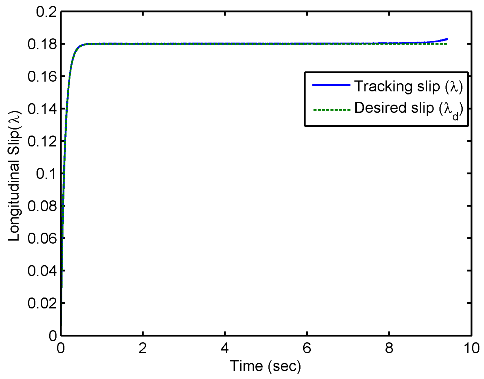


Figure 4.31: Slip tracking on low friction surface ($\mu = 0.2$) using FBLPID controller

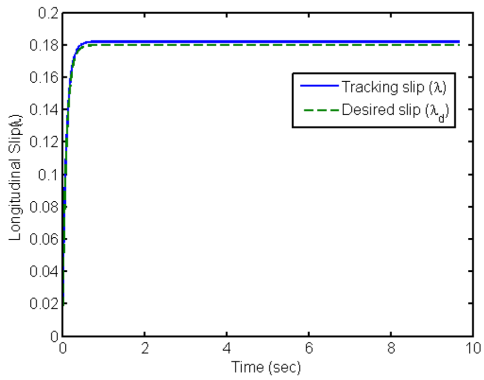


Figure 4.32: Slip tracking on low friction surface ($\mu = 0.2$) using NNFBL controller

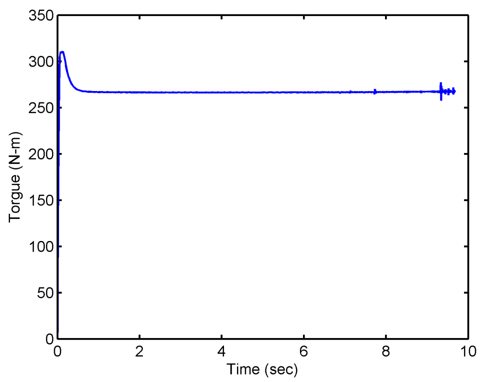


Figure 4.33: Braking torque on low friction surface ($\mu = 0.2$) using PID controller

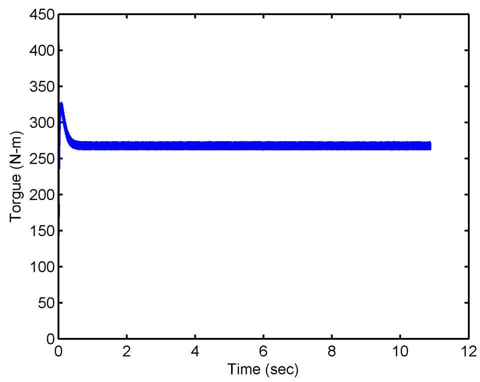


Figure 4.34: Braking torque on low friction surface ($\mu = 0.2$) using FBL controller

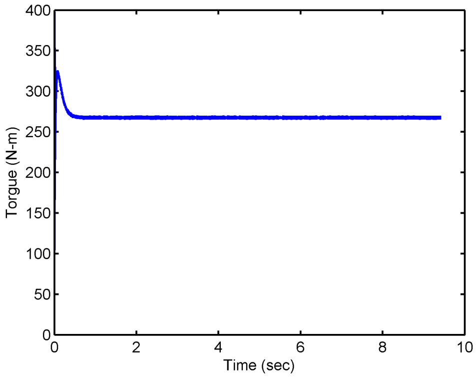


Figure 4.35: Braking torque on low friction surface ($\mu = 0.2$) using FBLPID controller

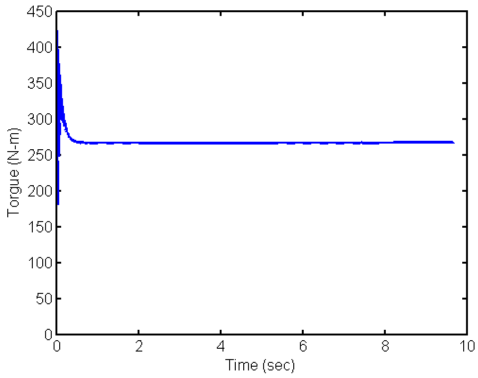


Figure 4.36: Braking torque on low friction surface ($\mu = 0.2$) using NNFBL controller

Table 4.4: Simulation results for $\mu = 0.2$ road condition

| Performance parameters | Specs | PID | FBL | FBLPID | NNFBL |
|---|---|---|---|---|---|
| Slip tracking - $\int_{t_0}^{t_f} (\lambda - \lambda_d)^2 dt$ $(10^{-6})$ | min | 10.860 | 1.412 | 4.148 | 0.439 |
| Braking torque - $\int_{t_0}^{t_f} {T_b}^2 dt$ $((Nm)^2)$ $(10^5)$ | min | 0.191 | 0.645 | 0.481 | 0.922 |
| Stopping distance - $\int_{t_0}^{t_f} v dt$ $(m)$ | $\leq 50m$ | 103 | 126 | 103 | 103 |

in Section 4.6. Figures 4.25 to 4.28 show the vehicle and wheel decelerations, Figures 4.29 to 4.32 are the plots for the slip tracking and Figures 4.33 to 4.36 are the plots of the braking torques. The plots are similar to the previous two road conditions.

## 4.6 Simulation Results Analysis

The main goal of the ABS is to achieve shorter stopping distance and provide steering control to the driver by regulating the slip value around the peak friction coefficient for different road conditions. The goal of the current work therefore, is for the controller to maintain the slip value around the optimum value of $\lambda_d = 0.18$ were the optimum friction coefficient for all road conditions is located. A rise time of $0.25sec$ for the slip to achieve 90% value of its final desired value of $(\lambda_d = 0.18)$ is desirable. The case of no overshoot is superior performance to over-shoots, however, a maximum limit of 5% over-shoot is specified. It is also specified that the slip should settle about $\pm 5\%$ of its final values. A stopping distance of $\leq 50m$ from an initial velocity of $80km/h$ is the standard performance requirement (Dietsche and

Klingebiel, 2007), on all road conditions, however on icy road much longer stopping distances are recorded, as expected. In this section, therefore, a quantitative as well as a qualitative analysis of the performances of the four controllers is discussed.

### 4.6.1 General performance

Some general comments on the simulation results will be given in this section, while a comparative analysis will follow in the subsequent sections. In general, the overall performances of the four controllers can be considered to be in-line with results obtained by other researches and industry for the ABS (Jiang and Gao, 2001; Mirzaeinejad and Mirzaei, 2010; Shelley, 2012; Solyom, 2004). The convergent rate of the slip for all controllers on all road conditions does not exhibit any over-shoot (see Figures 4.5 - 4.8 for dry asphalt road, 4.17 - 4.20 for the gravel road and 4.29 - 4.32 for the icy road condition). The braking torques remain below the set-limit of $1200Nm$ (Figures 4.9 - 4.12 for dry asphalt road; 4.21 - 4.24 for gravel road and 4.33 - 4.36 for the icy road conditions). These general observations may give the impression that any of the controllers could be picked at random for application to the ABS. However, for every performance it is necessary to evaluate with respect to the other factors. The following sections present a comparative analysis of these controllers.

### 4.6.2 PID vs FBL

The two standard linear and non-linear controllers, PID and FBL respectively are discussed first. This provides the basis for the comparison of the subsequent proposed alternatives; namely the FBLPID and the NNFBL. The PID is a well known and broadly applied controller in industry due to its simple design and ease of tuning (O'Dwyer, 2009). Even for non-linear systems like the ABS, the PID gives good results (Pedro et al., 2009; Solyom, 2004). Some non-linear PID structures have been proposed in the literature as well (Jiang and Gao, 2001; Tanelli et al., 2006). The PID structure employed in this work is the classical one (see Section 3.2.2).

The PID controller achieved stooping distances of $29.26m$ on high friction road $40m$ on medium friction road and $103m$ on low friction road. The FBL controllers achieved stopping distances of $30.58m$, $42.9m$ and $126m$ for high, medium and low friction roads respectively. Both PID and FBL meet the stopping distance requirements for high and medium friction coefficient road conditions. As expected, a longer stopping distance is recorded for the low friction coefficient road condition. The PID in total achieved shorter stopping distances in comparison to the FBL controller.

For slip tracking, both controllers meet the desired performance criteria (see Section 3.1.2). A comparison of the slip plots for the PID controller shown in Figures 4.5, 4.17 and 4.29 to those for the FBL controller shown in Figures 4.6, 4.18 and 4.30, reveal the FBL controller to have a superior performance of regulating the longitudinal slip with respect to the desired slip value ($\lambda_d$) (green dashed lines). The FBL slip plots do not exhibit over-shoot and settle far below the $\pm 5\%$ specified thereby giving almost perfect tracking of the desired slip trajectory. The PID controller, exceeds the rise time requirement by 30% and 19% on the high and medium friction road conditions respectively. The slip tracking for both the PID and the FBL controller are unstable towards the end of the simulation. This is more obvious with the PID controller than the FBL and could account for the relatively higher values of the slip variations performance index in Tables 4.2, 4.3 and 4.4 for the PID.

The slip tracking and stopping distances are the result of the effective braking torque. The braking torque is limited to $1200Nm$. The PID accomplished the braking using effective braking torques of $1130Nm$, $800Nm$ and $267Nm$ on the high, medium and low friction road conditions respectively and the FBL recorded effective braking torques of $1122Nm$, $800Nm$ and $263Nm$ for the same road conditions respectively. Both PID and FBL accomplished the braking operation with torque values lower than the maximum allowable torque for all road conditions. However, the FBL has pronounced chattering effect observed in Figures 4.10, 4.22 and 4.34. This accounts for the relatively high effective braking torque performance index for the FBL in Tables 4.2, 4.3 and 4.4.

The chattering problem in the FBL motivates the investigation of a hybrid controller as a possible solution. Chattering deteriorates the life-span of the ABS, and may give the driver an unpleasant pulsation sensation on the brake pedal. This could lead to improper application of braking application by the driver and hence compromise the advantages of the ABS. The hybrid controller is a combination of the FBL and PID controllers and the outcome of this synergy is the topic of the next section.

### 4.6.3 Hybrid FBLPID

The hybrid controller combines the PID and the FBL controller. The primary objective for developing the hybrid system is to solve the chattering effect observed in the FBL controller performance by enhancing the FBL controller with a PID controller to smooth-out the control action. In other works, a sliding mode controller has been employed (Buckholtz, 2002; Lin and Hsu, 2003; Park and Lim, 2008). This latter approach however, introduces a steady-state error in the solution. The proposed hybrid controller achieves stopping distances of $28.83m$, $39.61m$ and $103m$ on high, medium and low friction road conditions respectively. This yields a 6% improvement on high friction road, 8% improvement on medium friction road and 18% improvement on the low friction road when compared to the standard FBL controller.

The hybrid system equally utilises less effective braking torques to the maximum allowable. It recorded effective braking torque of $1135Nm$ on the high friction road, which is about 1% higher than the standard FBL, $800Nm$ on the medium friction road condition, same as that of the standard FBL and $267Nm$ on low friction road about 1.5% above that of the standard FBL. Comparing the plots of the hybrid system in Figures 4.11, 4.23 and 4.35 to those of the standard FBL in Figures 4.10, 4.22 and 4.34 chattering has been reduced considerably. The slightly higher braking torques utilised by the hybrid system is compensated by reduced chattering. The effective braking torques plots showed high initial torque values on the on-set of the braking on all road conditions, but this phenomenon is more pronounced on the medium and low friction road conditions. Taking this situation into consideration therefore, the hybrid controller out-performs the standard FBL as revealed on the effective braking torque performance index in Tables 4.2, 4.3 and 4.4.

The slip tracking plots for the hybrid system are shown in Figures 4.7, 4.19 and 4.31. The hybrid system exhibits slight unstable slip situation towards the end of the simulation for the high and medium friction road conditions. It however, gives almost perfect slip tracking on the low friction road condition. The hybrid system records lower performance index values than the FBL and the PID with respect to slip tracking, as indicated in Tables 4.2, 4.3 and 4.4.

In conclusion the hybrid control scheme reduced chattering, achieved 6%, 8% and 18% improvement on stopping distance on high, medium and low friction road conditions respectively, against the standard FBL. This encouraging results informed the investigation of a neural network-based FBL (NNFBL) whose performance is evaluated in the next section.

### 4.6.4 Neural network-based FBL

The PID, FBL and the hybrid systems are model-based, their performances are based on the accuracy of the mathematical model used. Under changing conditions therefore, these controllers may not perform optimally due to the ideal mathematical conditions in which they are developed. One of the goals of introducing the neural network-based FBL is to overcome the uncertainties in the model of the system due to the assumptions made (see section 2.2).

The NNFBL achieved a stopping distance of $28.88m$ on high friction road, $39.67m$ on medium road condition and $103m$ on the low friction road condition. These stopping distances are comparable with those for the FBLPID system, but are better than those for the PID and FBL controllers. The FBLPID has less than 1% lower stopping distance than the NNFBL on high and medium friction roads and on low friction road both achieved the same stopping distances.

The slip tracking results of the NNFBL controller, exhibits no over-shoot, and gives almost perfect tracking of the desired slip as can be seen in Figures 4.8, 4.20 and 4.32. It outperforms the hybrid system on all road conditions and does not exhibit any unstable situation like observed in the FBLPID case, particularly on the high friction road condition (Figure 4.7). The NNFBL maintains superior performance over the PID and FBL control schemes on all three road conditions. This can be seen from the slip tracking performance index in Tables 4.2, 4.3 and 4.4.

The plots for the effective braking torques for the NNFBL are presented in Figures 4.12, 4.24 and 4.36. It accomplished the braking process with an effective braking torque of $1134Nm$ on high friction road, which is less than 1% higher than that for the FBLPID. Though the NNFBL is about 1% higher than the FBL in effective braking torque, the lack of chattering on the NNFBL is likely to give a better performance. An interesting situation observed for the effective braking torques on medium road is that all controllers utilised an average of $800N$ to bring the vehicle to rest (Figures 4.21, 4.22, 4.23, and 4.24).

In general the NNFBL controller exhibits promising results and hence provides an indication that a neural network-based ABS controller is feasible.

## 4.7 Conclusion

The objectives of this research can be broadly divided into two parts. The first part being the design, analysis and simulation evaluation of PID, FBl, FBLPID and NNFBL controllers. This represents the first two research objectives stated in Section 1.6. The second part of the research is the validation of the simulation performance of the proposed NNFBL using a quarter-car laboratory test rig.

The specifications of the slip control is to track the desired slip ($\lambda_d$) within a boundary of $\pm 5\%$ with a maximum over-shoot of 5%. The controller specifications require a rise time of $0.25sec$ and a stopping distance of $\leq 50m$ from an initial speed of $80km/h$.

All four controllers (PID, FBL, FBLPID and NNFBL) do not exhibit any over-shoot in the slip tracking. The PID performed relatively poor on the high friction road with a slightly higher rise time, but still within the limits of $0.25sec$. This result is not considered poor, for a linear PID controller. The slip performance index results, indicate the hybrid system (FBLPID) to have the best slip tracking when the response quality and stability are taken into consideration. Since this performance is consistent on the road conditions simulated, the controller can be said to be robust and it is likely to be consistent under some uncertainty, like loading of vehicle and road profile. The NNFBL although considered to be second best with respect to slip response quality, perform comparably well with the FBLPID controller. The NNFBL is expected to be even more robust as it is not model-dependent and can therefore adapt to different operating conditions.

One of the important goals of the ABS is to shorten the stopping distance during hard braking without slippage. The PID controller, the FBL controller and the proposed hybrid (FBLPID) and its neural network-based (NNFBL) equivalent met the stopping distance requirement of $\leq 50m$ on high and medium friction road conditions. However on low friction road conditions, the stopping distances achieved by all controllers is over 50%. This indicates that even when a vehicle is equipped with an ABS, drivers should maintain low speeds when driving on icy road. The FBLPID achieved a better result followed closely by the NNFBL which achieves less than 1% higher stopping distances than the FBLPID. However, both FBLPID and NNFBL achieve the same stopping distances on low friction road.

The FBLPID and the NNFBL controllers maintain their superiority with respect to the effective braking torque, with the FBLPID having the best results.

In conclusion, a hybrid system slip control (FBLPID) and a neural network-based feedback linearization slip control (NNFBL) for application in ABS has been proposed. The neural network-based controller, employed two neural networks that were tuned off-line using the back-propagation training method to estimate the non-linearities. The stability of the controller was investigated using Lyapunov stability theory. The performance of the two proposed controllers using a quarter-car model, demonstrates their superiority over standard FBL and PID controllers.

The proposed neural-network based controller and its hybrid equivalent, are tested on a laboratory ABS test bench for verification and validation. In the next chapter, a PID controller is used as a benchmark controller.

# 5 Experimental Study of the Proposed ABS Controller

## 5.1 Introduction

Following the promising performance of the proposed NNFBL controller by simulation, its physical performance on an experimental test bench is conducted. The PID and NNFBL controllers designed in Chapters 3.2 and 3.4 are applied to the experimental model. Similar simulations as the ones presented in Chapter 4 are conducted on a Simulink® model of the test rig, the results were used to tune the controllers.

This chapter gives a brief description of the experimental ABS test rig and its limitations, followed by the experimental set-up used for this work. Finally, the tuning of the controllers and the hardware-in-the-loop (HiL) experimental results for the laboratory ABS are presented.

## 5.2 The Experimental ABS Test Rig: Description and Limitations

The INTECO ABS laboratory system used for this work is shown in Figure 5.1. It is made up of two rolling wheels; the lower wheel represents the vehicle motion while the upper wheel represents the wheel motion. Two identical encoders are used to measure the wheel and vehicle rotational motions. The accuracy of measurement of the encoders is 2048 encoder counts per revolution, yielding $2\pi/2048 = 0.175^0$. Pulse width modulator (PWM) controlled DC motor of about $220W$ accelerates the lower wheel, the upper follower wheel also gains speed. The angular velocities of the wheels are estimated by differential quotients. The vehicle velocity is estimated by multiplying the angular velocity of the lower wheel $\omega_2$ with its radius $r_2$, while the wheel velocity is estimated by multiplying the angular velocity of the upper wheel $\omega_1$ with its radius $r_1$. When a pre-determined speed threshold value is reached, the power supply to the DC motor attached to the lower wheel cuts-off and the braking process is initiated. The braking is accomplished via a Shimano BR-M486 hydraulic braking system, used in bicycles. It consists of a thin disc and brake-pads arrangement, and has a cable wound on the shaft of the small PWM controlled DC motor and attached to the brake lever that transmits the braking torque to the upper wheel upon braking. Both DC motors are controlled by $3.5kHz$ frequency signals. The non-linear friction curve is generated by the contacting surfaces of the lower steel wheel and the upper plastic wheel.

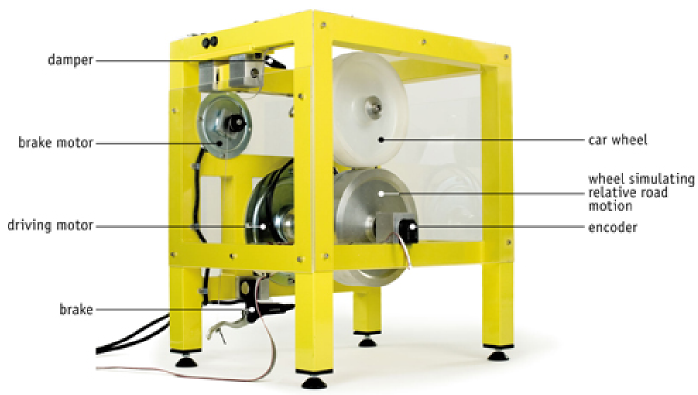


Figure 5.1: INTECO ABS physical model

Some of the limitations imposed by this experimental test rig include the following.

- The goal of the ABS is to maintain the slip at a desired value irrespective of road condition, this requires precise measurement of the wheel slip; the accuracy of the encoder therefore affects the slip estimation and hence the performance of the controller.
- The bicycle brake disk and hydraulic mechanism system introduces additional non-linearities.
- Experiments can only be run on one road condition; experiment on sudden changes in road conditions is not possible.

This section provides the description of the experimental ABS test rig and enumerates some limitations that the set-up imposes on the current work. The process of the data acquisition and computer interface is presented in the next section.

## 5.3 PC-Based ABS Controller Experimental Set-up

Control system design, analysis and prototyping is supported by software environments that provide real-life interaction between designers and hardware-in-the-loop (HiL) experimentation. This hardware-software prototyping process has several advantages; for example it helps to reduce the cost of off-the-self products and make them both available and affordable (Patil et al., 2003), and cuts down on time from design to mass production. The process used to implement the proposed ABS controllers is illustrated in Figure (5.2), where the arrows indicate the flow of activities.

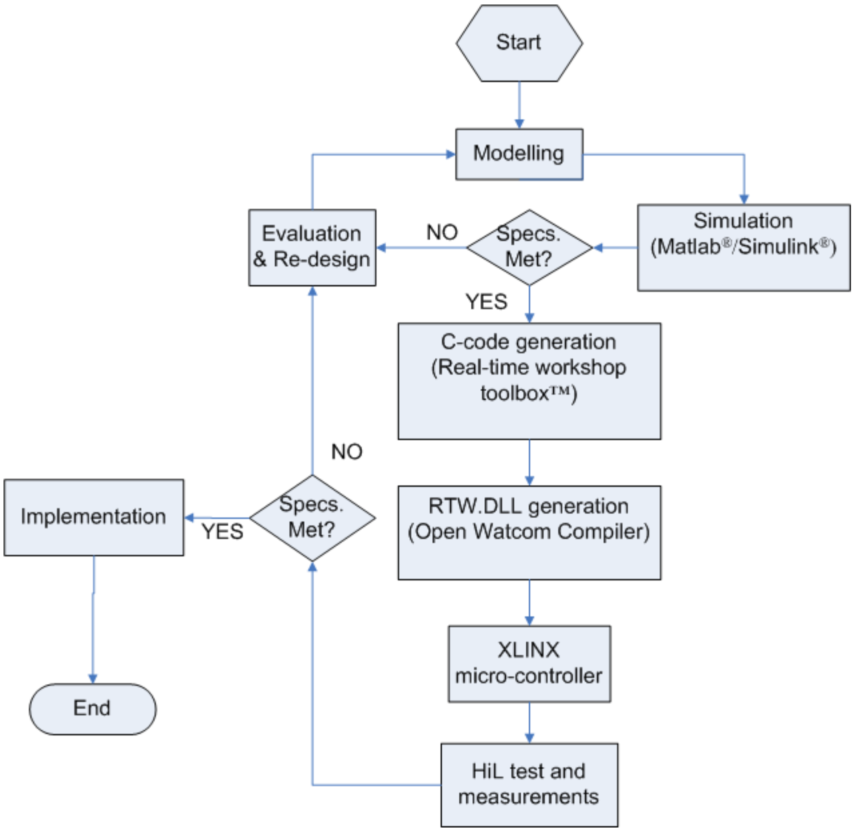


Figure 5.2: ABS controller prototyping process

The PC-based ABS set-up is shown in Figure 5.3. The set-up is made-up of the ABS mechanical unit, the power interface, the real time data acquisition card (RT-DAC) unit, the PC and the simulation environment. The mechanical unit is described in Section 5.2. This section describes the interaction between the PC interface with the mechanical unit through the data acquisition board and the power unit.

The power interface amplifies the control signals, which are transmitted from the

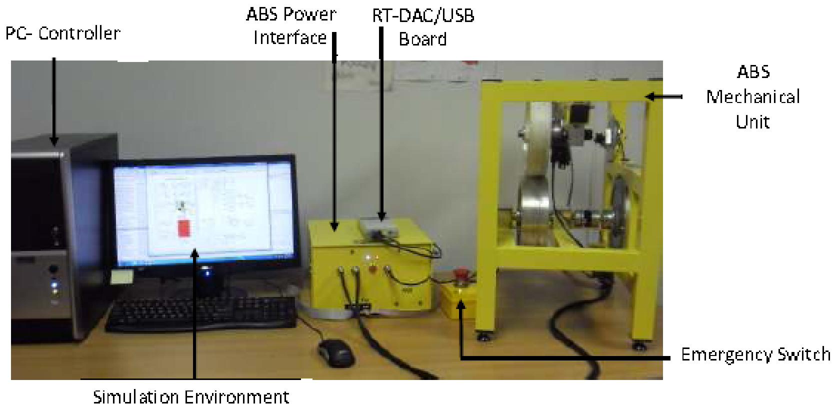


Figure 5.3: Experimental set-up

computer to the DC motors. It also converts the encoders pulse signals to a 16-bit digital form that makes it readable to the computer. The computer uses RT-DAC4/PCI-D multi-purpose digital I/O board to communicate with the power interface. The process logic for reading the encoders signals and for controlling the DC motors is configured in a Xilinx® micro-controller. The I/O board is accessed through the *ABS Toolbox*, which operates in the Matlab®/ Simulink® environment in conjunction with the Real Time Workshop (RTW) toolbox. The real-time implementation architecture for the ABS device driver is shown in Figure 5.4

The model of the ABS test rig is used for the implementation of the proposed controllers. The design cycle involves simulation, evaluation and re-design. Once a satisfactory performance of the controller is met, the real-time workshop is engaged to generate the C-codes. This is then compiled using open Watcom compiler; for compiling the code into a Real-Time-Workshop (RTW.DLL) executable file. Once the parameters are properly setted, a successful Real-Time Workshop (RTW) is then built for the model. This file is then downloaded onto the micro-processor located in the RTW Data Acquisition Card (RTW-DAC), which interfaced with the physical ABS mechanical system for testing and measurements. If the result of the test is satisfactory, the process stops, otherwise the cycle is repeated.

Once a satisfactory performance of the ABS controller is realised, the HiL experiments commenced. The remaining of this chapter describes the experimental process and presents the results for the proposed slip control schemes. The discussions on the results is presented in Chapter 5.7.

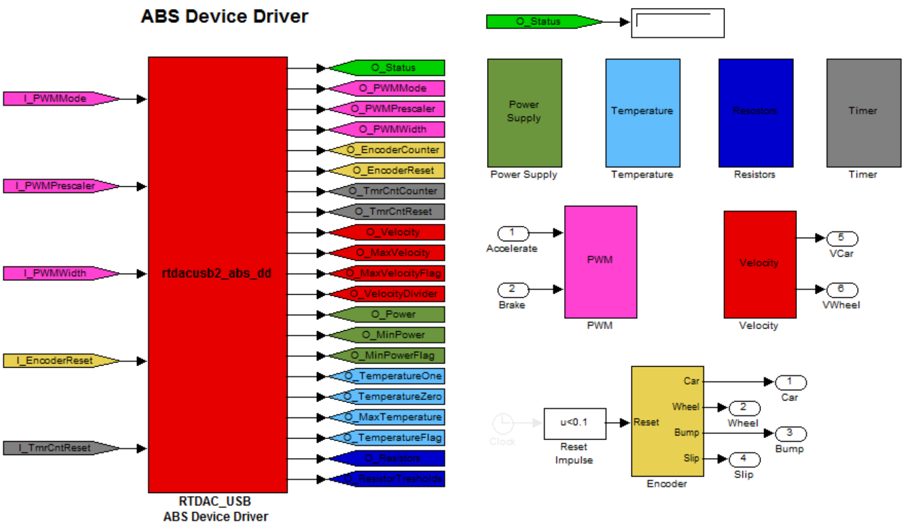


Figure 5.4: Real-time implementation architecture of ABS controller

## 5.4 Experimental Procedure

The experimental procedure describes here is followed for testing the PID, NNFBL and NNFBLPID controllers, using the same ABS test rig model. A description of the model and the parameters used are provided, followed by the experimental procedure.

### 5.4.1 Model description

The free-body diagram of the experimental rig is shown in Figure 5.5. The upper wheel represents the wheel motion while the lower wheel represents the vehicle motion. The radius of the upper wheel is $r_1$ and the radius of the lower wheel is $r_2$, while $\omega_1$ and $\omega_2$ represents the angular velocities of the upper and lower wheels respectively. The frictional force between the two wheels is given by the normal force $F_n$ multiplied by the friction coefficient $\mu$. There are three torques acting on the upper wheel, these are: the braking torque, the friction torque in the bearings and the friction torque between the wheels. Two torques act on the lower wheel; the frictional torque in the bearings and the friction torque between the wheels.

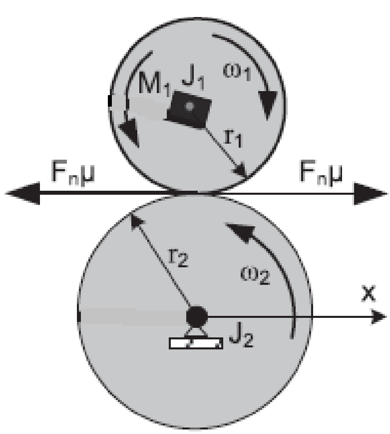


Figure 5.5: Free-body diagram of ABS test rig

The wheel slip for this set-up during braking is defined by Equation (5.1)

$$\lambda = \frac{r_2\omega_2 - r_1\omega_1}{r_2\omega_2} \tag{5.1}$$

a slip value $\lambda = 0$ indicates free rolling of the two wheels at the same angular speed, and a slip value $\lambda = 1$ indicates that the upper wheel has stopped rotating and skidding is taking place, which implies that the steering is not uncontrollable.

The friction coefficient between the two wheels is highly non-linear and is a function of the slip. Different friction models used in ABS design have been discussed in Section 1.4. However, the friction model supplied by INTECO Manual (2009) is used for the experimentation, and it is given by Equation (5.2)

$$\mu(\lambda) = \frac{c_4\lambda^p}{a + \lambda^p} + c_3\lambda^3 + c_2\lambda^2 + c_1\lambda \tag{5.2}$$

Table 5.1 presents the parameters and the numerical values for the laboratory ABS test rig.

To demonstrate the effectiveness of the proposed controller, simulations were first conducted on a Simulink® model of the experimental rig. The simulation performance of the controller is evaluated and fine-tuned to achieve the desired results. After this, the C-codes are generated, compiled and uploaded unto the micro-controller for the experimental run. Both the simulation and experimental results are provided in Section 5.6.

Table 5.1: Experimental system parameters and numerical values

| Symbol | Description | Value | Unit |
|---|---|---|---|
| $r_1$ | Radius of the upper wheel | 0.0995 | $m$ |
| $r_2$ | Radius of the lower wheel | 0.0990 | $m$ |
| $J_1$ | Moment of inertia for the upper wheel | 0.00753 | $kgm^2$ |
| $J_2$ | Moment of inertia for the lower wheel | 0.0256 | $kgm^2$ |
| $M_1$ | Static friction of the upper wheel | 0.0032 | $Nm$ |
| $M_2$ | Static friction of the lower wheel | 0.0925 | $Nm$ |
| $c_1$ | constant | -0.04240011450454 | - |
| $c_2$ | constant | 0.00000000029375 | - |
| $c_3$ | constant | 0.03508217905067 | - |
| $c_4$ | constant | 0.40662691102315 | - |
| $a$ | constant | 0.00025724985785 | - |
| $p$ | constant | 2.09945271667129 | - |

### 5.4.2 Experimental procedure

For each test run, the wheels are accelerated to a speed of approximately $68km/h$. Once the required speed is achieved, the braking process commenced. A fixed step size of $10ms$ is used for the experiments, which is the recommended value for the current experimental set-up Manual (2009) along with the fifth-order integration method. Three sets of test-run are conducted for each controller and the mean performance indices values are recorded. At the end of each test-run the data for the vehicle and wheel deceleration, applied torque, slip tracking and the stopping distances are logged to the workspace for plotting. These plots are presented in Section 5.6 and the analysis and discussion of the results is presented in Chapter 5.7. The tuning of the controllers for the HiL experimentation is described for each controller in the next section.

## 5.5 Tuning of Controllers

In this section, the tuning of the controllers is presented. Before deploying a controller to a hardware for experimentation or field testing, implementation of the controller to a simulation model is necessary for preliminary tuning of the controller. Though, perfect tuning is not obtained during this preliminary tuning, it provides a starting point for the experimentation tuning. The Simulink® model of the experimental ABS rig shown in Figure 5.6 is used for the tuning of the controllers. The process of the tuning for the PID and the NNFBL is described in the next section.

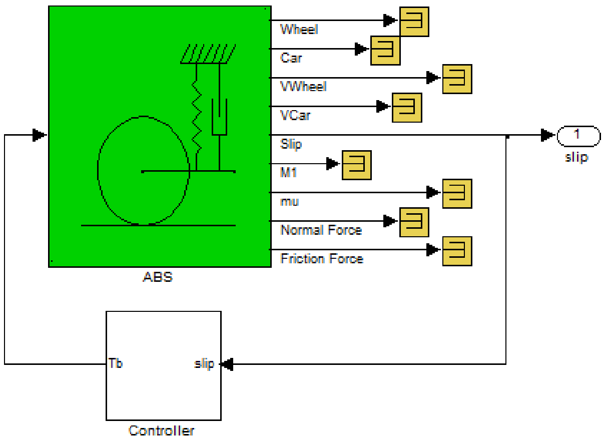


Figure 5.6: ABS rig Simulink® model

### 5.5.1 Tuning of the PID controller

The PID controller structure used for the experimentation is given by Equation (5.3),

$$U(s) = \left[ K_p \left( \frac{T_i s + 1}{T_i s} \frac{T_d s + 1}{\Psi T_d s + 1} \right) \right] E(s) \tag{5.3}$$

where $E(s)$ and $U(s)$ are the error signal and plant input signal respectively, $K_p$ is the proportional gain, $T_d$ is the derivative time constant, $T_i$ is the integral time constant and $\Psi$ is the lag factor in the derivative component of the PID.

The selection of the PID gains is carried out using the Simulink® optimization toolbox. The plant output ($\lambda$) is constrained to the desired signal response similar to the ones in Chapter 3, in-line with the performance criteria given in Section 3.1.2. A gradient descent method with a tolerance of 0.001 is used to search the optimal gains. The iterations is limited to 100, but the system stabilizes after 70 iterations. The gains are presented in Table 5.2.

Table 5.2: PID gains for ABS rig

| Parameter | Gain |
|---|---|
| $K_p$ | 5 |
| $T_i$ | 0.198223 |
| $T_d$ | 1 |
| $\Psi$ | 0.3 |

Table 5.3: System identification parameters and numerical values

| Parameters | Values |
|---|---|
| Number of layers | 2 |
| Number of hidden layer neurons | 9 |
| number of past outputs ($na$) | 2 |
| Number of past inputs ($nb$) | 2 |
| Number of iterations | 500 |
| Training algorithm | Levenberg-Marquardt |
| Sampling time | 0.01 sec |
| Maximum plant input | 1 Nm |
| Minimum plant input | 0 Nm |
| Maximum plant output | 0.4 |
| Minimum plant output | 0 |

Table 5.4: Result of system identification

| Parameters | Results |
|---|---|
| Performance (mse) | $1.99 \times 10^{-6}$ |
| Number of epoch | 6 |

### 5.5.2 Neural network controller training and adaptation

The NARMA-L2 toolbox in Matlab® / Simulink® is employed for the system identification. The structure of the neural network model, the parameters used for the neural network identification process and their numerical values are presented in Table 5.3. A sampling time of $0.01sec$ is used to conform with the micro-controller sampling time of the experimental rig. With this restriction, the results obtained are presented in Table 5.4. Figures 5.7, 5.8 and 5.9 show the plots of the training, testing and validation data respectively.

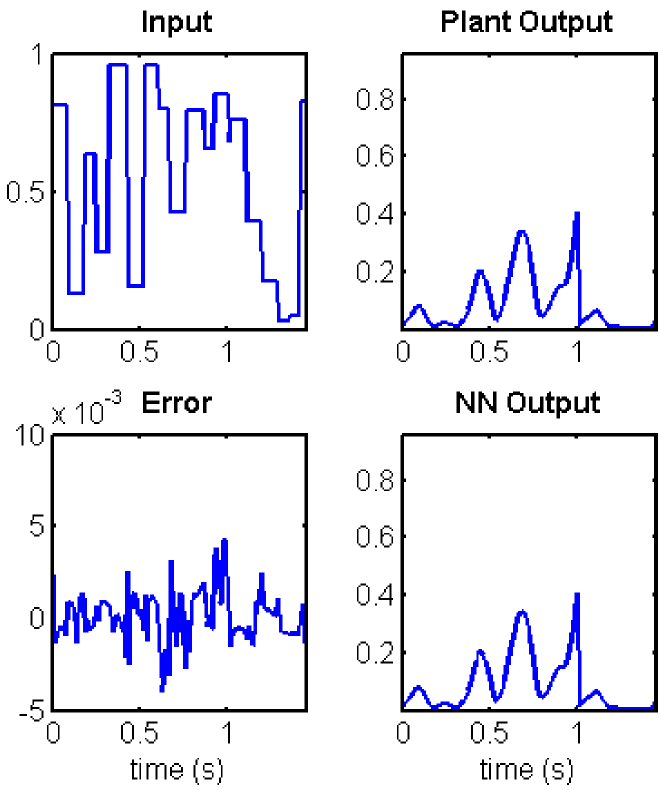


Figure 5.7: Training data for NNFBL ABS rig

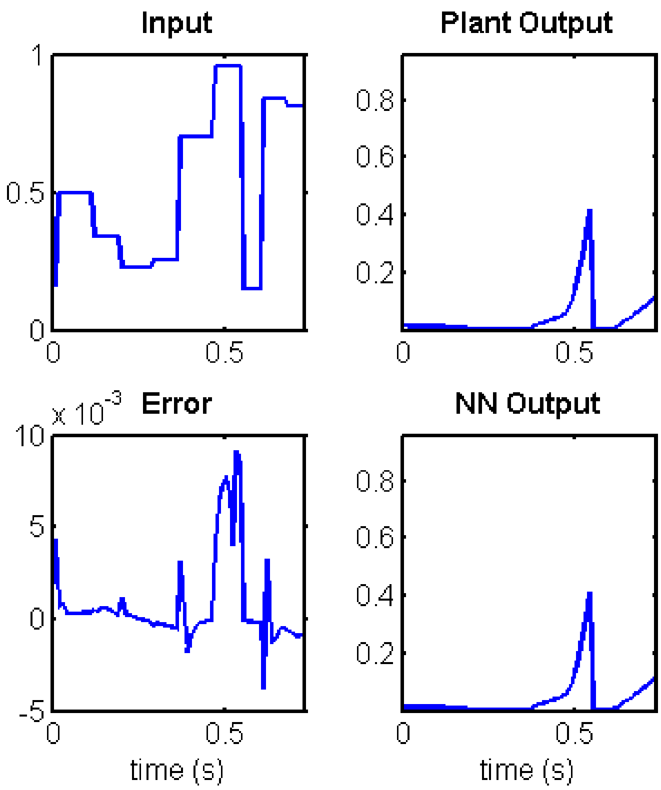


Figure 5.8: Testing data for NNFBL ABS rig

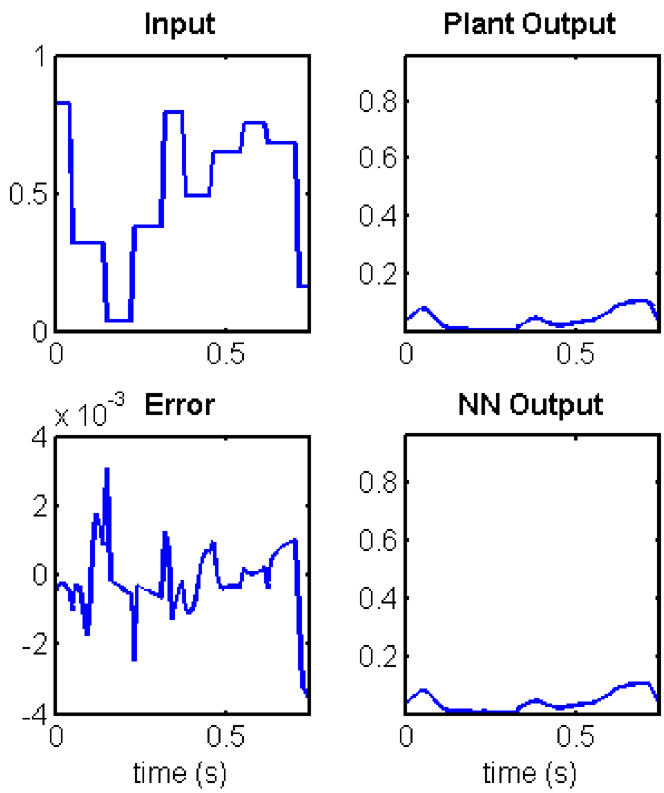


Figure 5.9: Validation data for NNFBL ABS rig

## 5.6 Experimental Results

Simulation and experimental results for three controllers will be presented: PID and the proposed NNFBL and NNFBL with PID. The current set-up does not provide the means of testing the controller on different road conditions (Topalov et al., 2011). Hence, experiments were conducted for a case of slip regulation at a desired slip value of $\lambda_d = 0.2$ and a case of slip tracking, in which the slip trajectory was varied from 0 to 0.3 to evaluate the slip tracking performance of the proposed controller, thereby imitating changes in road condition.

In the results that follow, the PID controller is used as a benchmark, because it is the most commonly used controller in industry (O'Dwyer, 2009) and it has been successfully applied to wheel slip control (Jiang and Gao, 2001; Yoo, 2006). The simulation and experimental results for each setting is presented side by side respectively.

### 5.6.1 Performance results for case of slip regulation

By slip regulation, it is inferred that no slip trajectory is imposed during the experimentation. The desired slip was set at $\lambda_d = 0.2$, braking commenced at an initial longitudinal velocity of $68km/h$ ($1500rpm$) until *rest*. However, the simulations on the background for the experimental tests continues until manually stopped. The maximum available torque from the motor is $30Nm$.

Figure 5.10 is the simulation result showing comparative plots for the case of constant slip regulation at a desired slip of $\lambda = 0.2$. The equivalent experimental plots are given in Figure 5.11. The plots for the applied torque and stopping distances are presented in Figures 5.12 and 5.14 respectively for the simulations and Figures 5.13 and 5.15 present the experimental equivalents respectively.

The deceleration of the vehicle and the wheel for the three controllers are equally presented in Figures 5.16 to 5.21

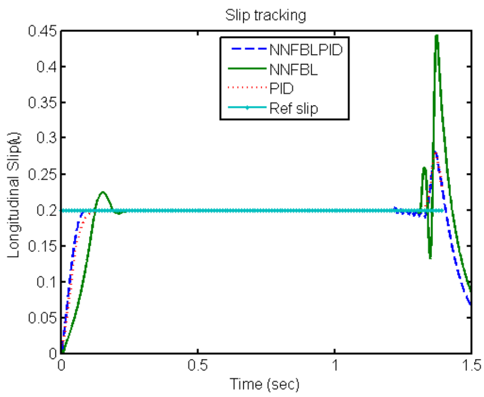


Figure 5.10: Simulation results for slip regulation at $\lambda = 0.2$

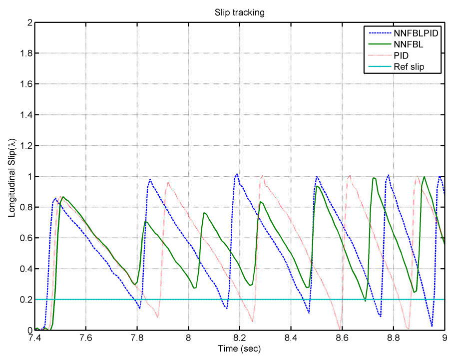


Figure 5.11: Experimental results for slip regulation at $\lambda = 0.2$

### 5.6.2 Performance results for case of slip tracking

For the case of slip tracking, a reference slip trajectory is imposed using the reference model given by Equation(4.1) for both simulation and experimentation. Like in the case of slip regulation, braking commenced at an initial longitudinal velocity of $68km/h$ ($1500rpm$) until *rest*. In this case as well, the simulations continue on the background until manually stopped. The maximum available torque from the motor is $30Nm$.

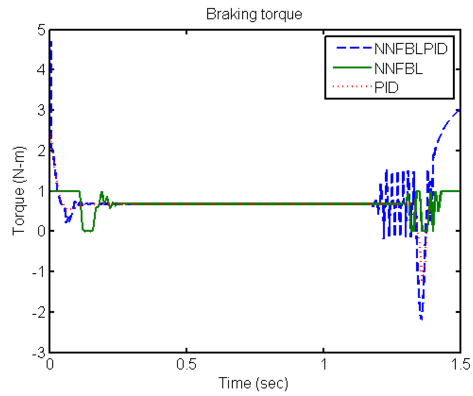


Figure 5.12: Simulation results for braking torques for the case of slip regulation

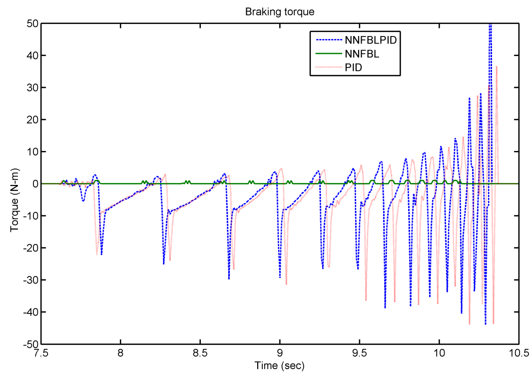


Figure 5.13: Experimental results for braking torques for the case of slip regulation

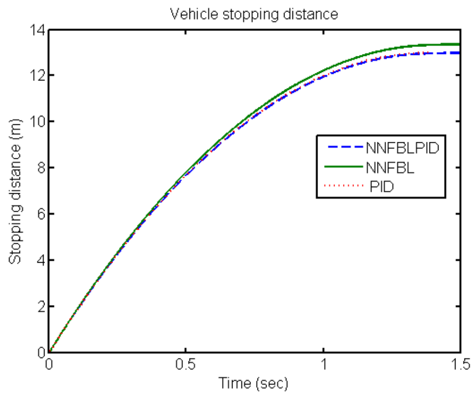


Figure 5.14: Simulation results for stopping distances for the case of slip regulation

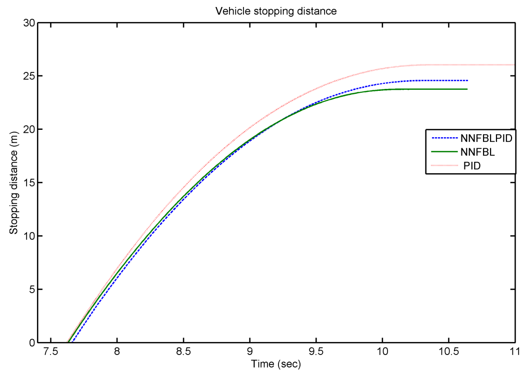


Figure 5.15: Experimental results for stopping distances for the case of slip regulation

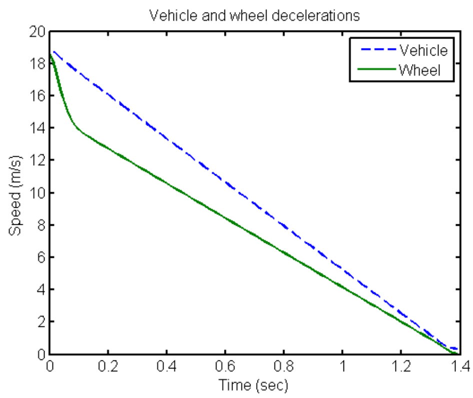


Figure 5.16: Simulation results for deceleration of vehicle and wheel using PID controller for the case of slip regulation

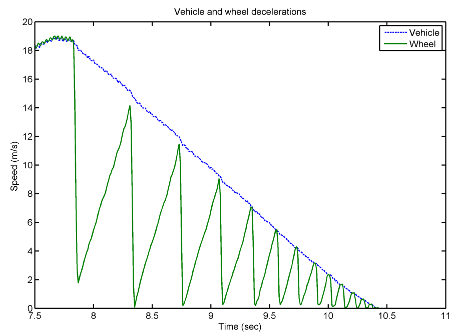


Figure 5.17: Experimental results for deceleration of vehicle and wheel using PID controller for the case of slip regulation

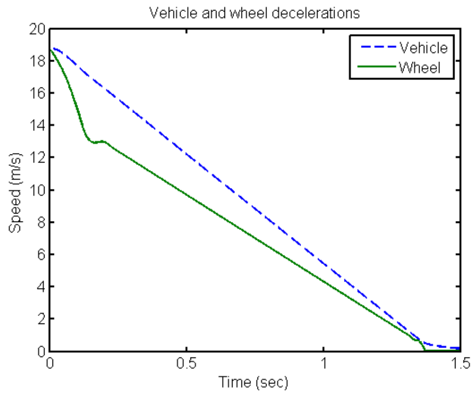


Figure 5.18: Simulation results for deceleration of vehicle and wheel using NNFBL controller for the case of slip regulation

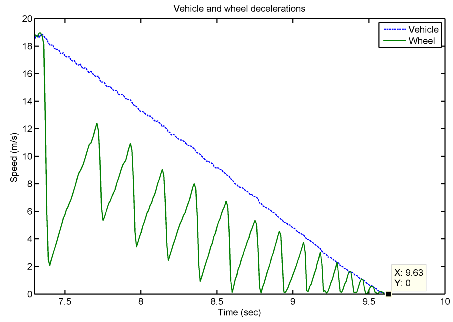


Figure 5.19: Experimental results for deceleration of vehicle and wheel using NNFBL controller for the case of slip regulation

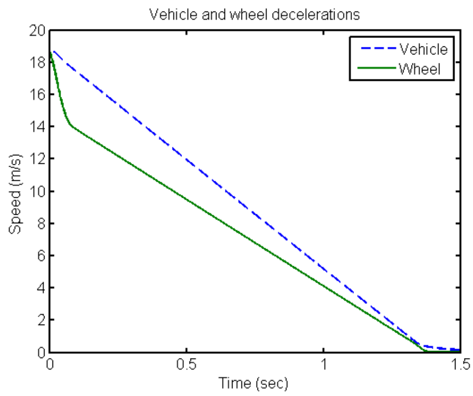


Figure 5.20: Simulation results for deceleration of vehicle and wheel using NNFBLPID controller for the case of slip regulation

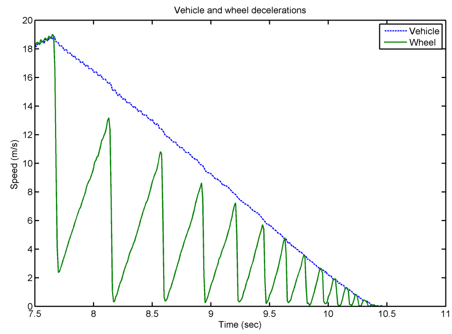


Figure 5.21: Experimental results for deceleration of vehicle and wheel using NNFBLPID controller for the case of slip regulation

Figure 5.22 is the simulation result showing comparative plots for the case of slip tracking from an initial slip of zero to a final slip value of $\lambda = 0.3$. The equivalent experimental plots are given in Figure 5.23. The plots for the applied torque and stopping distances are presented in Figures 5.24 and 5.26 respectively for the simulations and Figures 5.25 and 5.27 present the experimental equivalents respectively.

The deceleration of the vehicle and the wheel for the three controllers are equally presented in Figures 5.28 to 5.33

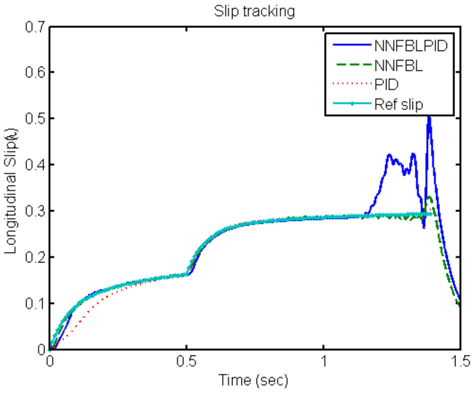


Figure 5.22: Simulation results for slip tracking

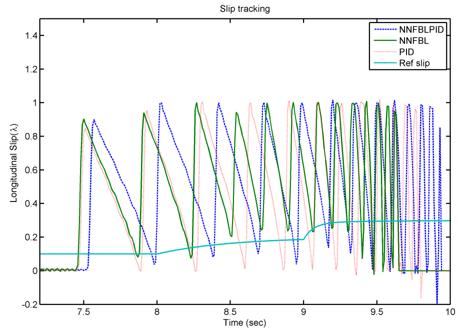


Figure 5.23: Experimental results for slip tracking

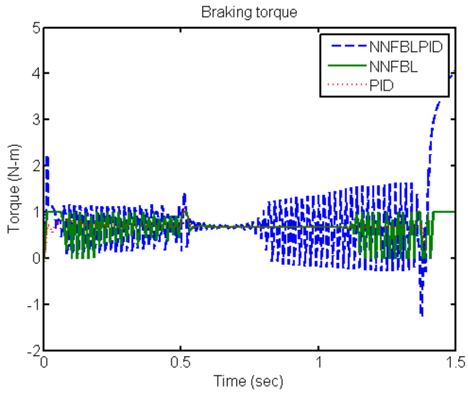


Figure 5.24: Simulation results for braking torques for the case of slip tracking

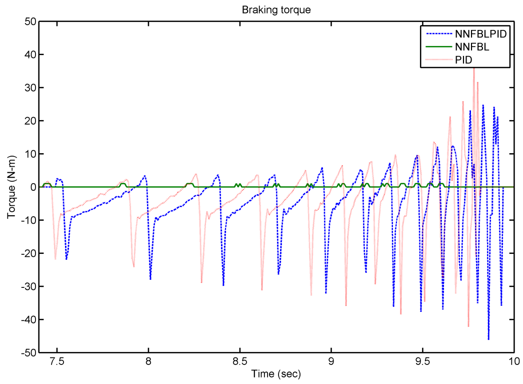


Figure 5.25: Experimental results for braking torques for the case of slip tracking

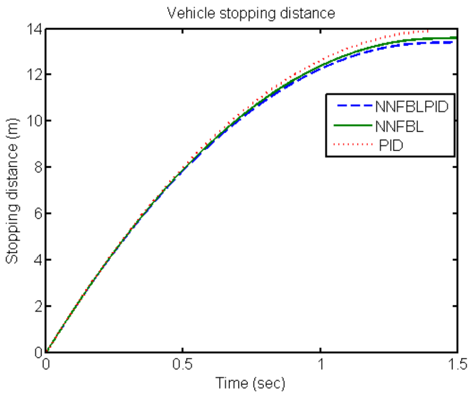


Figure 5.26: Simulation results for stopping distances for the case of slip tracking

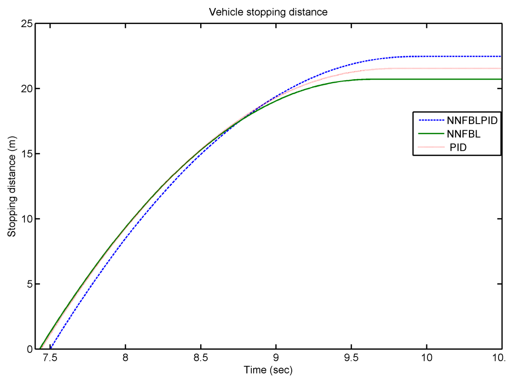


Figure 5.27: Experimental results for stopping distances for the case of slip tracking

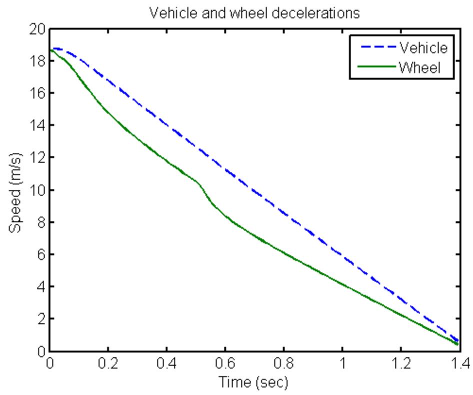


Figure 5.28: Simulation results for deceleration of vehicle and wheel using PID controller for the case of slip tracking

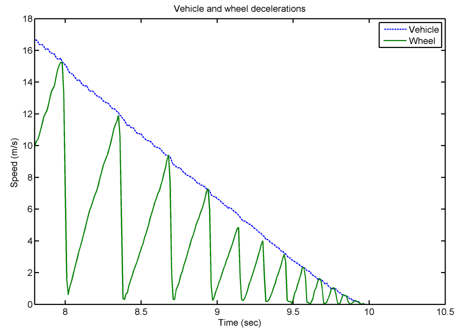


Figure 5.29: Experimental results for deceleration of vehicle and wheel using PID controller for the case of slip tracking

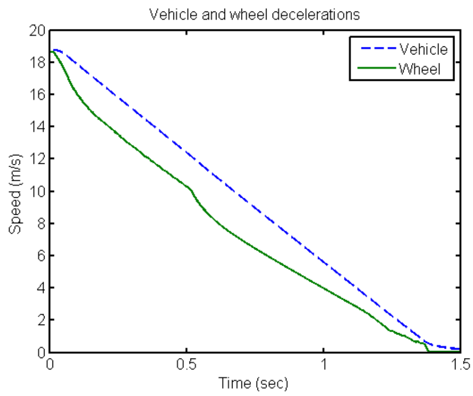


Figure 5.30: Simulation results for deceleration of vehicle and wheel using NNFBL controller for the case of slip tracking

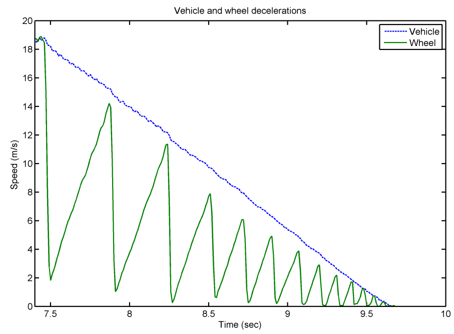


Figure 5.31: Experimental results for deceleration of vehicle and wheel using NNFBL controller for the case of slip tracking

### 5.6.3 Summary of performance results

The summary of the performance indices for the controllers for the case of slip regulation and slip tracking are presented in Tables 5.5 and 5.6 respectively for the simulation situation. The performance of each controller is evaluated on the stipulated criteria given in Section 3.1.2. For all three performance indices, the smaller the value the better the controller performance.

Tables 5.7 and 5.8 present the equivalent performance indices of the controllers in the experimental situation. It is worth mentioning that the values for the experimental situation are estimates. The reason being that the programme had to be stopped manually after the wheels come to a halt. This affects the slip tracking error and

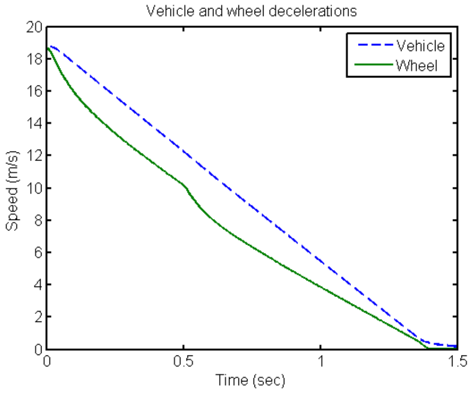


Figure 5.32: Simulation results for deceleration of vehicle and wheel using NNFBLPID controller for the case of slip tracking

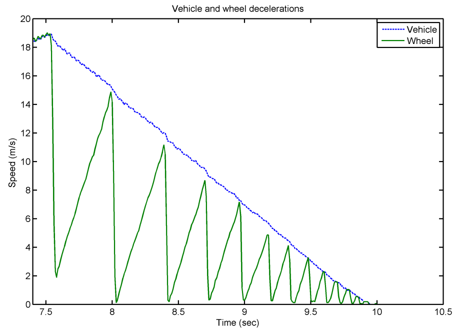


Figure 5.33: Experimental results for deceleration of vehicle and wheel using NNFBLPID controller for the case of slip tracking

Table 5.5: Performance indices for case of slip regulation in simulation

| Performance index | PID | NNFBL | NNFBLPID |
|---|---|---|---|
| Slip regulation - $\int_{t_0}^{t_f} (\lambda - \lambda_d)^2 dt$ $(10^{-3})$ | 1.233 | 3.669 | 2.543 |
| Braking torque - $\int_{t_0}^{t_f} {T_b}^2 dt$ $((Nm)^2)$ | 0.6145 | 0.6946 | 1.027 |
| Stopping distance - $\int_{t_0}^{t_f} v dt$ $(m)$ | 13.01 | 13.33 | 13.16 |

Table 5.6: Performance indices for case of slip tracking in simulation

| Performance index | PID | NNFBL | NNFBLPID |
|---|---|---|---|
| Slip tracking - $\int_{t_0}^{t_f} (\lambda - \lambda_d)^2 dt$ $(10^{-3})$ | 0.1479 | 2.308 | 0.0763 |
| Braking torque - $\int_{t_0}^{t_f} {T_b}^2 dt$ $((Nm)^2)$ | 0.383 | 0.703 | 0.705 |
| Stopping distance - $\int_{t_0}^{t_f} v dt$ $(m)$ | 13.90 | 13.57 | 13.44 |

the applied torque. This is because the slip and the braking torque become unstable towards low speeds. However, the stopping distances are more reliable indicators for this analysis.

The evaluation of these results is presented in Section 5.7.

Table 5.7: Performance indices for case of slip regulation from experiments

| Performance index | PID | NNFBL | NNFBLPID |
|---|---|---|---|
| Slip regulation -$\int_{t_0}^{t_f} (\lambda - \lambda_d)^2 dt$ | 0.7951 | 0.7356 | 0.8077 |
| Braking torque -$\int_{t_0}^{t_f} T_b{}^2 dt\ ((Nm)^2)$ | 108.5 | 39.15 | 108.7 |
| Stopping distance -$\int_{t_0}^{t_f} vdt\ (m)$ | 22.17 | 20.75 | 22.15 |

Table 5.8: Performance indices for case of slip tracking from experiments

| Performance index | PID | NNFBL | NNFBLPID |
|---|---|---|---|
| Slip tracking -$\int_{t_0}^{t_f} (\lambda - \lambda_d)^2 dt$ | 0.6397 | 0.6457 | 0.7222 |
| Braking torque -$\int_{t_0}^{t_f} T_b{}^2 dt\ ((Nm)^2)$ | 137.97 | 40.36 | 325.13 |
| Stopping distance -$\int_{t_0}^{t_f} vdt\ (m)$ | 22.15 | 21.32 | 21.77 |

## 5.7 Discussions of Experimental Results

### 5.7.1 Introduction

The main objective for the validation or verification of simulation results in an experimental test rig is to assess correlation between *theory* and *practice*. Secondly, experimental results provide some evidence for the real-life potential for a design. In this light the objectives of the ABS, which are; to achieve shorter stopping distance, provide steering wheel control by regulating the slip value around the peak friction coefficient, becomes the indicators for evaluating the experimental results in the current work. Due to the nature of the experimental results obtained, it is difficult to evaluate the slip response criteria, i.e. slip rise time, over-shoot and steady-state conditions in a quantitative manner. However, from the plots, qualitative analysis of these criteria are given. The stopping distance on the other hand is provided quantitatively. Since all controllers are tested under the same experimental conditions, the performance indices for all controllers are consistent, and hence the comparisons based on these results are valid. Speed of $68km/h$ was achieved on the rig when the wheels reached $1500rpm$ and hence was taken to be the initial speed, and braking commenced at this speed. Though higher speeds of up to $2000rpm$ could be achieved on the test rig, $1500rpm$ was chosen as a safe working speed. The results obtained through experimentation are hereby analysed. Possible sources of experimental errors are identified first, and this is followed by the discussion of the results.

### 5.7.2 Possible sources of experimental errors

Before presenting the validation results for the proposed slip control it will be expedient to identify some sources of experimental errors that could hamper the experimental results. Some sources of error are:

1. the simulation environment is in continuous time while the implementation through miro-controllers is in discrete time. Therefore, the A/D and D/A conversion required for processing the signals from continuous time to discrete time and vice-versa, introduces time delay that could degrade the performance of the controller;
2. the sampling time for the hardware implementation is $10ms$ whereas in the simulation environment the best controller performance was achieved with $0.1ms$ this accounts for the slow response of the controller in experimentation and hence the discrepancies between the the simulation and the experimental results;
3. the braking pressure is not as continuous as in electro-mechanical brake systems that are used in modern cars, the bicycle braking system used in the experiment could introduce errors on the braking torque;
4. the hydraulic hand braking system introduces additional non-linearities, which could affect the performance of the controllers. This, on the other-hand could be used to asses robustness of controllers;
5. in actual braking operation, the commanded brake pressure is usually supplied by the driver via the braking pedal, but for the experimental rig, there is no such manual initial braking pressure supplied, hence the high braking torque observed at the on-set of the braking operation;
6. the accuracy of the encoders used for measuring the speeds of the two wheels, affect the accuracy of the slip estimation.

### 5.7.3 Experimental results analysis

Experiments were conducted on the INTECO ABS laboratory equipment, using three controllers: PID, NNFBL and NNFBLPID. The PID controller is used as a benchmark controller, while the performance of the proposed NNFBL is compared to it. This work included the NNFBLPID to investigate its performance on the test rig, due to its good performance in the model-based simulation in Chapter 4. The result analysis is divided into two sections; controller performance during slip regulation and controller performance during slip tracking.

#### Performance of controllers in slip regulation

Simulations and experimentations in the case of slip regulation, is conducted at a fixed desired slip value of $\lambda_d = 0.2$. Braking commenced at an initial longitudinal velocity of $68km/h$ ($1500rpm$) until *rest*. Tuning of controllers is done in simulations, after achieving a satisfactory tuning, simulations were conducted on the Simulink® model of the experimental rig.

Figure 5.10 gives the results of the simulation results. The PID and NNFBLPID did not over-shoot, however, the NNFBL controller have an over-shoot of 12%, which is above the specified over-shoot of 5%. The best response time is $0.08sec$ and this is achieved by the PID controller. The NNFBLPID has a $0.11sec$ response time while NNFBL has $0.12sec$ response time. The two neural network-based controllers have similar convergence time while the PID outperformed them. The afore assertion is further confirmed by the low slip performance index of the PID and the relatively similar values of the NNFBL and the NNFBLPID in Table 5.5. Conversely, in experimentation, considering the plots of the slip regulation in Figure 5.11, NNFBLPID and the PID have similar performance, experiencing high slip values before the end of the experimentation. The NNFBL therefore gives a better performance, because it exhibit less slip values during the experimentation, and only towards the end that it reaches the slip peak value as expected in reality. This outcome is further confirmed with the low slip performance index of the NNFBL controller in Table 5.7.

It is however, necessary to point out that the bicycle hydraulic braking actuator used in the experiment, did not provide accurate slip regulation. This is because slip responses are sensitive to the inaccuracy of the actuator. However, the slip margin for the NNFBL is more superior in that the wheel did not lock during braking only towards the end of the braking operation when the wheels are allowed to lock.

Closely related to good slip tracking is the amount of braking torque expended to achieve it (see Figure 5.12). Since the PID controller gave a better result in simulations, it is expected that it will equally give good performance on its effective braking torque performance index. In Table 5.5, the PID has the less value on the braking torque, confirming the previous statement. Following in the same line of argument, in experimentation (see Figure 5.13), the NNFBL equally recorded the lowest effective braking torque performance index as indicated in Table 5.7.

The results of the deceleration of the vehicle and wheel in simulation are shown in Figures 5.16 ,5.18 and 5.20. The PID still retains its superiority with a stopping distance of 13.01$m$ which is less than those for NNFBL and NNFBLPID with stopping distances of 12.33$m$ and 13.16$m$ respectively. In experimentation, the NNFBL outperformed the PID and NNFBLPID controllers in slip and braking torques indices. It maintains its leads by recording the lowest stopping distance of 20.75$m$ as against 22.17$m$ and 22.15$m$ for the PID and NNFBLPID controllers respectively. The plots of the decelerations are given in Figures 5.17 ,5.19 and 5.21

### 5.7.4 Performance of controllers in slip tracking

In slip tracking, a reference slip trajectory is imposed using the reference model given by Equation(4.1) for both simulation and experimentation. This is done to imitate changes in road condition thereby evaluating the robustness of the controllers. Similar to the case of slip regulation, braking commenced at an initial longitudinal velocity of 68$km/h$ (1500$rpm$) until *rest*. There was no further tuning of the controllers to make the robustness evaluation consistent. Simulations were conducted on the Simulink® model of the experimental rig and the results compared to the experimental results.

The slip tracking plots in simulation for all three controllers are presented in Figure 5.22. A close examination of these plots reveal the PID and NFBL having a slower slip response time than the NNFBLPID. Table 5.6 indicates the NNFBLPID having the lowest slip variation performance index factor of 0.0763, with the PID and NNFBL recording 0.1479% and 2.308% values. The unstable situation towards the end of the plots is not unusual, as the simulation are run to *rest*. From the experimental plots (Figure 5.23) on the other hand, the three controllers exhibit high slip values, indicating locking of wheel for short periods of time. Using the slip performance index ( Table 5.8 ), however, reveals the PID to be leading, followed by the NNFBL controller with about 1% higher and the NNFBLPID coming last with about 12% higher than the PID.

Observing the effective braking torque plots for the simulation situation in Figure 5.24, it is immediately observed that the NNFBLPID controller exhibits more chattering than the NNFBL with the PID having no chattering effect. This is contrary to the results obtained in the model-based situation in Chapter 4. In simulations therefore, the PID recorded the lowest effective braking torque performance index, as shown in Table 5.6. Experimentation results however, recorded the NNFBL with the best index and the NNFBLPID the highest. This implies that the PID controller achieved good slip tracking at a high cost of the braking torque.

The deceleration of the vehicle and wheel in simulation for the slip tracking case are shown in Figures 5.29 ,5.31 and 5.33. In simulation as expected, based on the result of the slip and braking torque, the NNFBLPID achieved the shortest stopping distance of 13.44$m$ as against 13.90$m$ and 13.57$m$ for the PID and NNFBL controllers respectively. Though the PID controller had the best slip tracking result in experiment, this is at a high braking torque, and still it did not achieve the shortest stopping distance. The NNFBL recorded the shortest stopping distance in experiments of 21.32$m$ as against 22.15$m$ and 21.77$m$ by the PID and NNFBLPID controllers respectively.

# 6 Conclusions and Recommendations

## 6.1 Introduction

This chapter attempts to provide an over-all conclusion for the question as to which controller is best to implement further. It does this by consolidating results and discussions from previous chapters. Thus, it provides a way forward for future research.

There are several ABS control challenges that this research aimed to address (Section 1.3). The first is noise attenuation; which is common with the commercial ABS that uses table rule control method. This problem relates to the chattering of controllers. The second problem relates to robustness of the controller with respect to vehicle dynamics, road conditions and disturbance that might affect the control performance. Thirdly, the accuracy in slip tracking should be improved by future ABS controllers. Improving these factors will result in ride comfort, control of the steering wheel and shorter braking distance in emergency braking. Another problem associated with the commercial ABS is the long tuning time (Solyom, 2002). This last aspect is evaluated on the basis of the fine tuning that is required during hardware-in-the-loop (HIL) simulation.

In general, the work is consistent with other authors (Mirzaeinejad and Mirzael, 2011; Nyandoro et al., 2011; Poursamad, 2009) following the simulation results and test rig (Oniz et al., 2009; Precup et al., 2010; Topalov et al., 2011).

This work proposes a hybrid control (FBLPID) system and a neural-network based slip control (NNFBL) for use in ABS. Simulation implementation of both controllers is carried out. Comparative analyses of the controllers against the performance of a PID controller is presented in Chapter 4. Experimental validation of the NNFBL is conducted on a laboratory ABS test rig. The experimental results and analyses are presented in Chapters 5 and 5.7 respectively. Though some experimental errors are identified in Section 5.7.2, these errors are assumed to be consistent for all controllers. Therefore, the comparative analyses and conclusions are fair for all controllers.

## 6.2 Conclusions

Conclusions are based on the three performance indices used to evaluate the controllers: slip tracking variation, effective braking torque and the stopping distance. These indices relate to the research problem and the research objectives (Section 1.6). For example, a controller whose slip tracking performance is consistent on different road conditions is considered robust. The chattering effect is analysed by observation, in addition, a minimum effective braking torque performance index is an indication of the effectiveness of the controller. The stopping distance is also expected to be shortened.

To enable over-all conclusion, the *weighted objective method* (Cross, 2008) is employed. Accordingly, the performances of all controllers are rated on a scale of 5 to 1, with 5 points awarded to the best performed controller, 3 points to the second best controller, 2 points to the third best and 1 point to the worst performed controller. This ranking is applied to the slip variations (SV), braking torque (BT) and stopping distance (SD) performance indices on an equal weighting. Small or large margins in each performance index is treated the same. Differences are used to give qualitative conclusions. Table 6.1 presents the performance rankings of the controllers, for the model-based simulations (in Chapter 4).

For the model-based results presented and discussed in Chapter 4, the over-all performance of the proposed hybrid FBLPID controller is rated the best performed controller on high and medium road conditions while the FBL is the best on the low friction road, with a low margin of 2 points against the proposed FBLPID. The FBL performed poorer on high and medium road conditions and exhibits high chattering on the braking torque. The PID is the second best controller while the second proposed NNFBL controller comes third place. It is therefore concluded that the proposed FBLPID controller is the best controller for the ABS in the model-based

Table 6.1: Performance rankings of controllers (Model-based simulation)

| - | PID | | | FBL | | | FBLPID | | | NNFBL | | |
|---|---|---|---|---|---|---|---|---|---|---|---|---|
| Road condition | SV | BT | SD | SV | BT | SD | SV | BT | SD | SV | BT | SD |
| High friction | 1 | 5 | 2 | 2 | 2 | 1 | 5 | 3 | 5 | 3 | 1 | 3 |
| Medium friction | 2 | 5 | 2 | 1 | 2 | 1 | 3 | 3 | 5 | 5 | 1 | 3 |
| Low friction | 1 | 5 | 3 | 3 | 2 | 5 | 2 | 3 | 3 | 5 | 1 | 3 |
| Total | 4 | 15 | 7 | 6 | 6 | 7 | 10 | 9 | 13 | 13 | 3 | 9 |
| Over-all performance | 26 | | | 19 | | | 32 | | | 25 | | |

simulation results. It is also relatively more robust considering its consistent superior performance on all road conditions and the highly reduced chattering.

In Chapter 5, three controllers namely; PID, NNFBL and NNFBLPID are evaluated in hardware-in-the-loop (HiL) simulations. Simulations on the Simulink® model of the laboratory rig, is used to tune the controllers. The simulation and experimental results are categorised into slip regulation and slip tracking . The ranking of the controllers is based on a scale of 5 to 1, with 5 points awarded to the best performing controller, 3 points to the second best controller and 1 point to the worst performing controller. The rankings are presented in Tables 6.2 and 6.3 for laboratory rig simulation and HiL validation respectively. The PID scored the highest points in slip regulation while the NNFBLPID outperformed the PID and NNFBL in slip tracking scenario. The proposed NNFBL did not do so well on the laboratory rig simulations for both slip regulation and slip tracking. On the contrary, in HiL validation, the proposed NNFBL controller maintain a good lead on all performance indices. On the over-all performance, it scores 28 points against the 16 and 10 points scored by the PID and NNFBLPID controllers respectively. Though the PID is rated best in laboratory rig simulations and second best in HiL validation, its major short-coming is that it requires fine tuning in the HiL validation, whereas the proposed NNFBL does not require any fine tuning after the initial tuning. The proposed NNFBL therefore is concluded to be more robust, and a better controller due to its consistent superior performance in slip regulation and slip tracking in HiL validation. The HiL validation results are more indicative of real situations. The NNFBL controller also needs less tuning time due to its adaptation to un-modeled dynamics and external disturbances. This will reduce the associated cost.

Table 6.2: Performance rankings of controllers (Laboratory ABS model-based simulation)

| - | PID | | | NNFBL | | | NNFBLPID | | |
|---|---|---|---|---|---|---|---|---|---|
| Condition | SV | BT | SD | SV | BT | SD | SV | BT | SD |
| Slip regulation | 5 | 5 | 5 | 1 | 3 | 1 | 3 | 1 | 3 |
| Slip tracking | 3 | 5 | 1 | 1 | 3 | 3 | 5 | 1 | 5 |
| Total | 8 | 10 | 6 | 2 | 6 | 4 | 8 | 2 | 8 |
| Over-all performance | 24 | | | 12 | | | 18 | | |

Table 6.3: Performance rankings of controllers (Validation HiL simulation)

| - | PID | | | NNFBL | | | NNFBLPID | | |
|---|---|---|---|---|---|---|---|---|---|
| Condition | SV | BT | SD | SV | BT | SD | SV | BT | SD |
| Slip regulation | 3 | 3 | 1 | 5 | 5 | 5 | 1 | 1 | 3 |
| Slip tracking | 5 | 3 | 1 | 3 | 5 | 5 | 1 | 1 | 3 |
| Total | 8 | 6 | 2 | 8 | 10 | 10 | 2 | 2 | 6 |
| Over-all performance | 16 | | | 28 | | | 10 | | |

This thesis proposes a hybrid (FBLPID) and a neural network-based feedback linearization (NNFBL) slip control for application in ABS. The work covered, mathematical modeling, controller design and implementation of a model-based slip control using simulation and a laboratory ABS test bench. The FBLPID controller is evaluated in simulations and the NNFBL controller is evaluated in model-based simulation and with hardware-in-the-loop (HIL) experimentation. The proposed controllers exhibit good performances with respect to the objectives of slip control; they achieved relatively shorter stopping distances and exhibit good convergence of slip tracking. The NNFBL controller outperforms the PID in HiL experimentation and is the control of choice.

The results obtained from this work reveal that slip regulation using neural network-based controllers is feasible for different optimum slip values, and is robust to external disturbances. Hence, it is concluded that the proposed NNFBL solution demonstrates potential for implementation.

## 6.3 Recommendations for Future Work

There are a number of issues that are of interest not covered in this thesis. These have both theoretical and practical aspects. The proposed controller was tested on a laboratory test rig with the aim of correlating theory with practice, and not aimed at producing a prototype. Hence limited test runs were conducted and full evaluation of the controllers on a real vehicle was not carried out. A simple straight line braking was considered as the laboratory equipment can only be used for such an operation. However, a braking and cornering manoeuvre would be an interesting aspect to be investigated. Therefore, the following are recommended for future work.

1. The quarter-car model used in this work is sufficient for the current investigation. However, to move towards producing a prototype controller, a half-car or full-car model is recommended.

2. Some system dynamics that were not modeled in this work will be worthwhile considering. These are: the suspension dynamics and pitching effect which could improve the robustness of the controller and enhance its performance. Other dynamics to be considered include side-slip and the yaw rate.

3. It is recommended that further work should involve testing of the ABS controller on an actual vehicle.

4. Improvement in experimental results may be achieved if the experimental test rig uses an electro-mechanical braking system, that gives a more accurate continuous braking pressure. This is recommended for incorporation into the ABS laboratory test equipment.

5. Further investigation to be made into other hybrid systems; exploring intelligent with traditional control schemes.

# REFERENCES

Adaryani, M. R. and Afrakhte, H. (2011), NARMA-L2 controller for three-area load frequency control, *in* 'Proceedings of the 19th Iranian IEEE Conference on Electrical Engineering (ICEE), Tehran, Iran', pp. 1 –6.

Akbarimajd, A. and Kia, S. (2010), NARMA-L2 controller for 2-DoF underactuated planar manipulator, *in* 'Proceedings of the 11th International Conference on Control, Automation, Robotics and Vision, Singapore', pp. 195 – 200.

Alleyne, A. (1997), "Improved vehicle performance using combined suspension and braking forces", *Vehicle System Dynamics: International Journal of Vehicle Mechanics and Mobility* , Vol. 27, No. 4, pp. 235–265.

Aly, A. A. (2010), Intelligent fuzzy control for antilock brake system with road-surfaces identifier, *in* 'Proceedings of the International Conference on Mechatronics and Automation (ICMA), 2010 , Xian, China', pp. 699 –705.

Aly, A. A., Zeidan, E.-S., Hamed, A. and Salem, F. (2011), "An Antilock Braking Systems (ABS) control: A Technical Review", *Intelligent Control and Automation* , Vol. 2, No. 3, pp. 186 –195.

Anwar, S. (2004), An anti-lock braking control system for a hybrid electromagnetic/electrohydraulic brake-by-wire system, *in* 'Proceedings of the American Control Conference, Boston MA, USA', Vol. 3, pp. 2699 –2704.

Assadian, F. (2001), "Mixed $H_\infty$ and fuzzy logic controllers for the automobile ABS", *SAE Technical Paper 2001-01-0594* .

Austin, L. and Morrey, D. (2000), "Recent advances in antilock braking systems and traction control systems", *Proceedings of the Institution of Mechanical Engineers, Part D: Journal of Automobile Engineering* , Vol. 214, No.D6, pp. 625–638.

Awwad, A., Abu-Rub, H. and Toliyat, H. (2008), Nonlinear autoregressive moving average (NARMA-L2) controller for advanced ac motor control, *in* 'Proceedings of the 34th IEEE Conference on Industrial Electronics, IECON 2008, Orlando, Florida, USA', pp. 1287 –1292.

Bakker, E., Pacejka, H. and Lidner, L. (1989), "A new tire model with an application in vehicle dynamics studies", *SAE Technical Paper* , pp. 83 – 95.

Ball, S., Barany, E., Schaffer, S. and Wedeward, K. (2005), Nonlinear control of power network models using feedback linearization, *in* V. G. Oklobdzija, ed., 'Proceedings of the Third IASTED International Conference on Circuits, Signals and Systems, Marina CA, USA', pp. 493 – 800.

Behera, L. and Kar, I. (2009), *Intelligent Systems and Control Principles and Applications*, Oxford University Press, India.

Benine-Neto, A., Scalzi, S., Mammar, S. and Netto, M. (2010), Dynamic controller for lane keeping and obstacle avoidance assistance system, *in* 'Proceedings of the Intelligent Transportation Systems (ITSC), 2010 13th International IEEE Conference, Raffles City, Singapore', pp. 1363 –1368.

Berzeri, M., Dhir, A., Ranganathan, R., Balendran, B., Jayakumar, P. and O'Heron, P. J. (2004), A new tire model for road loads simulation: Full vehicle validation, *in* 'Proceedings of the ABS/TCS, Brake Technology and Foundation Brake NVH, and Tire and Wheel Technology', SAE Technical Paper 2004-01-1579, pp. 1 – 5.

Bevan, G. P., Gollee, H. and J, O. (2010), Trajectory generation for road vehicle obstacle avoidance using convex optimization, *in* 'Proceedings of the IMechE Part D:J. Automobile Engineering', Vol. 224 No.4, pp. 455 –473.

Bhattacharyya, S., Chapellat, H. and Keel, L. (1995), *Robust Control The Parametric Approach*, Prentice-Hall, Upper Saddle, NJ, USA.

Bian, M., Li, K., Feng, N. and Lian, X. (2004), "An empirical model for longitudinal tire-road friction estimation", *SAE Technical Paper 2004-01-1082* .

Bruckner, S. and Rudolph, S. (2000), Neural networks applied to smart structure control, *in* 'Proceedings of SPIE, San Jose, CA, USA', Vol. 4055, pp. 288 – 298.

Buckholtz, K. R. (2002), "Reference input wheel slip tracking using sliding mode control", *SAE Technical Paper* .

Burton, D., Delaney, A., Newstead, S., Logan, D. and Fildes, B. (2004), Effectiveness of ABS and vehicle stability control systems, Technical report, Royal Automobile Club of Victoria (RACV) Ltd.

Canudas-de Wit, C. and Horowitz, R. (1999), Observers for tire/road contact friction using only wheel angular velocity information, *in* 'Proceedings of the 38th IEEE Decision and Control Conference, Phoenix, Arizona, USA', Vol. 4, pp. 3932 –3937.

Canudas-de Wit, C. and Tsiotras, P. (1999), Dynamic tire friction models for vehicle traction control, *in* 'Proceedings of the 38th IEEE Conference on Decision and Control, Phoenix, Arizona, USA', Vol. 4, pp. 3746 –3751.

Cao, J., Liu, H., Li, P. and D.J., B. (2008), "State of the art in vehicle active suspension adaptive control systems based on intelligent methodologies", *IEEE Transactions on Intelligent Transportation Systems* , Vol. 9, No. 3, pp. 392 –405.

Cetinkunt, S. (2007), *Mechatronics*, John Wiley & sons, Inc., Hoboken, NJ, USA.

Chang, S. (2007), A Flexible Hierarchical Model-based Control Methodology for Vehicle Active Safety Systems, PhD thesis, The University of Michigan, Michigan, USA.

Chen, Y. and Wang, J. (2011), "Adaptive vehicle speed control with input injections for longitudinal motion independent road frictional condition estimation", *IEEE Transactions on Vehicle Technology* , Vol. 60, No.3, pp. 839 –848.

Chikhi, F., El Hadri, A. and Cadiou, J. (2005), ABS control design based on wheel-slip peak localization, *in* 'Proceedings of the Fifth International Workshop on Robot Motion and Control RoMoCo2005, Dymaczewo, Poland', pp. 73 – 77.

Claeys, X., Yi, J., Alvarez, L., Horowitz, R. and de Wit, C. (2001), A dynamic tire/road friction model for 3D vehicle control and simulation, *in* 'Proceedings of the IEEE Intelligent Transportation Systems Conference, Oakland, CA, USA', pp. 483 –488.

Cross, N. (2008), *Engineering Design Methods: strategies for product design*, John Wiley & Sons, Ltd., West Sussex PO19 8SQ, England.

Dietsche, K. and Klingebiel, M. (2007), *Automotive Handbook*, 7 edn, Robert Bosch GmbH, Plochingen, Germany.

Emereole, O. C. (2004), Antilock Performance Comparison Between Hydraulic and Electromechanical Brake Systems, PhD thesis, University of Melbourne, Australia.

Fritzson, P., Gunnarsson, J. and Jirstrand, M. (2002), Mathmodelica: An extensible modeling and simulation environment with integrated graphics and literate programming, *in* 'Proceedings of the 2nd International Modelica Conference, Deutsches Zentrum Fur Luft-und Raumfahr e.V (DLR), Germany', pp. 41 – 54.

Garces, F., Becerra, V. M. and Warwick, K. (2003), *Strategies for Feedback Linearisation, A Dynamic Neural Network Approach*, Springer, London, Great Britain.

Garcia, D., Karimi, A., Longchamp, R. and Dormido, S. (2006), PID controller design with constraints on sensitivity functions using loop slope adjustment, *in* 'Proceedings of the 2006 American Control Conference, Minneapolis, Minnesota, USA', pp. 268 – 273.

Gillespie, T. D. (1992), *Fundamentals of Vehicle Dynamics*, Society of Automotive Engineers, Inc, Warrendale, PA, USA.

Hagan, M. T., Demuth, H. B. and De-Jesus, O. (2002), "An introduction to the use of neural networks in control systems", *International Journal of Robust and Nonlinear Control* , Vol. 12, No. 11, pp. 959–985.

Hattori, Y., Ono, E. and Hosoe, S. (2006), "Optimum vehicle trajectory control for obstacle avoidance problem", *IEEE/ASME Transactions on Mechatronics* , Vol. 11, No. 5, pp. 507 –512.

Hedrick, J. and Girard, A. (2005), *Feedback Linearization.*
**URL:** *http://www.me.berkeley.edu/ME237/8feedbacklin.pdf, November 2011*

Henson, M. A. and Seborg, D. E. (1997), *Nonlinear Process Control*, Prentice-Hall, NJ, USA.

Hertz, E. (1998), Analysis of the crash experiences of vehicles equipped with antilock braking systems - an update, Technical report, U.S. Department of Transportation, NHTSA.

Hertz, E. (2000), Analysis of the crash experience of vehicles equipped with all wheel antilock braking systems (ABS)- a second update including vehicles with optional ABS, Technical report, U.S. Department of Transportation, NHTSA.

Hornik, K. M., Stinchcombe, M. and White, H. (1989), "Multilayer feedforward networks are universal approximators", *Journal of Neural Networks* , Vol. 2, No. 5, pp. 359 – 366.

Hsu, C.-F., Lee, T.-T., Hsu, C.-Y. and Lin, C.-M. (2008), Neurocontroller design and stability analysis for antilock braking systems, *in* 'Proceedings of the IEEE International Conference on Systems, Man and Cybernetics (SMC), Singapore', pp. 3388 –3393.

Jiang, F. and Gao, Z. (2001), An application of nonlinear PID control to a class of truck ABS problems, *in* 'Proceedings of the 40th IEEE Conference on Decision and Control, Orlando, Florida, USA', Vol. 1, pp. 516 –521.

Jing, Y., Mao, Y., Dimirovski, G., Zheng, Y. and Zhang, S. (2009), Adaptive global sliding mode control strategy for the vehicle antilock braking systems, *in* 'Proceedings of the American Control Conference (ACC '09), Missouri, USA', pp. 769 –773.

Johansen, T., Kalkkuhl, J., Ludemann, J. and Petersen, I. (2001), Hybrid control strategies in ABS, *in* 'Proceedings of the American Control Conference, Virginia, USA', Vol. 2, pp. 1704 –1705.

Johansen, T., Petersen, I., Kalkkuhl, J. and Ludemann, J. (2003), "Gain-scheduled wheel slip control in automotive brake systems", *IEEE Transactions on Control and Systems Technology* , Vol. 11, No. 6, pp. 799 – 811.

John, S. and Pedro, J. (2006), Review of tyre/road friction coefficient estimation for abs controller design, *in* 'Proceedings of the Fifth South African Conference on Computational and Applied Mechanics, Cape Town, South Africa'.

John, S. and Pedro, J. O. (2011), Performance of vehicle wheel slip controller combined with passive suspension system, *in* 'Proceedings of the IEEE International Conference (AFRICON), Livingstone, Zambia', pp. 1–6.

John, S., Pedro, J. O. and Koczy, L. (2011), Adaptive improvement of a passive antilock brake control, *in* 'Proceedings of the IEEE International Conference (AFRICON), Livingstone, Zambia'.

John, S., Pedro, J. and Pozna, C. (2011), Enhanced slip control performance using nonlinear passive suspension system, *in* 'Proceedings of the IEEE/ASME International Conference on Advanced Intelligent Mechatronics (AIM), Budapest, Hungary', pp. 277 –282.

Jun, C. (1998), The study of ABS control system with different control methods, *in* 'Proceedings of the 4th International Symposium on Advanced Vehicle Control, Nagoya, Japan', pp. 623 – 628.

Kahane, C. J. (1994), Preliminary evaluation of the effectiveness of antilock brake systems for passenger cars, Technical report, U.S. Department of Transportation, NHTSA.

Kayacan, E., Oniz, Y. and Kaynak, O. (2009), "A grey system modeling approach for sliding-mode control of antilock braking system", *IEEE Transactions on Industrial Electronics* , Vol. 56, No. 8, pp. 3244 –3252.

Kienhofer, F., Miller, J. and Cebon, D. (2008), "Design concept for an alternative heavy vehicles ABS system", *Vehicle System Dynamics: International Journal of Vehicle Mechanics and Mobility* , Vol. 46, No.51, pp. 571 – 583.

Lacombe, J. (2000), Tire model for simulations of vehicle motion on high and low friction road surfaces, *in* 'Simulation Conference Proceedings, Orlando, FL, USA', Vol. 1, pp. 1025 –1034.

Li, J., Yibo, Z. and Haipeng, P. (2008), Chattering-free grey sliding mode control for discrete time-delay systems with unmatched uncertainty, *in* 'Proceedings of the 3rd International Conference on Intelligent System and Knowledge Engineering (ISKE), Xiamen, China', Vol. 1, pp. 983 –986.

Li, L., Wang, F.-Y. and Zhou, Q. (2006), "Integrated longitudinal and lateral tire/road friction modeling and monitoring for vehicle motion control", *IEEE Transactions on Intelligent Transportation Systems* , Vol. 7, No. 1, pp. 1 –19.

Lidner, L. (1993), Experience with the magic formula tyre model, *in* H. B. Pacejka, ed., 'Proceedings of 1st International Colloquium on Tyre Models for Vehicle Dynamics Analysis (Supplement to Vehicle System Dynamics )', Vol. 21, SWETS & ZEITLINGER B.V. AMSTERDAM / LISSE, pp. 30– 46.

Lin, C.-M. and Hsu, C.-F. (2003), "Neural-network hybrid control for antilock braking systems", *IEEE Transactions on Neural Networks* , Vol. 14, No. 2, pp. 351 – 359.

Lin, J.-S. and Ting, W.-E. (2007), "Nonlinear control design of anti-lock braking systems with assistance of active suspension", *Control Theory Applications, IET* , Vol. 1, No. 1, pp. 343 –348.

Liu, Z. and Luo, C. (2006), Road adaptive active suspension control design, *in* 'Proceedings of the Multiconference on Computational Engineering in Systems Applications, IMACS, Beijing, China', pp. 1347 –1350.

Lu, H.-C. (2004), Grey prediction approach for designing grey sliding mode controller, *in* 'Proceedings of IEEE International Conference on Systems, Man and Cybernetics, Hague, The Netherlands', Vol. 1, pp. 403 – 408.

MacIsaac Jr, J. D. and Garrot, W. R. (2002), Preliminary findings of the effect of tire inflation pressure on the peak and slide coefficients of friction, Technical report, National Highway Traffic Safety Administration, 400 Seventh St., S.W. Washington, D.C. 20590, USA.

Manual, U. (2009), *The laboratory antilock braking system controlled from PC*, Inteco Ltd., Crakow, Poland.

Mao, Y., Stojanovski, G., Jing, Y., Stankovski, M. and Dimirovski, G. (2010), Sliding mode controller employing RBF-ANN for vehicle anti-lock braking system, *in* ‘Proceedings of the 14th International Conference on Power Electronics and Motion Control (EPE/PEMC), Ohrid, Macedonia’, pp. T10–55 –T10–60.

Mirzaei, A., Moallem, M., Dehkordi, B. and Fahimi, B. (2006), “Design of an optimal fuzzy controller for antilock braking systems”, *IEEE Transactions on Vehicular Technology* , Vol. 55, No. 6, pp. 1725 –1730.

Mirzaeinejad, H. and Mirzaei, M. (2010), “A novel method for non-linear control of wheel slip in anti-lock braking systems”, *Control Engineering Practice* , Vol. 18, No. 8, pp. 918 – 926.

Mirzaeinejad, H. and Mirzael, M. (2011), “A new approach for modelling and control of two-wheel anti-lock brake system”, *Proceedings of the Institution of Mechanical Engineers, Part K: Journal of Multi-body dynamics* , Vol. 225, No. 2, pp. 179 – 192.

Norgaard, M. (2000), Neural network based system identification toolbox, Technical report, Department of Automation, Technical University of Denmark.

Norgaard, M., Ravn, O., Poulsen, N. and Hansen, L. (2003), *Neural Networks for Modelling and Control of Dynamic Systems: A Practitioner’s Handbook*, Springer-Verlag, London.

Nyandoro, O. T., Pedro, J. O., Dahunsi, O. A. and Dwolatzky, B. (2011), Linear slip control formulation for vehicular anti-lock braking system with suspension effects, *in* ‘Proceedings of the 18th IFAC World Congress, Milano, Italy’, pp. 4779 – 4784.

O’Dwyer, A. (2009), *Handbook of PI and PID Controller Tuning Rules*, 3rd edn, Imperial College Press, London.

Ogata, K. (2002), *Modern Control Engineering*, fourth edn, Prentice-Hall, Inc. Upper Saddle River, New Jersey.

Olson, B. J. (2001), Nonlinear dynamics of longitudinal ground vehicle traction, Master’s thesis, Michigan State University, USA.

Oniz, Y., Kayacan, E. and Kaynak, O. (2007), Simulated and experimental study of antilock braking system using grey sliding mode control, *in* ‘IEEE International Conference on Systems, Man and Cybernetics (ISIC), Montreal, Canada’, pp. 90 –95.

Oniz, Y., Kayacan, E. and Kaynak, O. (2009), “A dynamic method to forecast the wheel slip for antilock braking system and its experimental evaluation”, *IEEE Transactions on Systems, Man, and Cybernetics, Part B: Cybernetics* , Vol. 39, No. 2, pp. 551 –560.

Oosten, J. V. and Bakker, E. (1993), Determination of magic tyre model parameters, *in* H. B. Pacejka, ed., 'Proceedings of 1st International Colloquium on Tyre Models for Vehicle Dynamics Analysis (Supplement to Vehicle System Dynamics Vol. 21)', Vol. 21, SWETS & ZEITLINGER B.V. AMSTERDAM / LISSE, pp. 19–29.

Pacejka, H. and Bakker, E. (1993), The magic formula tyre model, *in* H. B. Pacejka, ed., 'Proceedings of 1st International Colloquium on Tyre Models for Vehicle Dynamics Analysis (Supplement to Vehicle System Dynamics Vol. 21)', Vol. 21, SWETS & ZEITLINGER B.V. AMSTERDAM / LISSE, pp. 1–18.

Park, K.-S. and Lim, J.-T. (2008), Wheel slip control for ABS with time delay input using feedback linearization and adaptive sliding mode control, *in* 'Proceedings of the International Conference on Control, Automation and Systems (ICCAS), Seoul, Korea', pp. 290 –295.

Patil, C., Longoria, R. and Limroth, J. (2003), Control prototyping for an anti-lock braking control system on a scaled vehicle, *in* 'Proceedings of the 42nd IEEE Conference on Decision and Control, Hawaii, USA', Vol. 5, pp. 4962 – 4967.

Pedro, J., Nyandoro, O. and John, S. (2009), Neural network-based feedback linearisation slip control of an anti-lock braking system, *in* 'Proceedings of the 7th Asian Control Conference ( ASCC), Hong Kong', pp. 1251 –1257.

Petersen, I. (2003), Wheel Slip Control in ABS Brakes Using Gain Scheduled Optimal Control with Constraints, PhD thesis, Department of Enginnering Cybernetics, Norwegian University of Science and Technology, Trondheim, Norway.

Poursamad, A. (2009), "Adaptive feedback linearization control of antilock braking systems using neural networks", *Mechatronics* , Vol. 19, No. 5, pp. 767 – 773.

Precup, R. E., Spataru, S., Petriu, E. M., Preitl, S., Radac, M.-B. and Dragos, C.-A. (2010), Stable and optimal fuzzy control of a laboratory antilock braking system, *in* 'Proceedings of the IEEE/ASME International Conference on Advanced Intelligent Mechatronics (AIM), Montreal, Canada', pp. 593 –598.

Pukrittayakamee, A., De Jesus, O. and Hagan, M. (2002), Smoothing the control action for NARMA-L2 controllers, *in* 'The 45th Midwest Symposium on Circuits and Systems ( MWSCAS), Tulsa, Oklahoma, USA', Vol. 3, pp. III–37 – III–40.

Schofield, B. (2008), Model-based Vehicle Dynamics Control for Active Safety, PhD thesis, Department of Automatic Control, Lund University Sweden.

Shelley, T. (2012), 'Advances in pneumatics are being applied to improve dramatically the efficiency of lorry braking', Web-page.

**URL:** *http://www.eurekamagazine.co.uk/article/12898/braking-through.aspx, January 2012*

Shin, H.-S., Choi, H.-L. and Lim, J.-T. (2006), "Feedback linearisation of uncertain nonlinear systems with time delay", *IEE Proceedings on Control Theory and Applications* , Vol. 153, No.6, pp. 732 –736.

Slotine, J. J. and Li, W. (1991), *Applied Nonlinear Control*, Prentice-Hall, New Jersey, USA.

Solyom, S. (2002), Synthesis of a Model-based Tire Slip Controller, PhD thesis, Department of Automatic Control, Lund Institute of Technology, SE-221 00 Lund Sweden.

Solyom, S. (2004), Control of Systems with Limited Capacity, PhD thesis, Department of Automatic Control, Lund Institute of Technology, SE-221 00 Lund Sweden.

Srakaew, K., Kananai, J. and Chancharoen, R. (2011), "Trajectory control of a nonlinear dynamical system using NARMA L2 neurocontroller", *Journal of Computer and Information Technology* , Vol. 1, No. 1, pp. 11 – 17.

Svendenius, J. (2003), Tyre models for use in braking applications, PhD thesis, Lund Institute of Technology.

Tanelli, M., Astolfi, A. and Savaresi, S. (2006), Robust nonlinear proportional-integral control for active braking control systems, *in* 'Proceedings of the 45th IEEE Conference on Decision and Control, San Diego, USA', pp. 1745 –1750.

Topalov, A. V., Oniz, Y., Kayacan, E. and Kaynak, O. (2011), "Neuro-fuzzy control of antilock braking system using sliding mode incremental learning algorithm", *Neurocomputing* , Vol. 74, No.11, pp. 1883 – 1893.

Villella, M. (2004), Nonlinear modeling and control of automobiles with dynamic wheel-road friction and wheel torque inputs, Master's thesis, School of Electrical and Computer Engineering, Georgia Institute of Technology, USA.

Von Altrock, C. (1994), Fuzzy logic technologies in automotive engineering, *in* 'Proceedings of the WESCON/94. 'Idea/Microelectronics'. Conference Record, Anaheim, California, USA', pp. 110 –117.

Wahyudi, M., Mokri, S. and Shafie, A. (2008), Real time implementation of NARMA L2 feedback linearization and smoothed NARMA L2 controls of a single link manipulator, *in* 'Proceedings of the International Conference on Computer and Communication Engineering (ICCCE), Kuala Lumpur, Malaysia', pp. 691 –697.

Wang, F.-C. (2001), Design and Synthesis of Active and Passive Vehicle Suspensions, PhD thesis, Department of Engineering University of Cambridge.

Wang, H., Tanaka, K. and Griffin, M. (1995), Parallel distributed compensation of nonlinear systems by takagi-sugeno fuzzy model, *in* 'Proceedings of the 4th International Joint Conference on Fuzzy Systems, Yokohama, Japan', Vol. 2, pp. 531 –538.

Wang, K., Liu, C. and Tang, J. (2010), Research on control strategy of anti-lock brake system in cornering with braking based on electromechanical brake system, *in* 'Proceedings of the International Conference on Mechatronics and Automation (ICMA), X'ian, China', pp. 45 –48.

Wellstead, P. and Pettit, N. (1997), "Analysis and redesign of an antilock brake system controller", *IEE Proceedings on Control Theory and Applications* , Vol. 144, No. 5, pp. 413 –426.

Woods, R. L. (2004), Normalization of Pacejka tire model, *in* 'Proceedings of the 2004 SAE Motorsports Engineering Conference and Exhibition', number 2004-01-3528 *in* 'SAE Technical Paper Series'.

Xu, C., Cheng, K., Sha, L., Ting, W. and Ding, K. (2009), Simulation of the integrated controller of the anti-lock braking system, *in* 'Proceedings of the 3rd International Conference on Power Electronics Systems and Applications, Hong Kong', pp. 1 –3.

Yagi, K., Kyogoku, K. and Nakahara, T. (2005), "Relationship between temperature distribution in EHL film and dimple formation", *ASME Journal of Tribology* , Vol. 127, No. 3, pp. 658–665.

Yeşildirek, A. and Lewis, F. L. (2001), "Adaptive feedback linearization using efficient neural networks", *Journal of Intelligent and Robotic Systems* , Vol. 31, No. 1-3, pp. 253–281.

Yoo, D. (2006), Model based wheel slip control via constrained optimal algorithm, Master's thesis, RMIT University, Melbourne, Australia.

Yu, F., Feng, J. and Li, J. (2002), "A fuzzy logic controller design for vehicle ABS with a on-line optimized target wheel slip ratio", *International Journal of Automotive Technology* , Vol. 3, No. 4, pp. 165 –170.

Zanten, A., Erhardt, R. and Lutz, A. (1990), "Measurement and simulation of transients in longitudinal and lateral tire forces", *SAE Technical Paper* , Vol. 99, pp. 300 –318.

Zhang, D., Chen, Y., Xie, J., Ai, W. and Yuan, C. (2010), A hybrid control method of sliding mode and PID controllers based on adaptive controlled switching portion, *in* 'Proceedings of the 29th Chinese Control Conference (CCC), Beijing, China', pp. 439 –445.